



5

# Dating Oligocene-Recent siliciclastic sediment sequences from the Norwegian Sea

10 Tjerk J.T. Veenstra<sup>1</sup>, Francesca Sangiorgi<sup>1</sup>, Vidar B. Bakker<sup>1</sup>, Klaudia F. Kuiper<sup>2</sup>, Appy Sluijs<sup>1</sup>

<sup>1</sup>Marine Palynology and Paleoceanography, Laboratory of Palaeobotany and Palynology, Department of Earth Sciences, Faculty of Geosciences, Utrecht University, P.O. Box 80.115, 3508 TC Utrecht, the Netherlands

<sup>2</sup>Department of Sciences, Vrije Universiteit Amsterdam, De Boelelaan 1085, 1081 HV, Netherlands

15

PEER REVIEW STATUS:

This manuscript was submitted to the Journal of Micropaleontology (eISSN: 2041-4978). It has come back from review with recommendations for revision. The authors are currently in the process of revising the manuscript and expect no major changes of the age model presented in this version.

20

# Dating Oligocene-Recent siliciclastic sediment sequences from the Norwegian Sea

Tjerk J.T. Veenstra<sup>1</sup>, Francesca Sangiorgi<sup>1</sup>, Vidar B. Bakker<sup>1</sup>, Klaudia F. Kuiper<sup>2</sup>, Appy Sluijs<sup>1</sup>

<sup>1</sup>Marine Palynology and Paleoceanography, Laboratory of Palaeobotany and Palynology, Department of Earth Sciences,  
5 Faculty of Geosciences, Utrecht University, P.O. Box 80.115, 3508 TC Utrecht, the Netherlands

<sup>2</sup>Department of Sciences, Vrije Universiteit Amsterdam, De Boelelaan 1085, 1081 HV, Netherlands

*Correspondence to:* Tjerk J.T. Veenstra (t.j.t.veenstra@uu.nl)

**Abstract.** The Norwegian Sea is crucial for ocean circulation and global climate and has therefore long been a focus in paleoceanography. However, precise dating of sediments has often proved difficult, due to poor preservation and endemism among microfossils and the discontinuous nature of many records. One important Norwegian Sea Site, Ocean Drilling Program (ODP) Site 643, is of particular interest, because of its location and long stratigraphic reach. Previously published magneto- and biostratigraphic age models diverge by ~1 Myr in the lower and middle Miocene, insufficient for global correlations. Here we present new palynological, notably dinoflagellate cyst (dinocyst) data from the lower and middle Miocene of ODP Site 643 and integrate these with existing palynostratigraphies of ODP Site 643. Additionally, we perform  $^{40}\text{Ar}/^{39}\text{Ar}$  dating on selected tephra layers. We use these, combined with other microfossil bioevents, to reinterpret the existing magnetostratigraphy and construct a revised Oligocene to Recent biomagnetostratigraphic age model for this Site. We confirm the occurrence of three early and middle Miocene hiatuses and one early Pleistocene hiatus and refine their duration. Our age model further indicates a substantially older age for lower and middle Miocene sediments than previous dating has suggested. Finally, we combine our new age model with the integrated palynostratigraphy to provide updated ages 10 of dinocyst bioevents and zone boundaries, which are at least applicable to the Norwegian Sea.

## 1 Introduction

As the location of North Atlantic Deep Water (NADW) formation, the Nordic Seas are a crucial area for the Atlantic Meridional Overturning Circulation (AMOC) and hence for global climate. Oceanographic changes in this region during the Neogene have been linked to both tectonically induced gateway changes (Wright and Miller, 1996; Jakobsson et al., 2007; 15 Ehlers and Jokat, 2013, De Schepper et al., 2015) and global climate (Müller-Michaelis and Uenzelmann-Neben, 2014). A prerequisite to understand the governing mechanisms and the precise timing of important warming and cooling climate events, and their link to the AMOC, is the accurate dating of sediments. However, absolute dating of sediments in the Nordic Seas is problematic (Deep Sea Drilling Project (DSDP) Leg 38: Schrader et al., 1976; Ocean Drilling Project (ODP) Leg 20 104: Goll, 1989; ODP Leg 151: Hull et al., 1996; ODP Leg 162: Raymo et al., 1999).

30 Traditional biostratigraphy based on calcareous nannofossils and foraminifera is affected by low diversity and evolutionary turnover at high latitudes (Parker et al., 1999; Matthiessen et al., 2009). For sediments older than the Pliocene, poor preservation of calcareous fossils in the Nordic Seas due to a combination of low carbonate productivity and strong dissolution poses an additional complication (Spiegler and Jansen, 1989). Finally, the stratigraphic discontinuity of many records strongly reduces the applicability of carbonate-based oxygen and stable carbon isotope stratigraphy (e.g. Matthiessen  
35 et al., 2009).

Siliceous microfossils are more commonly preserved than calcareous fossils in Nordic Sea Neogene sediments (Schrader et al., 1976; Goll, 1989; Hull et al., 1996; Raymo et al., 1999) and have potential for regional biostratigraphy. Indeed, a wealth of biostratigraphic data on diatoms, radiolarians and silicoflagellates has been generated on DSDP (Leg 38) and ODP (Legs 104, 151 & 162) cores (Bjørklund, 1976; Dzinoridze et al., 1978; Martini and Müller, 1976; Schrader and Fenner, 1976;  
40 Ciesielski et al., 1989; Goll and Bjørklund, 1989; Locker and Martini, 1989; Koç and Scherer, 1996; Locker, 1996; Amigo, 1999). However, incomplete recovery and high proportions of endemic species – particularly among radiolarians – have hampered the development of a robust regional stratigraphic framework. Improvements in paleomagnetic calibrations for the middle Miocene through Pliocene at ODP Leg 151 Sites have provided much better constraints (Koç and Scherer, 1996; Channell et al., 1999). However, integrated biomagnetostratigraphic models at high temporal resolution at various sites are  
45 now needed to link regional paleoceanographic and paleoenvironmental proxy data to records from elsewhere.

Shipboard and shore-based palynologists working on DSDP and ODP legs in the final three decades of the previous millennium have established that organic-walled dinoflagellate cysts (dinocysts) are the only microfossils that are ubiquitous throughout the entire Nordic Sea Neogene (DSDP Leg 38: Manum, 1976; ODP Leg 104: Manum et al., 1989; Mudie, 1989; ODP Leg 151: Poulsen et al., 1996; ODP Leg 162: Williams and Manum, 1999; Smelror, 1999). Dinocyst biostratigraphy is  
50 therefore still regularly applied, for example to improve dating of the Tjörnes section on Iceland (Verhoeven et al., 2011) and ODP Leg 151 Site 911 in the Fram Strait (Grøsfjeld et al., 2014). Recent work has established magnetostratigraphic calibrations of dinocyst bioevents in sediments from ODP Leg 151 Site 907 in the Iceland Sea (Schreck et al., 2012) and ODP Leg 104 Site 642 in the Norwegian Sea (De Schepper et al., 2017), providing reliable ages for the middle Miocene through Pliocene (~14-2.6 Ma). The generally high Nordic Sea dinocyst diversity implies that multiple bioevents are  
55 available that can be correlated to regions outside the Nordic Seas. This, combined with taxonomic advances and improved dating of events over the last decades make dinocysts potentially the most powerful microfossil group for biostratigraphic correlations for the Neogene of the Nordic Seas.

In addition to the stratigraphic work carried out on sediments recovered during ODP Leg 151 (Koç and Scherer, 1996; Schreck et al., 2012), we here aim to develop an integrated age model for ODP Leg 104 Site 643 in the Norwegian Sea (Fig.  
60 1). At present, this Site is influenced by the Norwegian Atlantic Current, a northward branch of the North Atlantic Current (NAC) (Gascard et al., 2004; Newton et al., 2018). ODP Site 643 is therefore ideally located to serve as a bridge between

globally recognized bioevents and those of more endemic Nordic Sea species. A magnetic polarity record (Bleil, 1989), as well as biostratigraphic constraints (Goll, 1989 and references therein) are available, but were never fully integrated, resulting in discrepancies between the age models of up to ~1 Myr.

- 65 To establish an updated integrated biomagnetostratigraphy for Site 643 and thereby revisit magnetostratigraphic calibration ages for bioevents, we 1) perform a new stratigraphic study based on dinocysts and some acritarchs on lower and middle Miocene sediments, and integrate our results with previously published stratigraphies, 2) compile published ages for Oligocene-Pleistocene dinocyst, diatom, radiolarian and planktic foraminifer bioevents recorded at ODP Site 643, and 3) perform  $^{40}\text{Ar}/^{39}\text{Ar}$  dating on selected Miocene tephra layers at ODP Site 643. The compiled biostratigraphic ages and  
70  $^{40}\text{Ar}/^{39}\text{Ar}$  ages allow us to update the magnetostratigraphic interpretation based on inclination and newly azimuthally corrected declination, and properly identify hiatuses at ODP Site 643. Based on the integrated age model, we recalibrate dinocyst events to the Geological Time Scale 2012 (Gradstein et al., 2012).

## 2 Methods

### 2.1 Material

- 75 ODP Leg 104 Hole 643A ( $67^{\circ}42.9' \text{ N}$ ,  $1^{\circ}02.0' \text{ E}$ ) was drilled in 1985 on the lower western slope of the outer Vørings Plateau in the eastern Norwegian Sea at 2753 m water depth (Fig. 1; Shipboard Scientific Party, 1987). Drilling penetrated 565.2 metres of sediments, of which 449.2 m was recovered (total recovery: 79.5 %), with an estimated age range of 0 to 44.5 Ma (Goll, 1989). Based on shipboard analyses (Table S1), the sedimentary sequence was divided into five lithological units, of which unit II was subdivided into three subunits (Shipboard Scientific Party, 1987). Here we consider units I-IV and the  
80 upper part of unit V (Fig. 2; Fig. S1). Unit I (0-49.42 metres below seafloor (mbsf), Pleistocene to Recent) consists of alternating interbedded dark carbonate-poor glacial muds, sandy muds, and light carbonate-rich interglacial muds. Unit IIA (49.42-63.80 mbsf, Pliocene to Pleistocene) consists of siliceous nannofossil ooze and minor amounts of muds. Unit IIB (63.80-81.30 mbsf, upper Miocene to Pliocene) consists of sandy and siliceous muds with minor amounts of nannofossil ooze. Unit IIC (81.30-100.15 mbsf, upper Miocene) comprises diatomaceous nannofossil ooze and siliceous muds, with  
85 minor amounts of diatom ooze. Unit III (100.15-274.05 mbsf, lower to upper Miocene) primarily consists of diatom ooze, with minor amounts of siliceous muds and nannofossil-diatom ooze. Unit IV (274.05-400.70 mbsf, lower Miocene) consists of monotonous dark, compaction-laminated mudstone, with minor amounts of chalk and siliceous mudstone. Unit V (400.70-565.20 mbsf) consists of zeolitic mudstone, mostly intensively compacted and laminated. Tephra layers of varying composition are present in Units I-III. To achieve an integrated stratigraphy for the early Oligocene to Recent, we focus on  
90 the upper ~460 metres of the recovered section. Sediments below this interval have been biomagnetostratigraphically dated to the early Oligocene and Eocene by Eldrett et al. (2004).

## 2.2 Revised mbsf

Core expansion and generally good core recovery often led to individual core recovery percentages of >100% and overlapping depths in the shipboard mbsf scale between the lowermost parts of a core and the top of the directly underlying core (Shipboard Scientific Party, 1987). Because only one hole was drilled at Site 643, no direct information is available on the stratigraphic thickness of core gaps. This has to be accounted for in the identification of bioevents and hiatuses, particularly those located at or close to core boundaries. In the integrated biostratigraphy of Goll (1989), sample depths in cores with recovery >100% were rescaled to fit to a recovery of 100%, which prevents overlap between subsequent cores, but gaps between the cores, which typically comprise in the order of 0.5 m (e.g. Lisiecki and Herbert, 2007; Wilkens et al., 100 Dickens and Backman, 2013; Vallé et al., 2017) were not accounted for.

We here construct a revised mbsf (R-mbsf) in a pragmatic way (Table S2). Subsequent cores were appended to the recovered length of the previous core if the recovery of the latter was >100%, or to the drilled length if the recovery was <100%. Additionally, 0.5 m was added between each core to account for missing sediment in core gaps. Sample depths in mbsf (Shipboard Scientific Party, 1987) or rescaled mbsf (Goll, 1989) reported in previous studies were recalculated to mbsf from 105 the original ODP sample codes (Core-Section-cm), and subsequently converted to R-mbsf.

## 2.3 Palynological analyses

Thirty-one samples were selected for palynological analysis (Table S3). The samples were processed according to standard palynological processing techniques in use at Utrecht University (e.g. Brinkhuis et al., 2003). In short, the samples were crushed and weighted (~1 gram of sediment). A tablet with a known amount ( $20848 \pm 3.3\%$ ) of *Lycopodium clavatum* spores was added to each sample to facilitate quantification of palynomorphs. The samples were then treated with 30% HCl to remove carbonates and 38% cold HF to remove silicates. After each acid step, the samples were neutralised with water and centrifuged (after HCl) or left to settle for 20 hours (after HF) and decanted. The residues were sieved with 15 µm and 250 µm nylon meshes to obtain the 15–250 µm fraction. All samples were treated with ultrasound for five minutes to break up agglutinated particles of the residue. A droplet of homogenized residue was mixed with glycerine jelly, mounted on a microscope slide and sealed. A minimum of 250 marine palynomorphs was identified per sample and determined to the species level, where possible, with an Olympus CX21 light microscope at 400x magnification. All slides are stored in the collection of the Laboratory of Palaeobotany and Palynology, Department of Earth Sciences, Utrecht University.

## 2.4 Bioevents

Lowest Occurrences (LO) and Highest Occurrences (HO) represent the lowest and highest in-situ stratigraphic occurrences 120 of taxa, and we assign ages to these bioevents based on First Appearance Datums (FAD) and Last Appearance Datums (LAD). Similarly, LPOs and HPOs (FPADs/LPADs) represent the lowest and highest persistent (successive) occurrences of taxa. New results from palynology were combined with palynostratigraphy of Mudie (1989) and Manum et al. (1989) down

to Core 49X, resulting in a combined high-resolution dinocyst and acritarch stratigraphy for ODP Hole 643A. Where possible, species names were updated to the most recent nomenclature and taxonomy of DINOFLAJ3 (i.e. Williams et al., 125 2017). Taxonomic junior and senior synonyms were individually assessed before being synonymized. The processing of new palynological samples allowed the identification of known, but often also recently described species, which were not reported by Mudie (1989) or Manum et al. (1989). As a consequence, their work could not be included in determining their bioevent depths, leading to somewhat larger errors. We use diatom and planktic foraminifer bioevents identified by the Shipboard Scientific Party (1987) and Ciesielski and Case (1989). Radiolarian events were identified from Goll and 130 Bjørklund (1989). Species nomenclature mostly follows these authors, but has been updated when necessary for comparison with newer studies. We have noticed that sample codes in the older literature are sometimes inconsistent with the sampling reports from the ODP sampling data base. In those cases we have adopted the sampling codes of the data base.

Selected dinocyst event ages from literature are recalibrated to GTS2012 using available independent stratigraphy in the original publications. Selected diatom, planktic foraminifer and radiolarian ages are directly derived from the original 135 publications, but have been updated to GTS2012 using linear interpolation between rescaled magnetic reversals. Since the biostratigraphy in this study mainly serves as a means to constrain the magnetostratigraphic interpretation rather than as a direct age estimate, we chose to define confining bioevents at their extreme position: the globally first FAD or last LAD and the highest/lowest possible depth of a LO/HO, i.e. the lowest/highest sample with the presence of a species. This is based on 1) the plausibility that environmental factors caused a species to appear/disappear at Site 643 after/before the globally first 140 FAD/last LAD, while the opposite is unlikely, especially if the event has been documented by many studies, and 2) the plausibility that the real LO/HO of a species occurs below/above the reported LO/HO if the species has a very low abundance in these sediments, while the opposite can only be explained by sediment caving or reworking.

## 2.5 $^{40}\text{Ar}/^{39}\text{Ar}$ dating

145 Eighteen samples were selected for  $^{40}\text{Ar}/^{39}\text{Ar}$  dating. Sample selection was based on the description of tephras by the Shipboard Scientific Party (1987) and Despraires et al. (1989). One additional sample was taken after visual core inspection (Table S4). Samples were washed and sieved over a 90 µm sieve. Feldspar minerals were separated using standard heavy liquid (2.55 and 2.59 g cm<sup>-3</sup>) using a miniaturized centrifugal system. A subset of selected samples was further cleaned with distilled water in an ultrasonic bath. Finally, these samples were hand-picked under a microscope.

Samples were wrapped in 6 mm Al packages and loaded into 25 mm diameter Al cups together with Fish Canyon tuff 150 sanidine as neutron flux monitor. Samples were irradiated at the OSU Triga reactor in the CLICIT facility for 18 hours. After irradiation samples and standards were unpacked and loaded in a 185 hole Cu tray and baked overnight at 250 °C under vacuum. This tray is then placed in a doubly pumped vacuum chamber with Zn-S window and baked overnight at 120 °C under high vacuum. This sample chamber is connected to a ThermoFisher NGPrep gas purification line with four additional SEAS-NP10 getters, a cold finger, an ion gauge, two inlets and two pipette systems. We connected a CO<sub>2</sub> laser in 155 combination with the sample chamber to one inlet. Samples are heated using a 25W Synrad CO<sub>2</sub> laser. Sample gas is

exposed to three of the NP10 getters (two hot and 1 cold) in the gas purification line during 3 minutes before expansion into the ARGUS VI+ for analyses.

The ARGUS VI+ at the Vrije Universiteit, Amsterdam, is a high sensitivity, low resolution multi-collector noble gas mass spectrometer with an internal volume of 710 ml. The mass spectrometer is equipped with four Faraday cups at the H2, H1, AX and L1 positions and two compact discrete dynodes (CDDs) at positions L2 and L3. The system is equipped with a  $10^{12}$  Ohm amplifier on H2 and  $10^{13}$  Ohm amplifiers on H1, AX and L1 cups. The resolution of the system is  $\sim 200$  and therefore does not resolve hydrocarbon or chlorine interferences. The ARGUS VI+ has a NP10 getter and ion gauge on the source of the mass spectrometer. The NP10 getter is run cold and the ion gauge is turned off, because of its pumping capacity for argon. Depending on beam size, samples are either run on H2 – L2 for higher intensity samples, or H1 – L3 for low intensity samples (Table S5).

Bias between the different detectors has been monitored by 1) measurement of  $^{40}\text{Ar}$  air pipettes across the different Faraday cups; 2) measurement of  $^{40}\text{Ar}$  blanks on all detectors and 3) by measurement of mass 44 CO<sub>2</sub> in dynamic mode on all detectors. Systematic bias up to 7% is found, but is reproducible over periods of weeks. Similar to Phillips and Matchan (2013) we did not apply bias corrections, but analyzed samples and standards in the same tray (and thus at more or less the same time) alternating with air pipettes of different intensities in the same range as the samples and standards. Line blanks were measured every 2-3 unknowns and were subtracted from succeeding sample data. Data reduction is done in ArArCalc (Koppers, 2002). Ages are calculated with Min et al. (2000) decay constants and  $28.201 \pm 0.022$  Ma for FCs (Kuiper et al., 2008). The atmospheric air value of 298.56 from Lee et al. (2006) is used. The correction factors for neutron interference reactions are  $(2.64 \pm 0.02) \times 10^{-4}$  for  $(^{36}\text{Ar}/^{37}\text{Ar})_{\text{Ca}}$ ,  $(6.73 \pm 0.04) \times 10^{-4}$  for  $(^{39}\text{Ar}/^{37}\text{Ar})_{\text{Ca}}$ ,  $(1.21 \pm 0.003) \times 10^{-2}$  for  $(^{38}\text{Ar}/^{39}\text{Ar})_{\text{K}}$  and  $(8.6 \pm 0.7) \times 10^{-4}$  for  $(^{40}\text{Ar}/^{39}\text{Ar})_{\text{K}}$ . All errors are quoted at the  $1\sigma$  level, unless mentioned otherwise, and include all analytical errors.

## 2.6 Paleomagnetism

We use paleomagnetic data from Bleil (1989) (Fig. 2). In addition to measurements of natural remanent magnetization (NRM), Bleil (1989) presented inclination and declination data by applying systematic step-wise demagnetization treatments on each sample. Steps of 2.5 and 5 mT were typically applied up to 10 mT, followed by 5 mT steps up to 20 or 30 mT and 10 mT steps beyond that stage. For most samples, demagnetization was taken to the 50 mT level, which generally exceeded the median destructive field.

Absolute or relative azimuthal core orientations are not available for ODP Site 643, which has hampered the use of declination data for polarity interpretation. Bleil (1989) therefore based the polarity interpretation solely on inclinations, which, due to the steep geomagnetic field inclinations at high latitudes, can provide an unambiguous interpretation, but offers a less reliable result. In order to also use declination for assessing the polarity interpretation, we chose to azimuthally reorient the declination data. Assuming a general correlation between inclination and declination in each core, we rotated declination data such that mean (excluding outliers  $>1\sigma$ ) northward ( $360^\circ$ ) and southward ( $180^\circ$ ) core declination was

aligned with positive and negative inclination, respectively. The resulting correction factor was applied to all declination data  
190 in the core, preserving the intersample variability. The polarity signal was subsequently reinterpreted, in which inclination data was considered leading and declination and NRM intensity were used to assess confidence in the assigned polarity.

### 3 Results

#### 3.1 Palynostratigraphy

During palynological analysis of 31 new lower to middle Miocene samples, 105 dinocyst and 9 acritarch in-situ taxa were  
195 identified (Tables S6 & S7). Of these, 19 dinocyst and 2 acritarch taxa could not be identified at species level based on previous work at ODP Site 643 (Manum et al., 1989; Mudie, 1989) or other literature and are reported at the genus level or higher. These taxa are mostly rare and confined to a few samples and are therefore not further considered. Reworked Paleogene dinocysts were encountered in five samples, but did not exceed two specimens per sample.

Integration of our results with palynostratigraphy of Manum et al. (1989) and Mudie (1989) from the top of Hole 643A  
200 (recent) down to core 49X (lowest Oligocene) yielded a total of 216 dinocyst and 11 acritarch taxa. Of these, 55 dinocyst taxa remain in open nomenclature, while 12 dinocyst and 2 acritarch taxa have previously only been described informally. Taxa that are considered questionably synonymous are included both separately (*sensu stricto*, s.s.) and combined (*sensu lato*, s.l.). Full stratigraphic ranges of dinocyst and acritarch taxa are presented in Table S6 and explanations on the synonymization of individual taxa are included in Table S7.

#### 205 3.2 Bioevents

More than 300 bioevents were assessed for their potential to constrain the magnetostratigraphic interpretation and sediment age. However, many were not very useful due to problems with taxonomy or poor age constraints from the literature. Additionally, LOs/HOs with FADs/LADs  $>\sim 5$  Myr earlier/later than the expected age of the sediment (Bleil, 1989; Goll,  
210 1989) were excluded, as these LOs/HOs are assumed to be diachronous. These events are consistent with available age models for Site 643, but do not provide additional information on the sediment age for the here considered interval. This resulted in 45 useful dinocyst events, 16 diatom events, 1 planktic foraminifer event, and 1 radiolarian event (Table 1; Fig. 3; Fig. S1). Bioevents are present throughout the studied interval with a peak of bioevents in the middle Miocene. Siliceous bioevents are absent below the diagenetic front of opal at  $\sim 300$  R-mbsf. Updated nomenclature and some stratigraphic notes are included in Table S7 (dinocysts and acritarchs) and Table S8 (diatoms, planktic foraminifer and radiolarian). Tables S9  
215 and S10 list the literature used for age derivations of bioevents.

#### 3.3 $^{40}\text{Ar}/^{39}\text{Ar}$

Four of the eighteen samples analyzed contained sufficient amounts of material for radio-isotope dating. Due to initial calibration and blank problems with the novel ARGUS VI+ noble gas mass spectrometer, analysis occurred about one year

after irradiation. This implies that it was not possible to accurately measure the  $^{37}\text{Ar}$  signal ( $t_{1/2}$  of  $^{37}\text{Ar}$  is 35.5 days) required for neutron interference reactions on Ca. As a result, corrections for neutron interference reactions are less reliable and measured K/Ca values may be incorrect. In all cases where  $^{37}\text{Ar}$  signals were lower than blank values, we set negative intensities to zero (Table S11; Fig. S2). Note, that the density separation of 2.55-2.59 g cm $^{-3}$  should only include the K-rich sanidine fraction in our experiments, in which case impact of Ca neutron interference corrections is minor, and exclude the Ca rich plagioclase fraction.

Tephra T1 (sample 16H 6W 46.0-48.0 cm): 12 single grains have been analyzed. Intensities range from 2 – 60 times  $^{40}\text{Ar}$  blank. Most samples show low amounts of radiogenic  $^{40}\text{Ar}^*$ . The three samples with a radiogenic  $^{40}\text{Ar}^*$  yield >70% give a weighted mean age with full external error of 17.59 (2 SE:  $\pm$  0.94) Ma (and an outlier of ~21.8 Ma).

Tephra T2 (sample 17X 1W 41.0-43.5 cm): 10 single grains have been analyzed. Intensities range from 1.2 – 19 times  $^{40}\text{Ar}$  blank. Most samples show low amounts of radiogenic  $^{40}\text{Ar}^*$ . Samples with a radiogenic  $^{40}\text{Ar}^*$  yield >55% give a weighted mean age with full external error of 18.34 (2 SE:  $\pm$  1.79) Ma.

Tephra T3 (sample 22X 3W 128.0-130.0 cm): 16 single grains have been analyzed, but the measured  $^{40}\text{Ar}$  intensity is hardly above blank values. Three exceptions are two older Paleocene grains and one highly non-radiogenic sample. Therefore, no reliable age could be obtained.

Tephra T4 (sample 28X 2W: 148.0-150.0 cm): 19 grains have been analyzed of which 4 grains in two steps. The measured  $^{40}\text{Ar}$  intensities range from just >1 to 110 times above blank values with the majority between 3 and 10. The age range of samples with >60%  $^{40}\text{Ar}^*$  is 16.86-21.53 Ma and does not provide information on eruption age.

Overall, two (T3, T4) of the  $^{40}\text{Ar}/^{39}\text{Ar}$  experiments did not yield reliable data and two (T1, T2) of the experiments suggest an age of ~17-19 Ma. Highly precise ages were not obtained.

### 3.4 Magnetic polarity signal

Azimuthally reoriented declination data generally confirm the inclination-based magnetic polarity interpretation (Table S12; Fig. 2). Our interpretation differs slightly from that of Bleil (1989) (Fig. 3), mostly to the extent that we consider some excursions to represent true reversals and vice versa. We did not assign polarities to most of the interval between 230.60 R-mbsf and 266.94 R-mbsf, due to frequently changing polarity and poor directional stability of the demagnetization data, associated with extremely low ( $<10^{-4}$  A m $^{-1}$ ) NRM intensity (Bleil, 1989).

## 245 4 Discussion

### 4.1 New bio-magnetostratigraphic age model of ODP 643 Hole A

A revised age model for the Oligocene-recent section of ODP Hole 643A is constructed (Table 2; Figs. 3 & 4; Fig. S1) using the selected bioevents (Table 1) and tephra  $^{40}\text{Ar}/^{39}\text{Ar}$  ages (Table S11; Fig. S2) as constraints on the magnetostratigraphic interpretation. Recognized magnetostratigraphic tie points have been converted to the Geomagnetic Polarity Time Scale

250 (GPTS2012) of Ogg (2012) (Fig. 3). Below 315.16 R-mbsf, dated at ~19.73 Ma, magnetostratigraphic interpretation was not reliable and the age model is solely based on biostratigraphy (Fig. 4). At a depth of 491.89 R-mbsf, the top of magnetochron C13n was identified (Eldrett et al., 2004), which marks the earliest Oligocene (Fig. 4).

Our selected bioevent and tephra  $^{40}\text{Ar}/^{39}\text{Ar}$  ages, although partly in agreement with previous age models by Goll (1989) and Bleil (1989) (both recalibrated to GTS2012), differ in some key aspects (Fig. 3; Fig. S1). Our magnetostratigraphic interpretation of the lower-middle Miocene below 143.82 R-mbsf is ~1.5 Myr older than the interpretation of Bleil (1989) and slightly older than the age model of Goll (1989). Additionally, a different magnetostratigraphic interpretation was chosen for two upper Miocene-Pliocene sections (34.70-53.26 R-mbsf and 63.61-88.82 R-mbsf) and the magnetostratigraphy was refined for the middle Miocene section between 104.04 and 124.09 R-mbsf. The depth and duration of hiatuses of Goll (1989) have been evaluated, which has led to some minor changes in depth and larger adjustments in duration, including the removal of some hiatuses.

To understand correspondence and differences between our age model and that of previous work, we briefly discuss how Goll (1989) and Bleil (1989) constructed their models. The age model presented by Goll (1989) strongly relied on regional intercomparison of sediments recovered during DSDP Leg 38 in 1974 and ODP Leg 104. This allowed the identification of ten hiatus-bounded Neogene sequences of laterally strongly varying thickness, classified in a synthemic system (sensu Salvador, 1987), clustered into two synthems (NSN1.0 & NSN2.0) and ten subsynthems (NSN1.1-1.6 & NSN2.1-2.4) (Fig. 2). Subsynthem 1.3 is absent at Site 643 (Goll, 1989). Boundaries (i.e. hiatuses) were denoted by their encompassing (sub)synthem, e.g. H1.1/1.2. The synthemic system was based on assemblage zones and biostratigraphic events, rather than lithological criteria and most synthems and hiatuses were based on the radiolarian stratigraphy of Goll and Bjørklund (1989). While the use of this nomenclature was controversial at the time (Murphy and Salvador, 1988) and is still debated to date (Ruban, 2015; Lucchi, 2019), we adhere to the use of these synthems and bounding hiatuses as a means to easily compare our interpretation with that of Goll (1989).

Bleil (1989) principally focused on recognizing paleomagnetic reversals, rather than presenting a full age model. He acknowledged the existence of several hiatuses, based on the radiolarian stratigraphy of Goll and Bjørklund (1989), but did not assess their duration. Intervals surrounding possible hiatuses are therefore indicated with a dashed line in Fig. 4 and Fig. S1. The existence of some hiatuses between ~37 and ~113 R-mbsf has been questioned by Bruns et al. (1998) based on the lack of sedimentological evidence and they propose that H2.1/2.2, H2.2/2.3 and H2.3/2.4 are in fact artefacts of prolonged reduced sedimentation rates or reduced fossil preservation.

In the below discussion, we use our R-mbsf depth scale. To avoid confusion with depth scales used in previous work, we include sample codes where such confusion may occur.

## 280 **4.1.1 INTERVAL 0-63.61 R-mbsf, 0-4.30 Ma**

Our magnetostratigraphic interpretation in the interval 0-63.61 R mbsf (top of C3n.1r) is consistent with available biostratigraphic constraints (Table 1; Fig. 3; Fig. S1). It is also essentially identical to that of Bleil (1989), with the addition

that the single normal polarity sample at 37.11 R-mbsf is interpreted to represent C1r.2n and tied to the middle of this subchron (Table 2; Fig. 3). C2n and C2r.1n are absent in this record, which we interpret to represent a hiatus, consistent with 285 H2.3/2.4 of Goll (1989) (Fig. 4). Although Bruns et al. (1998) questioned the existence of this hiatus, we consider the lithological boundary between Unit I and Unit II at 52.97 R-mbsf to correspond to a hiatus. This implies that the reversed polarity interval at 37.41-52.49 R-mbsf represents a truncated C1r.3r. While it is unknown how much of the lower part of C1r.3r is missing, this subchron is probably mostly complete, as downward extrapolation of the sedimentation rate (22.5 m 290 Myr<sup>-1</sup>) between the overlying tie points suggests an age of 1.86 Ma, which is older than the onset of C1r.3r at 1.78 Ma. Any age much younger than 1.78 Ma at 52.49 R-mbsf would result in a sharp and unrealistic increase in sedimentation rate. We therefore assign an age of 1.78 Ma to 52.49 R-mbsf and derive an age of 1.80 Ma for the end of hiatus H2.3/2.4 (Table 2; Figs. 3 & 4), with the notion that this age could be slightly younger. The onset of H2.3/2.4 is placed at 2.52 Ma, based on extrapolation of the sedimentation rate (5.1 m Myr<sup>-1</sup>) between the underlying tie points. C2An.1r and C2An.2r are also absent in the paleomagnetic record, but are assumed to fall within the unsampled interval at 55.31-57.16 R-mbsf.

#### 295 4.1.2 INTERVAL 63.61-88.82 R-mbsf, 4.30-8.77 Ma

Our magnetostratigraphic interpretation between the top of C3n.1r at 63.61 R-mbsf and the top of C4An at 88.82 R-mbsf differs from that of Bleil (1989) and the age model of Goll (1989) (Figs. 3 & 4). While Goll (1989) proposed two hiatuses (H2.1/2.2 at ~73.85 R-mbsf and H2.2/2.3 at ~66.60 R-mbsf) in this interval, and Bleil (1989) inferred the existence of a longer single hiatus, we consider the paleomagnetic record to be consistent with continuous slow sedimentation because 300 there is no biostratigraphic or lithological evidence for gaps in the record (Goll, 1989; Bruns et al., 1998). The low resolution paleomagnetic sampling could have easily resulted in missing several subchrons in this condensed section. The average sedimentation rate between 63.61 and 75.48 R-mbsf of 3.8 m Myr<sup>-1</sup> (Table 2) is similar to the suggested sedimentation rate of 4.6 m Myr<sup>-1</sup> by Bruns et al (1998). The discrepancy between magnetostratigraphy and the biostratigraphic age model in this interval as noted by Goll (1989) is reduced with our new interpretation, compared to that of Bleil (1989).

305 Our interpretation of this interval is consistent with most available biostratigraphic constraints (Table 1; Fig. 3; Fig. S1). While the LAD of *Batiacasphaera hirsuta* (83.15 R-mbsf/8.35 Ma (Schreck et al., 2012)) suggests a slightly older age, its LAD may be younger if some specimens interpreted as reworked by Schreck et al. (2012) are in fact in situ. Additionally, its LAD is currently only described by Schreck et al. (2012) and some regional diachroneity is possible. The LAD of *Operculodinium piaseckii* (74.83 R-mbsf/7.90 Ma (Piasecki, 2003)) could not be reconciled with the magnetostratigraphic 310 interpretation and *O. piaseckii* may have a younger LAD at ODP Site 643.

#### 4.1.3 INTERVAL 88.82-107.15 R-mbsf, 8.77-9.90 Ma

The magnetostratigraphic interpretation in the interval 88.82-107.15 R-mbsf follows Bleil (1989), with the addition that the single reversed polarity sample at 105.34 R-mbsf is interpreted to represent C4Ar.3r and tied to the middle of this subchron (Table 2; Fig. 3). A major hiatus, consistent with H1.6/2.1 of Goll (1989) (Fig. 4) is placed at 107.15 R-mbsf. H1.6/2.1 was

315 originally based on the absence of the Radiolarian *Eucoronis fridtjofnanseni* Zone between 107.15 R-mbsf (11H-CC, 46-49) and 108.73 R-mbsf (12H-1, 105-107) (Goll and Bjørklund, 1989). Additionally, an abrupt change in the silicoflagellate assemblage was reported between 99.48 R-mbsf (11H-2, 70-72) and 109.88 R-mbsf (12H-2, 70-72), with fourteen HOs and one LO (Ciesielski et al., 1989). It is further accompanied by several closely spaced dinocyst and diatom bioevents. The HO of *Hystrichostrogylon membraniphorum* (s.l.) at 107.99 R-mbsf suggests the hiatus is located above this depth. The  
320 lithological boundary between subunit IIC and unit III has been defined at 106.63 R-mbsf (11H-7, 35), but may be more gradual considering the pattern of alternating lithology around this depth. The hiatus is therefore placed at 107.15 R-mbsf, close to the reported lithological boundary, but within the range of the radiolarian assemblage change.

The paleomagnetic signal is continuously normal across this depth and does not provide any diagnostic information. The termination of H1.6/2.1 is therefore dated at 9.90 Ma, based on downward extrapolation of the sedimentation rate (12.2 m  
325 Myr<sup>-1</sup>) between the overlying tie points (Table 2).

This interpretation is confirmed by most biostratigraphic constraints (Table 1; Fig. 3; Fig. S1), but some discrepancies exist between our magnetostratigraphic interpretation and biostratigraphy. The LAD of *Cerebrocysta irregularis* (93.57 R-mbsf/10.28 Ma (Schreck et al., 2012)) suggest an older age, but it has so far only been dated by Schreck et al. (2012) and may have a younger age at ODP Site 643. Following Schreck et al. (2012), we have tentatively synonymised *C. irregularis*  
330 with *Tectatodinium* sp. 4 of Manum et al. (1989). The highest confirmed specimen of *C. irregularis* occurs at 108.30 R-mbsf and is consistent with our magnetostratigraphic interpretation. The LAD of *Cerebrocysta poulsenii* (103.58 R-mbsf/9.87 Ma (De Verteuil and Norris, 1996)) suggests a slightly older age than our interpretation, but its age assignment is tied to 67% of NN9, and a slight deviation from this relatively imprecise assignment would be consistent with our interpretation.

#### 4.1.4 INTERVAL 107.15-122.11 R-mbsf, 13.30-14.29 Ma

335 This interval is equivalent with NSN1.6 and NSN1.5 of Goll (1989) (Fig. 4). Bleil (1989) did not provide a magnetostratigraphic interpretation for this interval due to insufficient biostratigraphic constraints. Our new biostratigraphic constraints (Table 1; Fig. 3; Fig. S1) indicate that the section 109.44-122.11 R-mbsf can be interpreted as a mostly complete sequence of reversals from C5ABn through C5ADn (Table 2; Fig. 3).

The interpretation of the overlying section 107.15-109.44 R-mbsf is less straightforward. A hiatus (H1.5/1.6) was proposed  
340 by Goll (1989) based on the absence of Radiolarian ‘Interzone B’ between 110.23 R-mbsf (12H-2, 105-107) and 111.73 R-mbsf (12H-3, 105-107) (Goll and Bjørklund, 1989). Silicoflagellate stratigraphy also indicates that a brief hiatus may exist between 109.88 R-mbsf (12H-2, 70-72) and 114.38 R-mbsf (12H-5, 70-72) (Ciesielski et al., 1989), based on the clustering of six HOs and five LOs between these two samples.

The presence of slump and debris flow deposits, alternating with normal pelagic sedimentation, between 109.18 and 113.23  
345 R-mbsf suggests that this interval may in fact be characterized by multiple small hiatuses. Their total duration, combined with periods of deposition, is constrained by the top of C5ABr (111.64-112.04 R-mbsf/13.61 Ma) and the HO of *H. membraniphorum* (s.l.) (107.99 R-mbsf/13.27 Ma (Zegarra and Helene, 2011)) and suggests a rapid alternation of

deposition and non-deposition. The apparent low sedimentation rate within C5ABr could either indicate another small hiatus in this subchron, or, if representing continuous sedimentation, may have contributed to a mistaken hiatus assignment by Goll and Bjørklund (1989) and Ciesielski et al. (1989). We therefore conclude that this interval is best approximated by continuous sedimentation. In the absence of clear magnetostratigraphic or biostratigraphic constraints, we infer ages for this interval by upward extrapolation of the average sedimentation rate ( $15.1 \text{ m Myr}^{-1}$ ) between the top of C5ABr and hiatus H1.4/1.5 (see next paragraph). The onset of hiatus H1.6/2.1 is accordingly dated at 13.30 Ma, consistent with the HO of *H. membraniphorum* (s.l.).

Another hiatus (H1.4/1.5) was proposed by Goll (1989) at the bottom of H1.5 (Fig. 4). It was originally defined by the absence of the Radiolarian *Actinomma plasticum* Zone and *Cyrtocapsella kladaros* Subzone B between 121.72 R-mbsf (13H-3, 104-107) and 123.22 R-mbsf (13H-4, 104-107) (Goll and Bjørklund, 1989), suggesting the absence of ~250 ky (*C. kladaros* Subzone B is located above Subzone A, but is erroneously depicted below Subzone A in Fig. 2 of Goll and Bjørklund (1989)). We interpret this hiatus to fall within C5ADn, consistent with Bleil (1989). As a result, this hiatus cannot be constrained by magnetostratigraphy. Several dinocyst events occur around this depth, but they do not unambiguously indicate a hiatus. Based on descriptions and photographs of the core material, a sudden lithological change from diatom ooze to diatom ooze/diatomaceous mud occurs at 122.11 R-mbsf (13H-3, 143) (Shipboard Scientific Party, 1987). Consequently, we tentatively confirm a hiatus (H1.4/1.5; Table 2; Figs. 3 & 4) at this depth. The termination of this hiatus could theoretically be anywhere between its onset at 14.53 Ma (see sect. 4.1.5) and the top of C5ADn at 14.16 Ma. Here we chose to date it at 14.29 Ma, at 1/3 between these tie points, which results in a similar duration as suggested by Goll and Bjørklund (1989).

#### 4.1.5 INTERVAL 122.11-143.82 R-mbsf, 14.53-15.04 Ma

The magnetostratigraphic interpretation in the interval 122.11-143.82 R-mbsf follows Bleil (1989) and includes a complete sequence of reversals from C5ADn through C5Bn.1r (Table 2; Fig. 3). Upward extrapolation of the average sedimentation rate between the top of C5Bn.1n and the top of C5ADr yields an age of 14.53 Ma for the onset of hiatus H1.4/1.5. A paleomagnetic reversed excursion is present from 122.24 through 123.34 R-mbsf, which could be synchronous with a similar tentative excursion reported by Sant et al. (2016) in the lower part of C5ADn in Serbia. Alternatively, the excursion could represent C5ADr and the underlying sequence would be interpreted as complete down to C5Br. Accordingly, this would imply an earlier onset and termination of hiatus H1.4/1.5 of 14.62 Ma and 14.32 Ma, as well as a minor change in the onset of hiatus H1.6/2.1, as this is calculated by upward extrapolation.

Both interpretations are in conflict with the FAD of *Achomosphaera andalousiensis* (127.40 R-mbsf/13.12 Ma (Dybkjær and Piasecki, 2010)) and the FAD of *Crucidenticula punctata* (130.20 R-mbsf/13.4 Ma (Barron Diatom Catalog in Lazarus et al., 2014)) (Table 1; Fig. 3; Fig. S1). The LO of *A. andalousiensis* occurs in an isolated sample, but its LPO occurs at 111.30 R-mbsf. This depth would be more, but not fully, consistent with the FAD of Dybkjær and Piasecki (2010). Our alternative interpretation is not supported by the FAD of *Denticulopsis hyalina* (134.70 R-mbsf/14.9 Ma (Barron et al., 1985a)) and the

FAD of *Unipontidinium aqueductum* (136.74 R-mbsf/15.16 Ma (Bijl et al., 2018)) and we therefore prefer the original interpretation for this interval of Bleil (1989), which is supported by most biostratigraphic constraints.

Hiatus H1.2/1.4 (Fig. 4), reported at the bottom of this section (Goll, 1989), is primarily based on the absence of the Radiolarian *Cyrtocapsella eldholmi* Zone (Goll and Bjørklund, 1989), between 142.75 R-mbsf (15H-4 25-27) and 145.05 R-

385 mbsf (15H-5 105-107), suggesting the absence of ~300 ky. The literature regarding diatom stratigraphy is confusing at best.

Goll (1989) noted that the initial diatom stratigraphy (Shipboard Scientific Party, 1987) suggests a much longer hiatus (absence of the *Denticulopsis lauta* Zone (termed NNPD4) and possibly portions of the upper *Actinocyclus ingens* Zone

390 (NNPD3) and lowermost *Denticulopsis hustedtii/D. lauta* Zone (NNPD5)). The absence of the *D. lauta* Zone was based on the concurrent LO of *D. lauta* and *D. hustedtii*. However, Ciesielski and Case (1989) have questionably adjusted the LO of

395 *D. hustedtii* from 137.10 R-mbsf (14H-CC, 48-51) to 125.97 R-mbsf (13H-6, 69-71), rendering the diatom zonation scheme of the Shipboard Scientific Party (1987) problematic. In addition, the species *D. hustedtii* was later emended, so that *D.*

399 *simonsenii* now includes specimens previously attributed to *D. hustedtii* (Yanagisawa and Akiba, 1990), making it unclear which species was found by the Shipboard Scientific Party (1987). Re-examination of the material is needed to clarify the taxonomy and stratigraphy of these taxa. Six silicoflagellate bioevents occur between 140.21 R-mbsf (15H-2, 71-73) and

400 150.20 R-mbsf (16H-2, 70-72) (Ciesielski et al., 1989), but none have been chronostratigraphically calibrated. A paleomagnetic reversal occurs between 143.46 R-mbsf and 143.86 R-mbsf. Finally, a 12 cm volcanic ash layer (Shipboard

Scientific Party, 1987) is present between 143.88 and 144.00 R-mbsf (15H-4, 138-150).

We constrain the depth of this hiatus between the LOs of *D. lauta* and *Cestodiscus peplum* at 143.77 R-mbsf and the uppermost normal polarity sample below this depth at 143.86 R-mbsf, which we interpret as the truncated upper part of

400 C5Cn.2n (see sect. 4.1.6). This puts the hiatus at 143.82 R-mbsf, just above the ash layer.

The termination of this hiatus falls within C5Bn.1r in our primary interpretation, identical to that of Bleil (1989). This subchron is probably mostly complete, as downward extrapolation of the sedimentation rate ( $15.7 \text{ m Myr}^{-1}$ ) between the overlying tie points suggests an age of 15.73 Ma, which is older than the onset of C5Bn.1r at 15.03 Ma. Any age much

405 younger than 15.03 Ma at 143.46 R-mbsf would result in a sharp and unrealistic increase in sedimentation rate. We therefore assign an age of 15.03 Ma to 143.46 R-mbsf and arrive at an age of 15.04 Ma for the end of hiatus H1.2/2.4 (Table 2; Figs. 3

& 4), with the notion that this age could be slightly younger. Similarly, if the termination falls within C5Br in our alternative interpretation, we could infer a maximal age of 16.00 Ma for the end of H1.2/1.4 based on downward extrapolation between the top of C5Br and the truncated bottom of C5Br, but this would be inconsistent with the global FAD of *D. lauta* (143.77 R-

599 mbsf/15.9 Ma (Barron Diatom Catalog in Lazarus et al., 2014)) and the more recent dating of 15.57-15.7 Ma by Cody et al.

410 (2008) (Table S10). Our primary interpretation is therefore preferred.

#### 4.1.6 INTERVAL 143.82-315.16 R-mbsf, 16.30-19.73 Ma

In contrast to Bleil (1989), who interpreted sedimentation to be continuous across hiatus H1.2/1.4, our new tephra  $^{40}\text{Ar}/^{39}\text{Ar}$  ages, as well as the LAD of *Thalassiosira fraga* (157.85 R-mbsf/15.96 Ma (Pälike et al., 2010)) suggest that sediments below 143.82 R-mbsf are substantially older than above this depth (Fig. 3; Fig. S1).

415  $^{40}\text{Ar}/^{39}\text{Ar}$  samples T1 and T2 suggest ages of 17.59 (2 SE:  $\pm 0.94$ ) Ma and 18.34 (2 SE:  $\pm 1.79$ ) Ma for 155.96 and 158.79 R-mbsf respectively. We therefore interpret the magnetostratigraphic record below 143.82 R-mbsf to represent a mostly complete reversal sequence from C5Cn.2n through C6r (Table 2; Fig. 3), which is consistent with available biostratigraphic constraints (Table 1; Fig. 3; Fig. S1). An assignment to older magnetochrons would lead to discrepancies with biostratigraphy.

420 Sediments directly below hiatus H1.2/1.4 are interpreted as the truncated top of C5Cn.2n. This subchron is probably mostly complete, as upward extrapolation of the sedimentation rate ( $19.7 \text{ m Myr}^{-1}$ ) between the underlying tie points suggests an age of 16.27 Ma, which is younger than the top of C5Cn.2n at 16.30 Ma. Any age much older than 16.30 Ma at 143.86 R-mbsf would result in a sharp and unrealistic increase in sedimentation rate. We therefore assign an age of 16.30 Ma to 143.86 R-mbsf and arrive at an age of 16.30 Ma for the onset of hiatus H1.2/1.4 (Table 2; Figs. 3 & 4), with the notion that this age 425 could be slightly older.

NRM intensities below 143.82 R-mbsf are often less than  $10^{-4} \text{ A m}^{-1}$  and directional stability of the demagnetization data is often poor in this interval (Bleil, 1989). Our polarity interpretation of the inclination and declination signal, which mostly follows Bleil (1989), is therefore tentative at places. C5Dr.1n could not be unequivocally recognized and the top of C5Er may be linked to two different depths. These have therefore not been used as tie points.

430 The top of C6r is tentatively recognized at 314.65 R-mbsf between a continuously normal polarity section and a single reversed polarity sample, below which there are insufficient paleomagnetic samples for further interpretation.

#### 4.1.7 INTERVAL 315.16-491.89 R-mbsf, 19.73-33.16 Ma

Age interpretation of this section relies on biostratigraphy only. A hiatus (H1.1/1.2) was tentatively proposed by Goll (1989) at the boundary of lithological units III and IV at 291.48 R-mbsf (Fig. 4), but we see no indication of a hiatus at this level.

435 Unit IV was originally classified as monotonous terrigenous mudstones, contrasting the highly productive biogenic siliceous oozes and muds in Unit III (Shipboard Scientific Party, 1987). Sedimentation of the two units was interpreted to be separated by a period of (deep) burial and subsequent uplift and erosion. This interpretation was questioned by Henrich (1989), who concluded that the boundary was purely the result of diagenesis during early burial and compaction.

Goll (1989) found only limited evidence for the existence of a hiatus. The top of NSN1.1 was dated at  $\sim 19.7$  Ma by 440 extrapolation of the sedimentation rate, such that the LO of *Evittosphaerula paratabulata* (Manum et al., 1989) was coeval with this event at Hole 642D. However, the use of *E. paratabulata* as a regional marker may be problematic, as this species

is known to occur in the Norwegian Sea from the middle Oligocene upwards (Manum, 1976; 1979). No other indications for a hiatus were found in biostratigraphy and we therefore assume that sedimentation was continuous across this boundary. Our biostratigraphy-based age model for this section should be regarded as tentative only. Tie points were chosen that are consistent with available bioevents, while minimizing changes in sedimentation rate. Sedimentation rates above ~455.81 R-mbsf appear to have been higher (~20 m Myr<sup>-1</sup>) than below this depth (~5.7 m Myr<sup>-1</sup>). We include the top of C13n at 491.89 R-mbsf as a tie point to the Eocene-Oligocene age model for Hole 643A by Eldrett et al. (2004).

## 4.2 New bioevent ages and revised zonation

Our new age model (Fig. 4) allows a revised dating of bioevents at ODP Site 643. Bioevent ages are here derived from the mean depth between the lowest/highest sample with the presence of a species and the adjacent sample, in contrast to the bioevents previously used for constructing the age model. Revised ages for palynological samples are included in Table 3 and Table S6, while revised sample and bioevent ages for other microfossils can be obtained by applying our age model to stratigraphies of Donally (1989) (Calcareous nannofossils), Ciesielski et al. (1989) (Silicoflagellates), Spiegler and Jansen (1989) (Planktic foraminifera), Goll and Bjørklund (1989) (Radiolarians) and Osterman and Qvale (1989) (Benthic foraminifera). While the Shipboard Scientific Party (1987) included an initial diatom stratigraphy, adapted diatom events were presented by Ciesielski & Case (1989). Updated ages of bioevents initially used as broad constraints to interpret the magnetostratigraphy in this study are included in Table 1 and Fig. 5 (dinocysts only).

The integration of our new palynological results with palynostratigraphies of Manum et al. (1989) and Mudie (1989) leads to modifications to their dinocyst zonations. We therefore provisionally include a revised Oligocene-recent dinocyst zonation scheme (Table 3; Fig. 5). Here we only assess the occurrences of zonation boundary markers and refer to Manum et al. (1989) and Mudie (1989) for full discussions on zonation assemblages. Ages and depths for the following zones are updated based on this study and are depicted in Table 4.

### 4.2.1 *Islandinium minutum* - *Brigantedinium simplex* Zone

This zone follows the *Multispinula minuta* – *B. simplex* Zone of Mudie (1989), who defined the lower boundary by the LOs of *I. minutum* (as *M. minuta*) and *B. simplex*.

### 4.2.2 *Filisphaera filifera* - *Achomosphaera andalousiensis* Zone

This zone combines the *F. filifera* Zone and *A. andalousiensis* Zone of Mudie (1989), who defined the boundary between these zones by the LOs of *F. filifera* and *Tectatodinium pellitum* and the HO of *A. andalousiensis*. The determination of *T. pellitum* by Mudie (1989) has been questioned by Head (1994) and its LO may therefore not be applicable as a boundary marker. Both *F. filifera* and *T. pellitum* have been found to occur further downcore (Manum et al., 1989 and this study), while *A. andalousiensis* is found within the *F. filifera* Zone by Mudie (1989). The lower boundary is defined by HO of *U. aquaeductus*.

#### **4.2.3 *Unipontidinium aqueductus* - *Achromosphaera andalousiensis* Zone**

This zone combines the *Impagidinium aqueductum* Zone of Mudie (1989) and the *A. andalousiensis* Zone of Manum et al.

475 who defined the lower boundary by the LO of *A. andalousiensis*. The lower boundary is here redefined by the LPO of *A. andalousiensis*, to exclude the isolated and possibly questionable occurrence further downcore of Mudie (1989).

#### **4.2.4 *Unipontidinium aqueductus* Zone**

This zone mostly follows the *I. aqueductum* Zone of Manum et al. (1989), who defined the lower boundary by the LO of *U.*

*aquaeductus* (as *I. aqueductum*). The lower boundary is here redefined by the LPO of *U. aqueductus*, to exclude the

480 isolated occurrence further downcore of Mudie (1989).

#### **4.2.5 *Labyrinthodinium truncatum* - *Apteodinium spiridoides* Zone**

This zone combines the *L. truncatum* Zone and *Emslandia spiridoides* Zone of Manum et al. (1989), who defined the

boundary between these zones by the LO of *L. truncatum* and the HOs of *A. spiridoides* (as *E. spiridoides*) and

*Cribroperidinium tenuitabulatum* as substitute. *L. truncatum* (s.s.) has been found to occur further downcore (Mudie, 1989

485 and this study), and *A. spiridoides* and *C. tenuitabulatum* have been found to occur near the top of the *L. truncatum* Zone (this study). The lower boundary is defined by the HO of *Cordosphaeridium cantharellus*.

#### **4.2.6 *Impagidinium patulum* Zone**

This zone mostly follows the *I. patulum* Zone of Manum et al. (1989), who defined the lower boundary by the LO of *I.*

*patulum*. The lower boundary is here redefined by the LPO of *I. patulum*, to exclude the two isolated and possibly

490 questionable occurrences further downcore of this study.

#### **4.2.7 *Evittosphaerula paratabulata* Zone**

This zone mostly follows the *E. paratabulata* Zone of Manum et al. (1989), who defined the lower boundary by the LO of *E.*

*paratabulata*. The lower boundary is here redefined by the LPO of *E. paratabulata*, to exclude the isolated and questionable

occurrence further downcore of this study. We note that the use of *E. paratabulata* as a regional marker may be problematic,

495 as this species is known to occur in the Norwegian Sea from the middle Oligocene upwards (Manum, 1976; 1979).

#### **4.2.8 *Cyclopsiella lusatica* Zone**

This zone follows the *Ascostomocystis granosa* Zone of Manum et al. (1989), who defined the lower boundary by the LO of

the acritarch *C. lusatica* (as *A. granosa*) and the LO of *Invertocysta tabulata* as substitute.

#### **4.2.9 *Systematophora*? sp. 1 Zone**

500 This zone follows the *Systematophora* sp. 1 Zone of Manum et al. (1989), who defined the lower boundary by the LO of *Systematophora*? sp. 1. The genus is here considered questionable.

#### **4.2.10 *Leptodinium italicum* Zone**

This zone follows the *Impagidinium* sp. 1 Zone of Manum et al. (1989), who defined the lower boundary by the LO of *L. italicum* (as *Impagidinium* sp. 1).

505 **4.2.11 *Reticulatosphaera actinocoronata* Zone**

This zone follows the *Areosphaeridium?* *actinocoronatum* Zone of Manum et al. (1989), who defined the lower boundary by the HO of *Enneadocysta arcuata* (as *Areosphaeridium arcuatum*).

#### **4.2.12 *Chiropteridium lobospinosum* Zone**

510 This zone mostly follows the *C. lobospinosum* Zone of Manum et al. (1989), who defined the lower boundary by the LO of *C. lobospinosum*, but included one lower sample without marker species ‘by implication’. This sample, which is below the interval considered in this study, is here excluded from the *C. lobospinosum* Zone.

## **5 Conclusions**

We present an improved biomagnetostratigraphic age model for Oligocene-recent sediments of ODP Hole 643A, which is confirmed by  $^{40}\text{Ar}/^{39}\text{Ar}$  dating. Our revised age model is similar to the magnetostratigraphic interpretation of Bleil (1989) for 515 Pleistocene to upper Miocene sediments, but indicates a substantially older age (~1.5 Myr) for middle and lower Miocene sediments. We confirm and refine four major hiatuses of Goll (1989), dated at 1.80-2.52 Ma, 9.90-13.30 Ma, 14.29-14.53 Ma and 15.04-16.30 Ma. Sedimentation is otherwise mostly continuous although sedimentation rates vary. Based on the revised age model, we update ages of bioevents and dinocyst zonal boundaries at ODP Hole 643A, which can be used as stratigraphic backbone for other Nordic Sea sites.

520 **Data availability**

All raw data associated with this paper are available in the Supplementary Tables and will be stored in the PANGAEA database upon publication of the paper.

## **Sample availability**

Palynological slides processed for this study are stored in the collection of the Laboratory of Palaeobotany and Palynology,

525 Department of Earth Sciences, Utrecht University, The Netherlands.

## **Author contributions**

TJTV led the study and designed the research with FS and AS. TJTV, VBB and FS carried out the palynology. KFK performed  $^{40}\text{Ar}/^{39}\text{Ar}$  dating and wrote the sections on this. TJTV compiled, integrated and interpreted the data with input from FS, KFK and AS. TJTV wrote the paper with input from all authors.

## **530 Competing interests**

FS is a member of the editorial board of the journal. The other authors declare that they have no conflict of interest.

## **Acknowledgements**

This research used samples and data provided by the International Ocean Discovery Program (IODP) and its predecessors. AS thanks the European Research Council for Consolidator Grant 771497 entitled SPANC. This work was carried out under 535 the program of the Netherlands Earth System Science Centre (NESSC), financially supported by the Dutch Ministry of Education, Culture and Science. We thank Natasja Welters (Utrecht University) for laboratory assistance, Roel van Elsas (Vrije Universiteit Amsterdam) for his support with mineral separation and Chris van Baak (formerly Utrecht University; now CASP) and Martin Head (Brock University) for discussions.

## **References**

- 540 Amigo, A.E., 1999. Miocene silicoflagellate stratigraphy: Iceland and Rockall Plateaus, in: Raymo, M.E., Jansen, E., Blum, P., Herbert, T.D. (Eds.), Proceedings of the Ocean Drilling Program, Scientific Results, Vol. 162. Ocean Drilling Program, College Station, TX, USA, pp. 63–81. <https://doi.org/10.2973/odp.proc.sr.162.001.1999>
- Barron, J.A., Keller, G., Dunn, D.A., 1985a. A multiple microfossil biochronology for the Miocene, in: Kennett, J.P. (Ed.), The Miocene Ocean: Paleoceanography and Biogeography, Memoir 163. The Geological Society of America, Boulder, CO, 545 USA, pp. 21–36.
- Bijl, P.K., Houben, A.J.P., Bruls, A., Pross, J., Sangiorgi, F., 2018. Stratigraphic calibration of Oligocene–Miocene organic-walled dinoflagellate cysts from offshore Wilkes Land, East Antarctica, and a zonation proposal. *J. Micropalaeontology* 37, 105–138. <https://doi.org/10.5194/jm-37-105-2018>

- Bjørklund, K.R., 1976. Radiolaria from the Norwegian Sea, Leg 38 of the Deep Sea Drilling Project, in: Talwani, M., Udintsev, G. (Eds.), Initial Reports of the Deep Sea Drilling Project, Vol. 38. U.S. Government Printing Office, Washington, D.C., USA, pp. 1101–1168. <https://doi.org/10.2973/dsdp.proc.38.131.1976>
- Bleil, U., 1989. Magnetostratigraphy of Neogene and Quaternary sediment series from the Norwegian Sea: Ocean Drilling Program, Leg 104, in: Eldholm, O., Thiede, J., Taylor, E. (Eds.), Proceedings of the Ocean Drilling Program, Scientific Results, Vol. 104, Proceedings of the Ocean Drilling Program. Ocean Drilling Program, College Station, TX, USA, pp. 829–901. <https://doi.org/10.2973/odp.proc.sr.104.1989>
- Brinkhuis, H., Munsterman, D.K., Sengers, S., Sluijs, A., Warnaar, J., Williams, G.L., 2003. Late Eocene–Quaternary Dinoflagellate Cysts from ODP Site 1168, off Western Tasmania, in: Exxon, N.F., Kennett, J.P., Malone, M.J. (Eds.), Proceedings of the Ocean Drilling Program, Scientific Results, Vol. 189. Ocean Drilling Program, College Station, TX, USA, pp. 1–36. <https://doi.org/10.2973/odp.proc.sr.189.105.2003>
- Brunn, P., Dullo, W.-C., Hay, W.W., Frank, M., Kubik, P., 1998. Hiatuses on Vøring Plateau: sedimentary gaps or preservation artifacts? *Mar. Geol.* 145, 61–84. [https://doi.org/10.1016/S0025-3227\(97\)00111-4](https://doi.org/10.1016/S0025-3227(97)00111-4)
- Channell, J.E.T., Amigo, A.E., Fronval, T., Rack, F., Lehman, B., 1999. Magnetic stratigraphy at Sites 907 and 985 in the Norwegian-Greenland Sea and a revision of the Site 907 composite section, in: Raymo, M.E., Jansen, E., Blum, P., Herbert, T.D. (Eds.), Proceedings of the Ocean Drilling Program, Scientific Results, Vol. 162. Ocean Drilling Program, College Station, TX, USA, pp. 131–148. <https://doi.org/10.2973/odp.proc.sr.162.036.1999>
- Ciesielski, P.F., Case, S.M., 1989. Neogene Paleoceanography of the Norwegian Sea Based Upon Silicoflagellate Assemblage Changes in ODP Leg 104 Sedimentary Sequences, in: Eldholm, O., Thiede, J., Taylor, E. (Eds.), Proceedings of the Ocean Drilling Program, Scientific Results, Vol. 104. Ocean Drilling Program, College Station, TX, USA, pp. 527–541. <https://doi.org/10.2973/odp.proc.sr.104.166.1989>
- Ciesielski, P.F., Hasson, P., Turner Jr., J.W., 1989. The Stratigraphy of Neogene Silicoflagellates from the Norwegian Sea, ODP Leg 104, in: Eldholm, O., Thiede, J., Taylor, E. (Eds.), Proceedings of the Ocean Drilling Program, Scientific Results, Vol. 104. Ocean Drilling Program, College Station, TX, USA, pp. 497–525. <https://doi.org/10.2973/odp.proc.sr.104.164.1989>
- Cody, R.D., Levy, R.H., Harwood, D.M., Sadler, P.M., 2008. Thinking outside the zone: High-resolution quantitative diatom biochronology for the Antarctic Neogene. *Palaeogeogr. Palaeoclimatol. Palaeoecol.* 260, 92–121. <https://doi.org/10.1016/j.palaeo.2007.08.020>
- De Schepper, S., Beck, K.M., Mangerud, G., 2017. Late Neogene dinoflagellate cyst and acritarch biostratigraphy for Ocean Drilling Program Hole 642B, Norwegian Sea. *Rev. Palaeobot. Palynol.* 236, 12–32. <https://doi.org/10.1016/j.revpalbo.2016.08.005>
- De Schepper, S., Schreck, M., Beck, K.M., Matthiessen, J., Fahl, K., Mangerud, G., 2015. Early Pliocene onset of modern Nordic Seas circulation related to ocean gateway changes. *Nat. Commun.* 6, 8659. <https://doi.org/10.1038/ncomms9659>

- de Verteuil, L., Norris, G., 1996. Miocene Dinoflagellate Stratigraphy and Systematics of Maryland and Virginia. *Micropaleontology* 42 Suppl., 186. <https://doi.org/10.2307/1485926>
- Despraires, A., Maury, R.C., Joron, J.-L., Bohn, M., Tremblay, P., 1989. Distribution, Chemical Characteristics, and Origin of Ash Layers from ODP Leg 104, Vøring Plateau, North Atlantic, in: Eldholm, O., Thiede, J., Taylor, E. (Eds.), *Proceedings of the Ocean Drilling Program, Scientific Results*, Vol. 104. Ocean Drilling Program, College Station, TX, USA, pp. 337–356. <https://doi.org/10.2973/odp.proc.sr.104.120.1989>
- Dickens, G.R., Backman, J., 2013. Core alignment and composite depth scale for the lower Paleogene through uppermost Cretaceous interval at Deep Sea Drilling Project Site 577. *Newsletters Stratigr.* 46, 47–68. <https://doi.org/10.1127/0078-0421/2013/0027>
- Donnally, D.M., 1989. Calcareous Nannofossils of the Norwegian-Greenland Sea: ODP Leg 104, in: Eldholm, O., Thiede, J., Taylor, E. (Eds.), *Proceedings of the Ocean Drilling Program, Scientific Results*, Vol. 104. Ocean Drilling Program, College Station, TX, USA, pp. 459–486. <https://doi.org/10.2973/odp.proc.sr.104.156.1989>
- Dybkjær, K., Piasecki, S., 2010. Neogene dinocyst zonation for the eastern North Sea Basin, Denmark. *Rev. Palaeobot. Palynol.* 161, 1–29. <https://doi.org/10.1016/j.revpalbo.2010.02.005>
- Dzinoridze, R.N., Jousé, A.P., Koroleva-Golikova, G.S., Kozlova, G.E., Nagaeva, G.S., Petrushevskaya, M.G., Strelnikova, N.I., 1978. Diatom and Radiolarian Cenozoic Stratigraphy, Norwegian Basin; DSDP Leg 38, in: Talwani, M., Udistsev, G. (Eds.), *Initial Reports of the Deep Sea Drilling Project*, Vol. 38, 39, 40, 41 (Suppl.). U.S. Government Printing Office, Washington, D.C., USA, pp. 289–427. <https://doi.org/10.2973/dsdp.proc.38394041s.119.1978>
- Ehlers, B.-M., Jokat, W., 2013. Paleo-bathymetry of the northern North Atlantic and consequences for the opening of the Fram Strait. *Mar. Geophys. Res.* 34, 25–43. <https://doi.org/10.1007/s11001-013-9165-9>
- Eldrett, J.S., Harding, I.C., Firth, J. V., Roberts, A.P., 2004. Magnetostratigraphic calibration of Eocene–Oligocene dinoflagellate cyst biostratigraphy from the Norwegian–Greenland Sea. *Mar. Geol.* 204, 91–127. [https://doi.org/10.1016/S0025-3227\(03\)00357-8](https://doi.org/10.1016/S0025-3227(03)00357-8)
- Gascard, J.-C., Raisbeck, G., Sequeira, S., Yiou, F., Mork, K.A., 2004. The Norwegian Atlantic Current in the Lofoten basin inferred from hydrological and tracer data (129I) and its interaction with the Norwegian Coastal Current. *Geophys. Res. Lett.* 31, L01308. <https://doi.org/10.1029/2003GL018303>
- Goll, R.M., 1989. A Synthesis of Norwegian Sea Biostratigraphies: ODP Leg 104 on the Vøring Plateau, in: Eldholm, O., Thiede, J., Taylor, E. (Eds.), *Proceedings of the Ocean Drilling Program, Scientific Results*, Vol. 104. Ocean Drilling Program, College Station, TX, USA, pp. 777–826. <https://doi.org/10.2973/odp.proc.sr.104.203.1989>
- Goll, R.M., Bjørklund, K.R., 1989. A New Radiolarian Biostratigraphy for the Neogene of the Norwegian Sea: ODP Leg 104, in: Eldholm, O., Thiede, J., Taylor, E. (Eds.), *Proceedings of the Ocean Drilling Program, Scientific Results*, Vol. 104. Ocean Drilling Program, College Station, TX, USA, pp. 697–737. <https://doi.org/10.2973/odp.proc.sr.104.205.1989>
- Gradstein, F.M., Ogg, J.G., Schmitz, M.D., Ogg, G.M., 2012. *The Geologic Time Scale 2012*. Elsevier, Amsterdam, The Netherlands. <https://doi.org/10.1016/C2011-1-08249-8>

- Grøsfjeld, K., De Schepper, S., Fabian, K., Husum, K., Baranwal, S., Andreassen, K., Knies, J., 2014. Dating and palaeoenvironmental reconstruction of the sediments around the Miocene/Pliocene boundary in Yermak Plateau ODP Hole 911A using marine palynology. *Palaeogeogr. Palaeoclimatol. Palaeoecol.* 414, 382–402. <https://doi.org/10.1016/j.palaeo.2014.08.028>
- 620 Head, M.J., 1994. Morphology and Paleoenvironmental Significance of the Cenozoic Dinoflagellate Genera *Tectatodinium* and *Habibacysta*. *Micropaleontology* 40, 289–321. <https://doi.org/10.2307/1485937>
- Henrich, R., 1989. Diagenetic Environments of Authigenic Carbonates and Opal-CT Crystallization in Lower Miocene to Upper Oligocene Deposits of the Norwegian Sea (ODP Site 643, Leg 104), in: Eldholm, O., Thiede, J., Taylor, E. (Eds.), *Proceedings of the Ocean Drilling Program, Scientific Results, Vol. 104. Ocean Drilling Program, College Station, TX, USA*, pp. 233–247. <https://doi.org/10.2973/odp.proc.sr.104.119.1989>
- 625 Hull, D.M., Osterman, L.E., Thiede, J., 1996. Biostratigraphic Synthesis of Leg 151, North Atlantic-Arctic Gateways, in: Thiede, J., Myhre, A.M., Firth, J. V., Johnson, G.L., Ruddiman, W.F. (Eds.), *Proceedings of the Ocean Drilling Program, Scientific Results, Vol. 151. Ocean Drilling Program, College Station, TX, USA*, pp. 627–644. <https://doi.org/10.2973/odp.proc.sr.151.146.1996>
- 630 Jakobsson, M., Backman, J., Rudels, B., Nylander, J., Frank, M., Mayer, L., Jokat, W., Sangiorgi, F., O'Regan, M., Brinkhuis, H., King, J., Moran, K., 2007. The early Miocene onset of a ventilated circulation regime in the Arctic Ocean. *Nature* 447, 986–990. <https://doi.org/10.1038/nature05924>
- Koç, N., Scherer, R.P., 1996. Neogene Diatom Biostratigraphy of the Iceland Sea Site 907, in: Thiede, J., Myhre, A.M., Firth, J. V., Johnson, G.L., Ruddiman, W.F. (Eds.), *Proceedings of the Ocean Drilling Program, Scientific Results, Vol. 151. Ocean Drilling Program, College Station, TX, USA*, pp. 61–74. <https://doi.org/10.2973/odp.proc.sr.151.108.1996>
- 635 Koppers, A.A.P., 2002. ArArCALC—software for  $^{40}\text{Ar}/^{39}\text{Ar}$  age calculations. *Comput. Geosci.* 28, 605–619. [https://doi.org/10.1016/S0098-3004\(01\)00095-4](https://doi.org/10.1016/S0098-3004(01)00095-4)
- Kuiper, K.F., Deino, A., Hilgen, F.J., Krijgsman, W., Renne, P.R., Wijbrans, J.R., 2008. Synchronizing Rock Clocks of Earth History. *Science* (80-. ). 320, 500–504. <https://doi.org/10.1126/science.1154339>
- 640 Lazarus, D., Barron, J.A., Renaudie, J., Diver, P., Türke, A., 2014. Cenozoic Planktonic Marine Diatom Diversity and Correlation to Climate Change. *PLoS One* 9, e84857. <https://doi.org/10.1371/journal.pone.0084857>
- Lee, J.-Y., Marti, K., Severinghaus, J.P., Kawamura, K., Yoo, H.-S., Lee, J.B., Kim, J.S., 2006. A redetermination of the isotopic abundances of atmospheric Ar. *Geochim. Cosmochim. Acta* 70, 4507–4512. <https://doi.org/10.1016/j.gca.2006.06.1563>
- 645 Lisiecki, L.E., Herbert, T.D., 2007. Automated composite depth scale construction and estimates of sediment core extension. *Paleoceanography* 22, PA4213. <https://doi.org/10.1029/2006PA001401>
- Locker, S., 1996. Cenozoic Siliceous Flagellates from the Fram Strait and the East Greenland Margin: Biostratigraphic and Paleoceanographic Results, in: Thiede, J., Myhre, A.M., Firth, J. V., Johnson, G.L., Ruddiman, W.F. (Eds.), *Proceedings of*

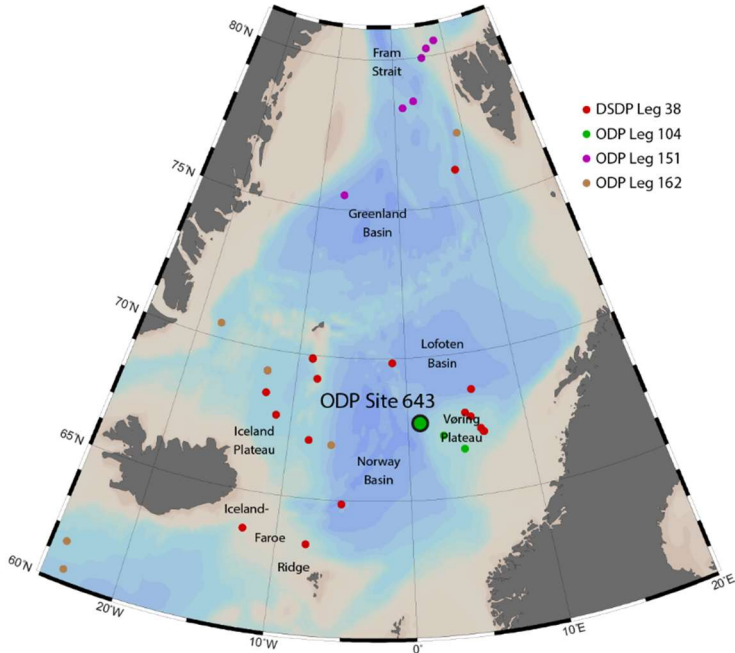
- the Ocean Drilling Program, Scientific Results, Vol. 151. Ocean Drilling Program, College Station, TX, USA, pp. 101–124.
- 650 https://doi.org/10.2973/odp.proc.sr.151.102.1996
- Locker, S., Martini, E., 1989. Cenozoic Silicoflagellates, Ebriidians, and Actiniscidians from the Vøring Plateau (ODP Leg 104), in: Eldholm, O., Thiede, J., Taylor, E. (Eds.), Proceedings of the Ocean Drilling Program, Scientific Results, Vol. 104. Ocean Drilling Program, College Station, TX, USA, pp. 543–585. https://doi.org/10.2973/odp.proc.sr.104.204.1989
- Lucchi, F., 2019. On the use of unconformities in volcanic stratigraphy and mapping: Insights from the Aeolian Islands (southern Italy). *J. Volcanol. Geotherm. Res.* 385, 3–26. https://doi.org/10.1016/j.jvolgeores.2019.01.014
- 655 Manum, S.B., Boulter, M.C., Gunnarsdottir, H., Rangnes, K., Scholze, A., 1989. Eocene to Miocene Palynology of the Norwegian Sea (ODP Leg 104), in: Eldholm, O., Thiede, J., Taylor, E. (Eds.), Proceedings of the Ocean Drilling Program, Scientific Results, Vol. 104. Ocean Drilling Program, College Station, TX, USA, pp. 611–662. https://doi.org/10.2973/odp.proc.sr.104.176.1989
- 660 Manum, S.B., 1976. Dinocysts in Tertiary Norwegian-Greenland Sea Sediments (Deep Sea Drilling Project Leg 38), with Observations on Palynomorphs and Palynodebris in Relation to Environment, in: Talwani, M., Udintsev, G. (Eds.), Initial Reports of the Deep Sea Drilling Project, Vol. 38. U.S. Government Printing Office, Washington, D.C., USA, pp. 897–919. https://doi.org/10.2973/dsdp.proc.38.129.1976
- Manum, S.B., 1979. Two new Tertiary dinocyst genera from the Norwegian Sea: *Lophocysta* and *Evittosphaerula*. *Rev. Palaeobot. Palynol.* 28, 237–248. https://doi.org/10.1016/0034-6667(79)90026-5
- 665 Martini, E., Müller, C., 1976. Eocene to Pleistocene Silicoflagellates from the Norwegian-Greenland Sea (DSDP Leg 38), in: Talwani, M., Udintsev, G. (Eds.), Initial Reports of the Deep Sea Drilling Project, Vol. 38. U.S. Government Printing Office, Washington, D.C., USA, pp. 857–895. https://doi.org/10.2973/dsdp.proc.38.128.1976
- Matthiessen, J., Knies, J., Vogt, C., Stein, R., 2009. Pliocene palaeoceanography of the Arctic Ocean and subarctic seas.
- 670 Philos. Trans. R. Soc. A Math. Phys. Eng. Sci. 367, 21–48. https://doi.org/10.1098/rsta.2008.0203
- Min, K., Mundil, R., Renne, P.R., Ludwig, K.R., 2000. A test for systematic errors in  $^{40}\text{Ar}/^{39}\text{Ar}$  geochronology through comparison with U/Pb analysis of a 1.1-Ga rhyolite. *Geochim. Cosmochim. Acta* 64, 73–98. https://doi.org/10.1016/S0016-7037(99)00204-5
- Mudie, P.J., 1989. Palynology and Dinocyst Biostratigraphy of the Late Miocene to Pleistocene, Norwegian Sea: ODP Leg 104, Sites 642 to 644, in: Eldholm, O., Thiede, J., Taylor, E. (Eds.), Proceedings of the Ocean Drilling Program, Scientific Results, Vol. 104. Ocean Drilling Program, College Station, TX, USA, pp. 587–610. https://doi.org/10.2973/odp.proc.sr.104.174.1989
- Müller-Michaelis, A., Uenzelmann-Neben, G., 2014. Development of the Western Boundary Undercurrent at Eirik Drift related to changing climate since the early Miocene. *Deep. Res. Part I Oceanogr. Res. Pap.* 93, 21–34.
- 680 https://doi.org/10.1016/j.dsr.2014.07.010
- Murphy, M.A., Salvador, A., 1988. Unconformity-bounded stratigraphic units: Discussion and reply. *Geol. Soc. Am. Bull.* 100, 155–156. https://doi.org/10.1130/0016-7606(1988)100<0155:UBSUDA>2.3.CO;2

- Newton, A.M.W., Huuse, M., Brocklehurst, S.H., 2018. A Persistent Norwegian Atlantic Current Through the Pleistocene Glacials. *Geophys. Res. Lett.* 45, 5599–5608. <https://doi.org/10.1029/2018GL077819>
- 685 Ogg, J.G., 2012. Geomagnetic Polarity Time Scale, in: Gradstein, F.M., Ogg, J.G., Schmitz, M.D., Ogg, G.M. (Eds.), *The Geologic Time Scale 2012*. Elsevier, Amsterdam, The Netherlands, pp. 85–113. <https://doi.org/10.1016/B978-0-444-59425-9.00005-6>
- Osterman, L.E., Qvale, G., 1989. Benthic Foraminifers from the Vøring Plateau (ODP Leg 104), in: Eldholm, O., Thiede, J., Taylor, E. (Eds.), *Proceedings of the Ocean Drilling Program, Scientific Results, Vol. 104*. Ocean Drilling Program, College 690 Station, TX, USA, pp. 745–768. <https://doi.org/10.2973/odp.proc.sr.104.159.1989>
- Pälike, H., Lyle, M., Nishi, H., Raffi, I., Gamage, K., Klaus, A., the Expedition 320/321 Scientists, 2010. *Proceedings of the Integrated Ocean Drilling Program, vol. 320/321*. Integrated Ocean Drilling Program Management International, Inc., Tokyo, Japan.
- Parker, W.C., Feldman, A., Arnold, A.J., 1999. Paleobiogeographic patterns in the morphologic diversification of the 695 Neogene planktonic foraminifera. *Palaeogeogr. Palaeoclimatol. Palaeoecol.* 152, 1–14. [https://doi.org/10.1016/S0031-0182\(99\)00049-8](https://doi.org/10.1016/S0031-0182(99)00049-8)
- Phillips, D., Matchan, E.L., 2013. Ultra-high precision  $^{40}\text{Ar}/^{39}\text{Ar}$  ages for Fish Canyon Tuff and Alder Creek Rhyolite sanidine: New dating standards required? *Geochim. Cosmochim. Acta* 121, 229–239. <https://doi.org/10.1016/j.gca.2013.07.003>
- 700 Piasecki, S., 2003. Neogene dinoflagellate cysts from Davis Strait, offshore West Greenland. *Mar. Pet. Geol.* 20, 1075–1088. [https://doi.org/10.1016/S0264-8172\(02\)00089-2](https://doi.org/10.1016/S0264-8172(02)00089-2)
- Poulsen, N.E., Manum, S.B., Williams, G.L., Ellegaard, M., 1996. Tertiary Dinoflagellate Biostratigraphy of Sites 907, 908, and 909 in the Norwegian-Greenland Sea, in: Thiede, J., Myhre, A.M., Firth, J. V., Johnson, G.L., Ruddiman, W.F. (Eds.), *Proceedings of the Ocean Drilling Program, Scientific Results, Vol. 151*. Ocean Drilling Program, College Station, TX, 705 USA, pp. 255–287. <https://doi.org/10.2973/odp.proc.sr.151.110.1996>
- Raymo, M.E., Jansen, E., Blum, P., Herbert, T.D., 1999. *Proceedings of the Ocean Drilling Program, Scientific Results, vol. 162*. Ocean Drilling Program, College Station, TX, USA.
- Ruban, D.A., 2015. Worldwide application of synthem stratigraphy in the 21st century: a bibliographical survey. *Proc. Geol. Assoc.* 126, 307–313. <https://doi.org/10.1016/j.pgeola.2015.03.008>
- 710 Salvador, A., 1987. Unconformity-bounded stratigraphic units. *Geol. Soc. Am. Bull.* 98, 232–237. [https://doi.org/10.1130/0016-7606\(1987\)98<232:USU>2.0.CO;2](https://doi.org/10.1130/0016-7606(1987)98<232:USU>2.0.CO;2)
- Sant, K., Mandic, O., Rundić, L., Kuiper, K.F., Krijgsman, W., 2018. Age and evolution of the Serbian Lake System: integrated results from Middle Miocene Lake Popovac. *Newsletters Stratigr.* 51, 117–143. <https://doi.org/10.1127/nos/2016/0360>
- 715 Schlitzer, R., 2016. Ocean Data View. <https://odv.awi.de>.

- Schrader, H.-J., Fenner, J., 1976. Norwegian Sea Cenozoic Diatom Biostratigraphy and Taxonomy, in: Talwani, M., Udintsev, G. (Eds.), Initial Reports of the Deep Sea Drilling Project, Vol. 38. U.S. Government Printing Office, Washington, D.C., USA, pp. 921–1099. <https://doi.org/10.2973/dsdp.proc.38.130.1976>
- Schrader, H.-J., Bjørklund, K.R., Manum, S.B., Martini, E., van Hinte, J., 1976. Cenozoic Biostratigraphy, Physical  
720 Stratigraphy and Paleoceanography in the Norwegian-Greenland Sea, DSDP Leg 38 Paleontological Synthesis, in: Talwani, M., Udintsev, G. (Eds.), Initial Reports of the Deep Sea Drilling Project, Vol. 38. U.S. Government Printing Office, Washington, D.C., USA, pp. 1197–1211. <https://doi.org/10.2973/dsdp.proc.38.133.1976>
- Schreck, M., Matthiessen, J., Head, M.J., 2012. A magnetostratigraphic calibration of Middle Miocene through Pliocene dinoflagellate cyst and acritarch events in the Iceland Sea (Ocean Drilling Program Hole 907A). *Rev. Palaeobot. Palynol.*  
725 187, 66–94. <https://doi.org/10.1016/j.revpalbo.2012.08.006>
- Shipboard Scientific Party, 1987. Site 643: Norwegian Sea, in: Eldholm, O., Thiede, J., Taylor, E. (Eds.), Proceedings of the Ocean Drilling Program, Initial Reports, Vol. 104. Ocean Drilling Program, College Station, TX, USA, pp. 455–615. <https://doi.org/10.2973/odp.proc.ir.104.105.1987>
- Smelror, M., 1999. Pliocene–Pleistocene and redeposited dinoflagellate cysts from the western Svalbard margin (Site 986):  
730 biostratigraphy, paleoenvironments, and sediment provenance, in: Raymo, M.E., Jansen, E., Blum, P., Herbert, T.D. (Eds.), Proceedings of the Ocean Drilling Program, Scientific Results, Vol. 162. Ocean Drilling Program, College Station, TX, USA, pp. 83–97. <https://doi.org/10.2973/odp.proc.sr.162.011.1999>
- Spiegler, D., Jansen, E., 1989. Planktonic Foraminifer Biostratigraphy of Norwegian Sea Sediments: ODP Leg 104, in: Eldholm, O., Thiede, J., Taylor, E. (Eds.), Proceedings of the Ocean Drilling Program, Scientific Results, Vol. 104. Ocean  
735 Drilling Program, College Station, TX, USA, pp. 681–696. <https://doi.org/10.2973/odp.proc.sr.104.157.1989>
- Vallé, F., Westerhold, T., Dupont, L.M., 2017. Orbital-driven environmental changes recorded at ODP Site 959 (eastern equatorial Atlantic) from the Late Miocene to the Early Pleistocene. *Int. J. Earth Sci.* 106, 1161–1174. <https://doi.org/10.1007/s00531-016-1350-z>
- Verhoeven, K., Louwey, S., Eiríksson, J., De Schepper, S., 2011. A new age model for the Pliocene–Pleistocene Tjörnes  
740 section on Iceland: Its implication for the timing of North Atlantic–Pacific palaeoceanographic pathways. *Palaeogeogr. Palaeoclimatol. Palaeoecol.* 309, 33–52. <https://doi.org/10.1016/j.palaeo.2011.04.001>
- Wilkins, R.H., Dickens, G.R., Tian, J., Backman, J., the Expedition 320/321 Scientists, 2013. Data report: revised composite depth scales for Sites U1336, U1337, and U1338, in: Pälike, H., Lyle, M.W., Nishi, H., Raffi, I., Gamage, K., Klaus, A., the  
745 Expedition 320/321 Scientists (Eds.), Proceedings of the Integrated Ocean Drilling Program, Vol. 320/321. Integrated Ocean Drilling Program Management International, Inc., Tokyo, Japan, p. 158. <https://doi.org/10.2204/iodp.proc.320321.209.2013>
- Williams, G.L., Fensome, R.A., MacRae, R.A., 2017. The Lentin and Williams index of fossil dinoflagellates 2017 edition. *Am. Assoc. Stratigr. Palynol. Contrib. Ser.* 48.

- Williams, G.L., Manum, S.B., 1999. Oligocene–early Miocene dinocyst stratigraphy of Hole 985A (Norwegian Sea), in: Raymo, M.E., Jansen, E., Blum, P., Herbert, T.D. (Eds.), Proceedings of the Ocean Drilling Program, Scientific Results, Vol. 162. Ocean Drilling Program, College Station, TX, USA, pp. 99–109. <https://doi.org/10.2973/odp.proc.sr.162.030.1999>
- Wright, J.D., Miller, K.G., 1996. Control of North Atlantic Deep Water Circulation by the Greenland-Scotland Ridge. *Paleoceanography* 11, 157–170. <https://doi.org/10.1029/95PA03696>
- Yanagisawa, Y., Akiba, F., 1990. Taxonomy and phylogeny of the three marine diatom genera, Crucidenticula, Denticulopsis and Neodenticula. *Bull. Geol. Surv. Japan* 41, 197–301.

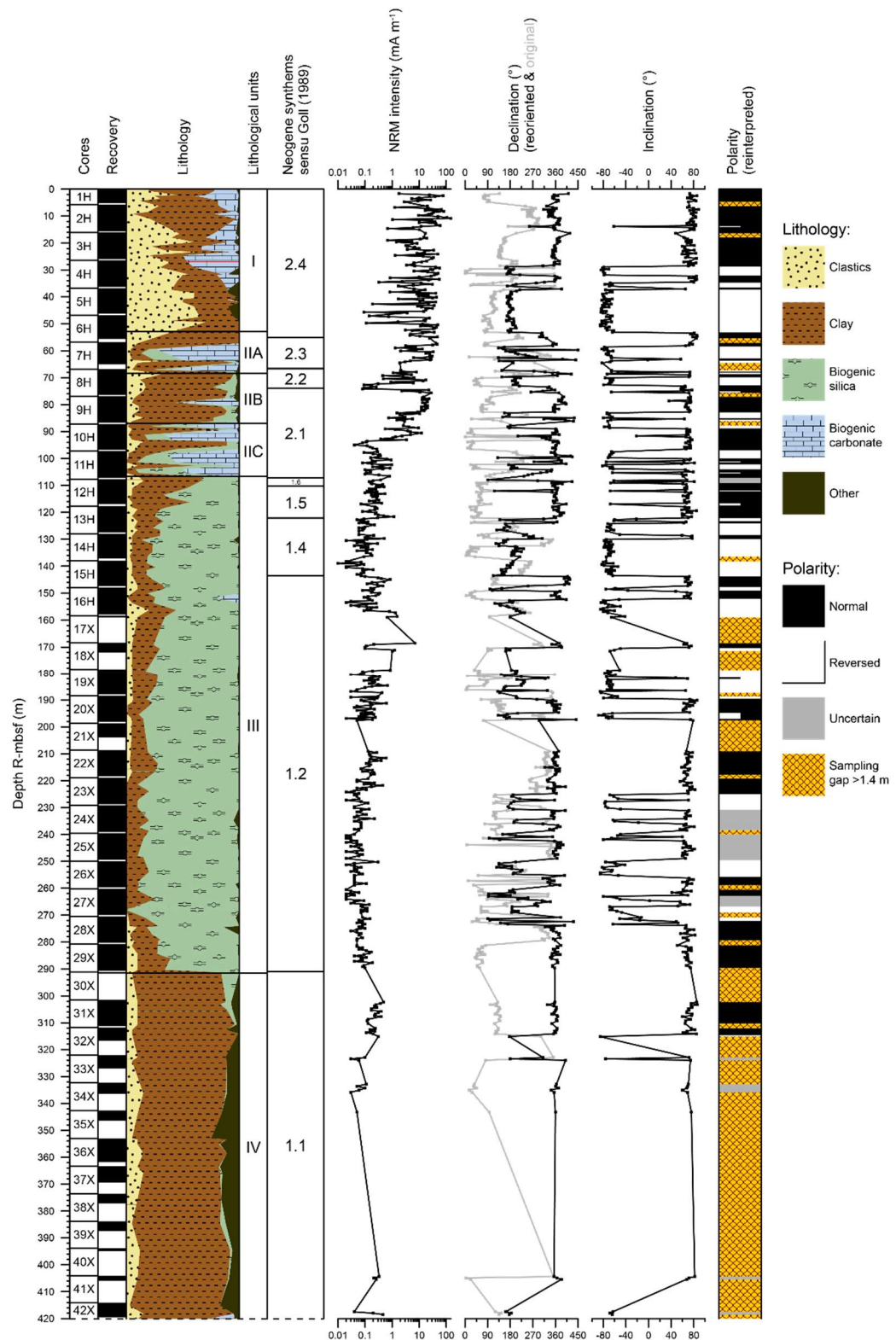
- Zegarra, M., Helenes, J., 2011. Changes in Miocene through Pleistocene dinoflagellates from the Eastern Equatorial Pacific (ODP Site 1039), in relation to primary productivity. *Mar. Micropaleontol.* 81, 107–121. <https://doi.org/10.1016/j.marmicro.2011.09.005>



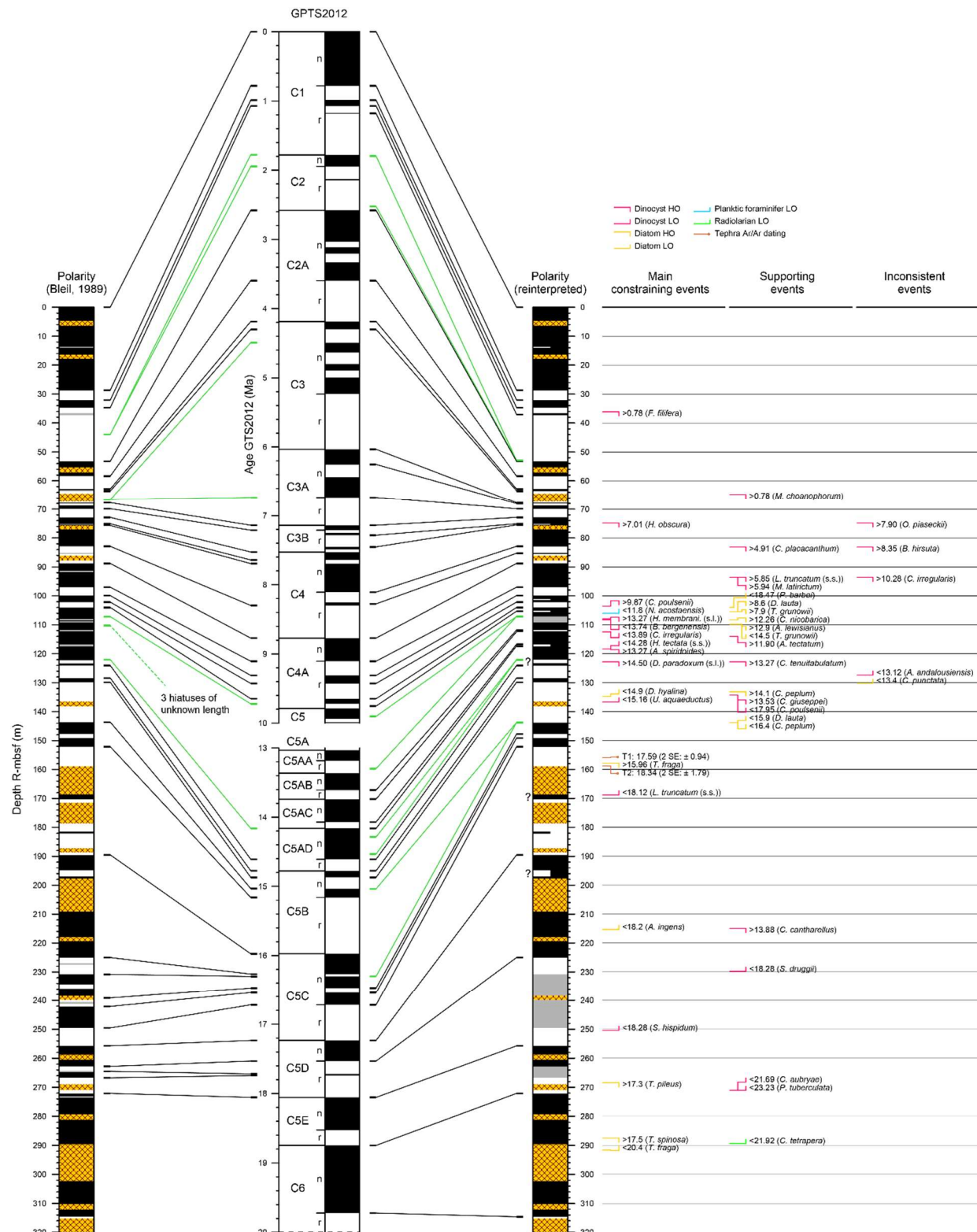
760 **Figure 1: Map of the modern Nordic Seas with the location of ODP Site 643 and other DSDP and ODP Sites. Map generated with Ocean Data View (Schlitzer, 2016).**

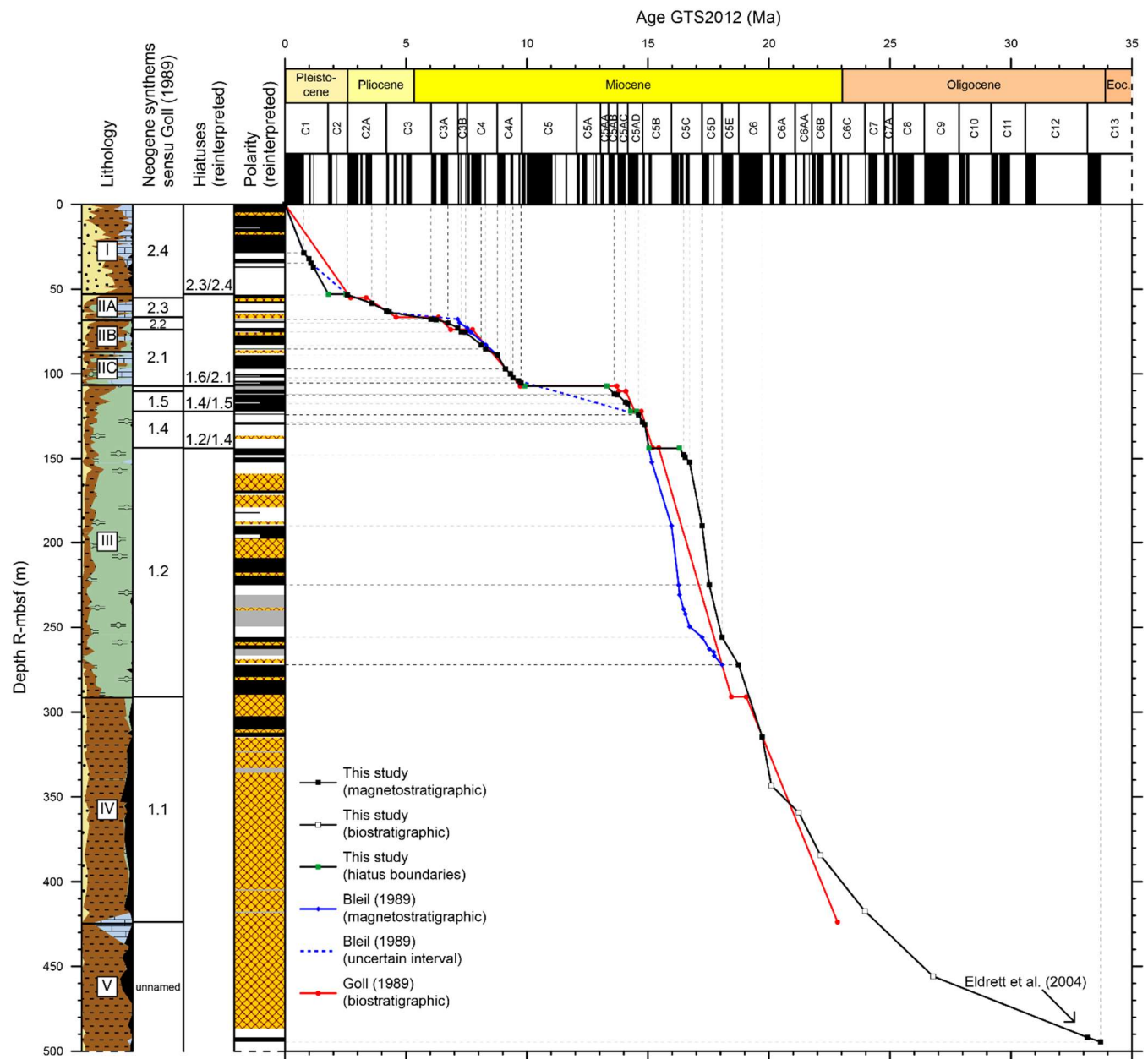
**Figure 2: Recovery, lithology, synthems and polarity interpretation of ODP Hole 643A for the interval with paleomagnetic data.**  
Recovery and lithology from the Shipboard Scientific Party (1987) (data available in Tables S1 and S2). Synthems according to  
Goll (1989). Original paleomagnetic data from Bleil (1989), with azimuthally reoriented declination and reinterpretation of the  
polarity signal from this study (data available in Table S12).

765



**Figure 3: Correlation of the paleomagnetic polarity signal to GPTS2012, with constraining ages (GTS2012, in Ma) of bioevents and  $^{40}\text{Ar}/^{39}\text{Ar}$  dating (data available in Tables 1 and 2 and Tables S11 and S12). Bioevents are indicated at the depth of the lowest/highest sample with the presence of a species and ages indicate the global FAD/LAD (see sect. 2.4). Question marks indicate unexplained subchrons or excursions. Colours used for the polarity record are explained in Fig. 2. The correlation of Bleil (1989), updated to GPTS2012, is displayed for comparison.**

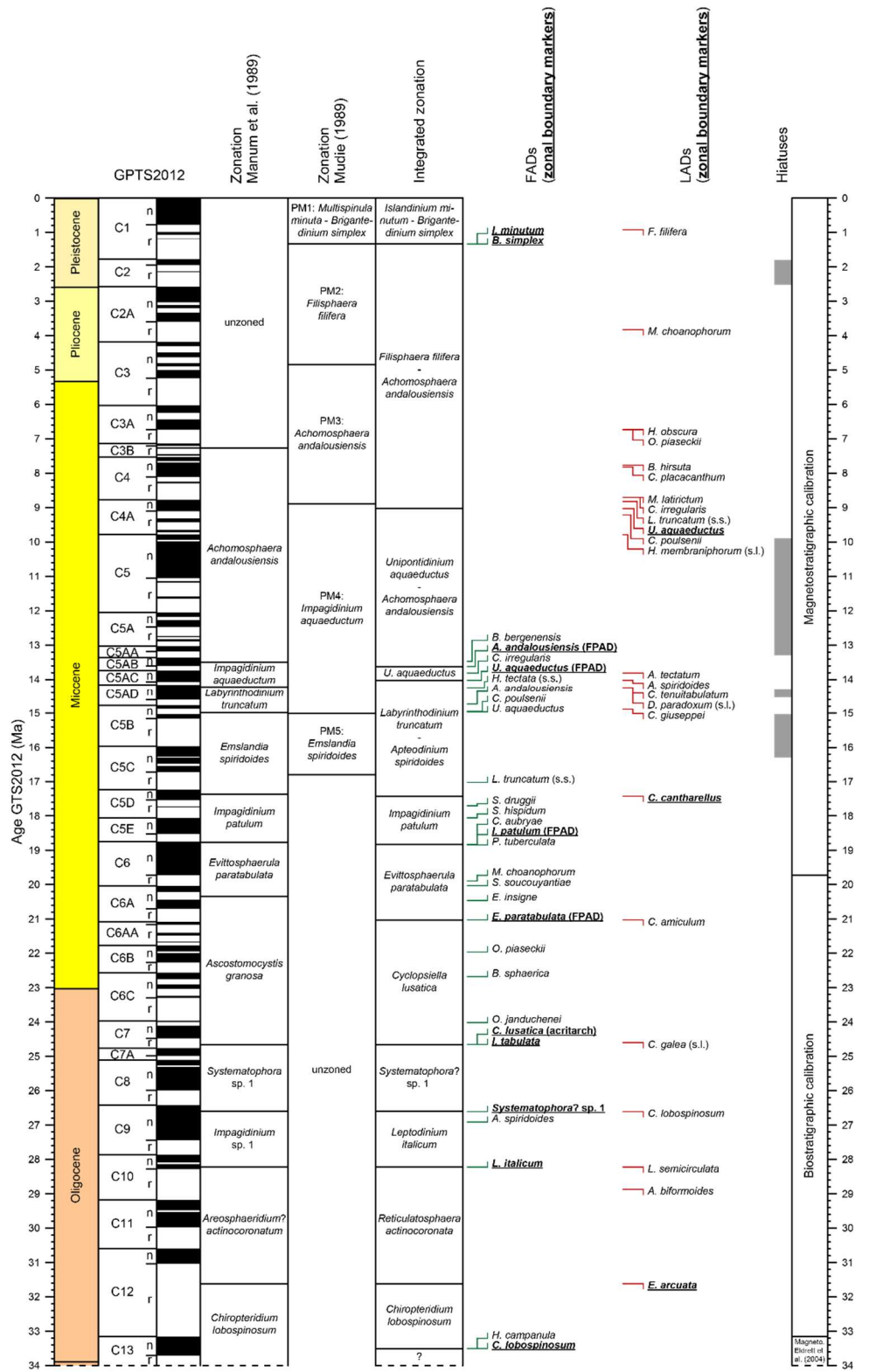




775

**Figure 4:** Age-depth plots for Oligocene to Recent sediments of ODP Hole 643A. Colours used for the lithology and the polarity record are explained in Fig. 2. Magnetostriatigraphic tie points of Bleil (1989) are directly linked to GPTS2012 and tie points of Goll (1989) were updated to GTS2012 using linear interpolation between rescaled magnetic reversals.

780 **Figure 5: Revised dinocyst bioevents and zonation of ODP Hole 643A, based on integration of new dinocyst counts with those of**  
**Manum et al. (1989) and Mudie (1989), calibrated to GTS2012 with the revised age model (data available in Tables 1, 3 and 4).**  
**Bioevent ages are derived from the mean depth between the lowest/highest sample with the presence of a species and the adjacent**  
**sample.**



785 **Table 1: Bioevents used for constraining the biomagnetostratigraphic interpretation.** TS = This study, Ma = Manum et al. (1989),  
Mu = Mudie (1989), CC = Ciesielski and Case (1989), SP = Shipboard Scientific Party (1987), GB = Goll and Bjørklund (1989).  
Taxonomic and stratigraphic comments are listed in Tables S7 and S8. Sample depths are indicated by their top depth. References  
for global FADs and LADs are listed in Tables S9 and S10. Global FADs and LADs in bold are considered consistent with the  
revised age model, while those in italics are inconsistent.

Species reported by:

Event

Species

			Upper sample		Lower sample		Upper sample (rbmsf)		Lower sample (rbmsf)		Upper sample (rbmsf)		Lower sample (rbmsf)		Mean depth (rbmsf)		LO/HO depth (rbmsf)		Global FAD/LAD (Ma)		Revised age at LO/HO depth (Ma)		Revised age at mean depth (Ma)		Comments in Table:				
TS, Ma, Mu	Dc	Microfossil																											
TS, Ma, Mu	Dc	LAD	<i>Filisphaera filifera</i>	3H	CC	W 18-20	4H	CC	W 9-11	24,610	33,980	25,920	36,120	31,020	36,120	0.78	1.14	0.92	Magn.										
TS, Ma, Mu	Dc	LAD	<i>Melitasphaeridium choanophorum</i>	6H	CC	W 7-9	7H	CC	W 7-9	51,890	60,760	55,440	64,810	60,125	64,810	0.78	4.80	3.82	Magn.										
TS, Ma, Mu	Dc	LAD	<i>Labyrinthodinium truncatum</i> (s.s.)	9H	CC	W 30-32	10H	5	W 31-33	81,640	87,610	86,690	93,570	90,130	93,570	5.85	8.96	8.82	Magn.										
TS, Ma, Mu	Dc	LAD	<i>Hystriochospaeropsis obscura</i>	7H	CC	W 25-27	8H	6	W 48-50	60,940	70,280	64,990	74,830	69,910	74,830	7.01	7.27	6.74	Magn.										
TS, Ma, Mu	Dc	LAD	<i>Operculodinium piaseckii</i>	7H	CC	W 25-27	8H	6	W 48-50	60,940	70,280	64,990	74,830	69,910	74,830	7.90	7.27	6.74	Magn.	S7									
TS, Ma, Mu	Dc	LAD	<i>Cleistosphaeridium placacanthum</i>	8H	CC	W 28-30	9H	5	W 30-32	71,580	78,100	76,130	83,150	79,640	83,150	4.91	8.12	7.82	Magn.	S7									
TS, Ma	Dc	LAD	<i>Batiacapsphaera hirsuta</i>	8H	6	W 48-50	9H	5	W 30-32	70,280	78,100	74,830	83,150	78,990	83,150	8.35	8.12	7.76	Magn.	S7									
TS, Ma	Dc	LAD	<i>Minisphaeridium latirictum</i>	9H	5	W 30-32	10H	5	W 31-33	78,100	87,610	83,150	93,570	88,360	93,570	5.94	8.96	8.71	Magn.										
TS, Ma	Dc	LAD	<i>Cerebrocysta irregularis</i>	9H	5	W 30-32	10H	5	W 31-33	78,100	87,610	83,150	93,570	88,360	93,570	10.28	8.96	8.71	Magn.	S7									
TS, Ma	Dc	LAD	<i>Cerebrocysta poulsenii</i>	10H	5	W 31-33	11H	5	W 30-32	87,610	97,100	93,570	103,580	98,575	103,580	9.87	9.59	9.21	Magn.	S7									
CC	D	FAD	<i>Proboscia barbii</i>	11H	5	W 70-72	11H	6	W 70-72	97,500	99,000	103,980	105,480	104,730	103,980	18.47	9.64	9.70	Magn.										
CC	D	LAD	<i>Thalassiosira grunowii</i>	11H	5	W 70-72	11H	6	W 70-72	97,500	99,000	103,980	105,480	104,730	105,480	8.6	9.76	9.70	Magn.										
CC	PF	FAD	<i>Neogloboquadra acostaensis</i>	11H	6	W 130-136	?			99,600	?	106,080	?	106,080	106,080	11.8	9.81	9.81	Magn.										
TS, Ma	Dc	LAD	<i>Hystriostrogylion membraniphorum</i> (s.l.)	11H	5	W 30-32	12H	1	W 31-33	97,100	100,610	103,580	107,990	105,785	107,990	13.27	13.35	9.79	Magn.										
TS	Dc	FAD	<i>Batiacapsphaera bergenensis</i>	12H	1	W 62-64	12H	3	W 62-64	100,920	103,920	108,300	111,300	109,800	108,300	13.74	13.37	13.47	Magn.										
CC	D	LAD	<i>Crucidenticula nicobarica</i>	11H	6	W 70-72	12H	1	W 70-72	99,000	101,000	105,480	108,380	106,930	108,380	12.26	13.38	9.88	Magn.										
CC	D	LAD	<i>Araniscus lewisiensis</i>	11H	4C	W 46-49	12H	2	W 70-72	100,670	102,500	107,150	109,880	108,515	109,880	12.9	13.48	13.39	Magn.										
CC	D	FAD	<i>Thalassiosira grunowii</i>	12H	2	W 70-72	12H	3	W 70-72	102,500	104,000	109,880	111,380	110,630	109,880	14.5	13.48	13.53	Magn.										
TS, Ma	Dc	FAD	<i>Cerebrocysta irregularis</i>	12H	4	W 31-33	12H	5	W 31-33	105,110	106,610	112,490	113,990	113,240	112,490	13.89	13.76	13.81	Magn.										
TS, Ma	Dc	LAD	<i>Aptedionium tectatum</i>	12H	4	W 31-33	12H	5	W 31-33	105,110	106,610	112,490	113,990	113,240	113,990	11.90	13.87	13.81	Magn.	S7									
TS, Ma, Mu	Dc	LAD	<i>Aptedionium spinoides</i>	12H	5	W 31-33	13H	1	W 64-66	106,610	110,440	113,990	118,320	116,155	118,320	13.27	14.19	14.03	Magn.										
TS	Dc	FAD	<i>Habibacysta tectata</i> (s.s.)	13H	1	W 64-66	13H	4	W 62-64	110,440	114,920	118,320	122,800	120,560	118,320	14.28	14.19	14.25	Magn.										
TS, Ma	Dc	LAD	<i>Cribroperdinium tenuitabulatum</i>	13H	1	W 64-66	13H	4	W 62-64	110,440	114,920	118,320	122,800	120,560	122,800	13.27	14.56	14.25	Magn.										
TS, Ma, Mu	Dc	LAD	<i>Distatodinium paradoxum</i> (s.l.)	13H	1	W 64-66	13H	4	W 62-64	110,440	114,920	118,320	122,800	120,560	122,800	14.50	14.56	14.25	Magn.										
TS, Ma, Mu	Dc	FAD	<i>Achromosphaera andalusiensis</i>	13H	CC	W 20-22	13H	CC	W 28-30	119,520	119,600	127,400	127,480	127,440	127,400	13.12	14.74	14.74	Magn.	S7									
CC	D	FAD	<i>Crucidenticula punctata</i>	14H	2	W 70-72	14H	3	W 70-72	121,500	123,000	130,200	131,700	130,950	130,200	13.4	14.87	14.88	Magn.	S8									
CC	D	LAD	<i>Cestodiscus peplum</i>	14H	3	W 70-72	14H	4	W 70-72	123,000	124,500	131,700	133,200	132,450	133,200	14.1	14.91	14.90	Magn.										
TS, Ma	Dc	FAD	<i>Cribroperdinium giuseppei</i>	14H	1	W 68-70	14H	5	W 32-34	119,980	125,620	128,680	134,320	131,500	134,320	13.53	14.92	14.89	Magn.										
TS, Ma	Dc	FAD	<i>Cerebrocysta poulsenii</i>	14H	5	W 32-34	15H	1	W 68-70	125,620	128,480	134,320	138,680	136,500	134,320	17.95	14.92	14.95	Magn.										
CC	D	FAD	<i>Denticulopsis hyalina</i>	14H	5	W 70-72	14H	6	W 70-72	126,000	127,500	134,700	136,200	135,450	134,700	14.9	14.93	14.94	Magn.	S8									
TS, Ma, Mu	Dc	FAD	<i>Unipontidinium aquaeductus</i>	14H	CC	W 12-14	15H	1	W 68-70	128,040	129,480	136,740	138,680	137,710	136,740	15.16	14.95	14.96	Magn.										
CC	D	FAD	<i>Denticulopsis lauta</i>	15H	4	W 127-129	15H	5	W 71-73	134,570	135,510	143,770	144,710	144,240	143,770	15.9	15.04	16.32	Magn.										
CC	D	FAD	<i>Cestodiscus peplum</i>	15H	4	W 127-129	15H	5	W 71-73	134,570	135,510	143,770	144,710	144,240	143,770	16.4	15.04	16.32	Magn.										
SP	D	LAD	<i>Thalassiosira fraga</i>	15H	CC	W 39-42	16H	CC	W 26-28	138,190	148,150	147,390	157,850	152,620	157,850	15.96	16.80	16.73	Magn.										
TS, Ma, Mu	Dc	FAD	<i>Labyrinthodinium truncatum</i> (s.s.)	18X	1	W 48-50	19X	1	W 50-52	157,780	167,300	168,860	178,880	173,870	168,860	18.12	16.95	17.02	Magn.										
TS, Ma	Dc	LAD	<i>Cordosphaeridium cantharellus</i>	22X	1	W 55-57	22X	5	W 30-32	195,850	201,600	209,170	214,920	212,045	214,920	13.88	17.45	17.42	Magn.										
CC	D	FAD	<i>Actinocyclus ingens</i>	22X	5	W 69-71	23X	2	W 70-72	201,990	207,300	215,310	221,120	218,215	215,310	18.2	17.45	17.48	Magn.										
TS	Dc	FAD	<i>Sumatradiinium druggii</i>	24X	1	W 55-57	25X	1	W 52-54	215,450	225,220	229,790	240,060	234,925	229,790	18.28	17.61	17.70	Magn.										
TS	Dc	FAD	<i>Sumatradiinium hispidum</i>	26X	1	W 52-54	27X	1	W 59-61	235,020	244,890	250,410	260,800	255,605	250,410	18.28	17.97	18.05	Magn.										
CC	D	LAD	<i>Triceratium pileus</i>	27X	2	W 70-72	27X	6	W 70-72	246,500	252,500	262,410	268,410	265,410	268,410	17.3	18.59	18.46	Magn.										
TS, Ma	Dc	FAD	<i>Cousteaudinium Aubryae</i>	28X	1	W 52-54	28X	7	W 30-32	28X	1	W 50-52	28X	2	W 70-72	266,100	270,600	283,010	287,510	285,260	287,510	17.5	19.10	19.05	Magn.				
CC	D	LAD	<i>Thalassiosira spinosa</i>	29X	2	W 70-72	29X	5	W 70-72	272,450	273,690	289,360	290,600	289,980	289,360	21.92	19.14	19.16	Magn.	S8									
GB	R	FAD	<i>Cyrtocapsella tetrapera</i>	30X	CC	W 52-55	31X	CC	W 42-45	274,220	293,310	291,650	311,240	301,445	291,650	20.4	19.20	19.42	Magn.	S8									
TS, Ma, Mu	Dc	FAD	<i>Melitasphaeridium choanophorum</i>	33X	1	W 62-64.5	34X	1	W 47.5-49.5	303,725	313,375	322,695	332,845	327,770	322,695	22.96	19.83	19.89	Bio.										
TS	De	FAD	<i>Sumatradiinium soucouyaniae</i>	34X	1	W 47.5-49.5	35X	1	W 62-64	313,375	323,320	332,845	343,290	338,068	332,845	21.69	19.96	20.03	Bio.										
TS	Ma	Dc	FAD	35X	1	W 62-64	36X	1	W 59-61	323,320	333,090	343,290	353,560	348,425	343,290	20.10	20.10	20.46	Bio.										
TS, Ma, Mu	Dc	LAD	<i>Caligodinium amiculum</i>	36X	1	W 59-61	36X	5	W 30-32	333,090	338,800	335,560	359,270	356,415	359,270	21.23	21.23	21.03	Bio.	S7									
TS, Ma, Mu	Dc	FAD	<i>Operculodinium piaseckii</i>	38X	2	W 29-31	39X	1																					

**Table 2: Magnetostratigraphic and biostratigraphic tie points for the revised Oligocene to Recent age model of ODP Hole 643A.**  
Hiatus ages are extrapolated from surrounding tie points. Notes: A. Extrapolated using minimal age of C4Ar.3r; B. Extrapolated using maximal age of C4Ar.3r; C. Sedimentation rate extrapolated from average between the top of C5ABr and H1.4/1.5; D. The termination of H1.4/1.5 could theoretically be anywhere between its onset at 14.533 Ma and the top of C5ADn at 14.163 Ma. Here dated at 14.286 Ma, at 1/3 between these tie points.

795

Tie point	Min. depth (R-mbsf)	Max. depth (R-mbsf)	Chosen depth (R-mbsf)	Min. age (Ma)	Max. age (Ma)	Chosen age (Ma)	Sed. rate (m Myr <sup>-1</sup> )
Top C1n	0.000	0.000	0.000				
Top C1r.1r	28.500	28.900	28.700		0.781	36.75	
Top C1r.1n	31.900	32.260	32.080		0.988	16.33	
Top C1r.2r	34.500	34.900	34.700		1.072	31.19	
Middle C1r.2n			37.110	1.173	1.185	1.179	22.52
Truncated bottom C1r.3r			52.490		1.778	1.778	25.68
H2.3/2.4			52.970	?	?	1.80 2.52	
Top C2An.1n	53.110	53.410	53.260		2.581	5.05	
Top C2Ar	58.190	58.590	58.390		3.596	5.05	
Top C3n.1n	62.640	63.100	62.870		4.187	7.58	
Top C3n.1r	63.420	63.800	63.610		4.300	6.55	
Top C3An.1n	67.570	67.920	67.745		6.033	2.39	
Top C3An.1r	67.920	68.230	68.075		6.252	1.51	
Top C3Ar	69.660	70.100	69.880		6.733	3.75	
Top C3Bn	72.670	73.100	72.885		7.140	7.38	
Top C3Br.2r	74.930	75.280	75.105		7.285	2.22	
Top C3Br.2n	75.280	75.680	75.480		7.454	11.36	
Top C4r.1r	82.710	83.110	82.910		8.108		
Middle C4r.1n			85.310	8.254	8.300	8.277	14.20
Top C4An	88.620	89.020	88.820		8.771	7.11	
Top C4Ar.1r	96.520	97.540	97.030		9.105	24.58	
Top C4Ar.1n	99.740	100.140	99.940		9.311	14.13	
Top C4Ar.2r	102.040	102.340	102.190		9.426	19.57	
Top C4Ar.2n	103.840	104.240	104.040		9.647	8.37	
Middle C4Ar.3r			105.340	9.721	9.786	9.754	
H1.6/2.1	107.150	107.990	107.150	9.82 A ?	9.98 B ?	9.90 13.30	
Top C5ABr	111.640	112.040	111.840		13.608	15.14 C	
Top C5ACn	112.040	112.440	112.240		13.739	3.05	
Top C5ACr	116.540	116.950	116.745		14.070	13.61	
Top C5ADn	116.950	117.940	117.445		14.163	7.53	
H1.4/1.5	122.110	122.110	122.110	14.16	14.53	37.81	
Top C5ADr	123.940	124.240	124.090		14.609	26.08	
Top C5Bn.1n	128.260	128.580	128.420		14.775	26.08	
Top C5Bn.1r	129.760	130.060	129.910		14.870	15.68	
Truncated bottom C5Bn.1r			143.460		15.032	83.64	
H1.2/1.4	143.770	143.860	143.815	?	?	15.04 16.30	
Truncated Top C5Cn.2n			143.860	16.303	16.303	23.08	
Top C5Cn.2r	147.260	148.260	147.760		16.472	23.08	
Top C5Cn.3n	148.960	149.360	149.160		16.543	19.72	
Top C5Cr	151.960	152.360	152.160		16.721	16.85	
Top C5Dn	189.340	189.740	189.540		17.235	72.72	
Top C5Dr.1r	224.780	225.280	225.030		17.533	119.09	
Top C5En	255.250	256.250	255.750		18.056	58.74	
Top C6n	271.870	272.370	272.120		18.748	23.66	
Top C6r	314.130	315.160	314.645		19.722	43.66	
LO E. insigne			343.290		20.10	76.59	
HO C. amiculum			359.270	21.23	21.23	14.08	
LO B. sphaerica			384.320		22.12	28.07	
LO O. janducheneei			417.360		23.96	17.97	
HO C. lobospinosum & LO A. spiridoides mean			455.810	22.98	30.58	13.66	
Top C13n	491.010	492.770	491.890		33.157	5.66	
Top C13r	493.810	495.070	494.440		33.705	4.65	
						Sensu Eldrett et al. (2004)	

Table 3: Integrated range chart of selected dinocyst and acritarch species, sorted by lowest occurrence. TS = This study, Ma = Manum et al. (1989), Mu = Mudie (1989). Species abundance is maximum of abundances if multiple species have been combined (Table S7): e.g. R + C = C. ? = uncertain determination, cf = specimens resembling the described species, r = suspected reworking. Species abundance: This study: A = abundant (>25%), C = common (2-25%), R = rare (<2%), - = not present. Percentage relative to total dinocysts. Manum et al. (1989): A = abundant (>25%), C = common (2-25%), R = rare (<2%), - = not present. Percentages relative to total marine palynomorphs. Mudie (1989): A = abundant (>49%), C = common (10-49%), R = rare to frequent (1-9%), - = not present. Percentages relative to total marine palynomorphs. Hashed fields indicate samples with species not reported on by Manum et al. (1989) or Mudie (1989), while their presence is likely in their studied interval, based on the counts by other authors, including this study. Events used in this study are indicated in grey, with solid lines indicating LO/HO and dashed lines indicating LPO/HPO.



**Table 4: Revised zonation boundaries and markers. Sample depths are indicated by their top depth.**

Zone	Event	Species	Upper sample	Lower sample	Upper sample (mbsf)	Lower sample (mbsf)	Upper sample (R-mbsf)	Lower sample (R-mbsf)	Mean depth (R-mbsf)	Revised age at mean depth (Ma)
<i>Islandinium minutum - Brigantedinium simplex</i>	FAD	<i>Islandinium minutum</i>	4H CC W 9-11	5H CC W 8-10	33.980	43.050	36.120	46.100	41.110	1.33
<i>Filisphaera filifera - Achomosphaera andalousiensis</i>	FAD	<i>Brigantedinium simplex</i>								
	LAD	<i>Unipontidinium aqueductus</i>	10H 5 W 31-33	10H CC W 5-7	87.610	90.770	93.570	96.730	95.150	9.03
<i>Unipontidinium aqueductus - Achomosphaera andalousiensis</i>	FPAD	<i>Achromosphaera andalousiensis</i>	12H 3 W 62-64	12H 4 W 31-33	103.920	105.110	111.300	112.490	111.895	13.63
<i>Unipontidinium aqueductus</i>	FPAD	<i>Unipontidinium aqueductus</i>	12H 5 W 31-33	13H 1 W 64-66	106.610	110.440	113.990	118.320	116.155	14.03
<i>Labyrinthodinium truncatum - Aptoidinium spiridoides</i>	LAD	<i>Cordosphaeridium cantharellus</i>	22X 1 W 55-57	22X 5 W 30-32	195.850	201.600	209.170	214.920	212.045	17.42
<i>Impagidinium patulum</i>	FPAD	<i>Impagidinium patulum</i>	28X 1 W 52-54	28X 7 W 30-32	254.620	263.400	271.030	279.810	275.420	18.82
<i>Evittosphaerula paratabulata</i>	FPAD	<i>Evittosphaerula paratabulata</i>	36X 1 W 59-61	36X 5 W 30-32	333.090	338.800	353.560	359.270	356.415	21.03
<i>Cyclopsiella lusatica</i>	FAD	<i>Cyclopsiella lusatica</i> (acritarch)	42X 4 W 19-21	44X 1 W 30-32	395.390	410.300	418.860	434.770	426.815	24.65
<i>FAD</i>		<i>Invertocysta tabulata</i>								
<i>Systematophora ? sp. 1</i>	FAD	<i>Systematophora ? sp. 1</i>	45X 5 W 29-31	46X 1 W 82-84	425.990	430.220	451.080	455.810	453.445	26.60
<i>Leptodinium italicum</i>	FAD	<i>Leptodinium italicum</i>	46X 5 W 82-84	47X 1 W 90-92	436.220	440.000	461.810	466.140	463.975	28.22
<i>Reticulatosphaera actinocoronata</i>	LAD	<i>Enneadocysta arcuata</i>	48X 5 W 90-92	48X 6 W 90-92	455.600	457.100	482.440	483.940	483.190	31.62
<i>Chiropteridium lobospinosum</i>	FAD	<i>Chiropteridium lobospinosum</i>	49X 4 W 30-32	50X 1 W 30-32	463.200	468.400	490.660	496.400	493.530	33.51

## Supplementary Figures and Tables

Figure S1: Age-depth plots for Oligocene to Recent sediments of ODP Hole 643A, with constraining bioevents and  $^{40}\text{Ar}/^{39}\text{Ar}$  dating. Bioevents are indicated at the depth of the lowest/highest sample with the presence of a species and ages indicate the global FAD/LAD (see sect. 2.4). Colours used for the lithology and the polarity record are explained in Fig. 2. Magnetostratigraphic tie points of Bleil (1989) are directly linked to GPTS2012 and tie points of Goll (1989) were updated to GTS2012 using linear interpolation between rescaled magnetic reversals.

Figure S2:  $^{40}\text{Ar}/^{39}\text{Ar}$  ages of single grains both for  $^{37}\text{Ca}$  corrected and uncorrected samples. See sect. 2.5 and 3.3 for explanation. Errors are  $1\sigma$  analytical uncertainty.

Table S1: Sediment composition of Hole 643A (Shipboard Scientific Party, 1987). Percentages, when necessary, rescaled to a total of 100%. Trace amounts not included.

Table S2: Applied R-mbsf offsets for ODP Hole 643A.

Table S3: Newly processed palynological samples from ODP Hole 643A.

Table S4: Sampled and selected tephra layers.

Table S5: Detectors ARGUS VI+.

Table S6: Integrated range chart of dinocyst and acritarch species, sorted by nomenclatural status and lowest occurrence. TS = This study, Ma = Manum et al. (1989), Mu = Mudie (1989). Species abundance is maximum of abundances if multiple species have been combined (Table S7): e.g. R + C = C. ? = uncertain determination, cf = specimens resembling the described species, r = suspected reworking. Species abundance: This study: A = abundant (>25%), C = common (2-25%), R = rare (<2%), - = not present. Percentage relative to total dinocysts. Manum et al. (1989): A = abundant (>25%), C = common (2-25%), R = rare (<2%), - = not present. Percentages relative to total marine palynomorphs. Mudie (1989): A = abundant (>49%), C = common (10-49%), R = rare to frequent (1-9%), - = not present. Percentages relative to total marine palynomorphs.

Table S7: Synonymization and updated nomenclature of dinocysts and acritarchs, and stratigraphic notes. Taxa are sorted by nomenclatural status and lowest occurrence (see Table S6). TS: This study, Ma: Manum et al. (1989), Mu: Mudie (1989). Species with open nomenclature retain the name of Mudie (1989) or Manum et al. (1989), unless an identical name is used in this study or the other publication, in which case the source publication is added to the name. Arabic and roman numbers are considered synonymous. E.g. "Pyxidiella sp. 1 of Manum et al. (1989)" and "Pyxidiella sp. 1 of Mudie (1989)", but "Aireinana sp. 1".

Table S8: Updated nomenclature of diatoms, radiolarians and planktic foraminifers, and stratigraphic notes. CC: Ciesielski and Case (1989), SP: Shipboard Scientific Party (1987), GB: Goll and Bjørklund (1989).

Table S9: Ages and references used for deriving global FADs and LADs of dinocyst events used for constraining the revised biomagnetostratigraphic age model of Hole 643A. Events are sorted by their stratigraphic occurrence in Hole 643A (See Table 1).

Table S10: Ages and references used for deriving global FADs and LADs of diatom, planktic foraminifer and radiolarian events used for constraining the revised biomagnetostratigraphic age model of Hole 643A. Events are sorted by their stratigraphic occurrence in Hole 643A (See Table 1).

Table S11:  $^{40}\text{Ar}/^{39}\text{Ar}$  results on single grains and calculations for the applied ages.

Table S12: Paleomagnetic results of Bleil (1989), calculations for azimuthally reoriented declination and polarity interpretation.

## Supplementary references

Açıklarlı, S., Vellekoop, J., Ocakoğlu, F., Yılmaz, İ.Ö., Smit, J., Altiner, S.Ö., Goderis, S., Vonhof, H., Speijer, R.P., Woelders, L., Fornaciari, E., Brinkhuis, H., 2015. Geochemical and palaeontological characterization of a new K-Pg Boundary locality from the Northern branch of the Neo-Tethys: Mudurnu – Göynük Basin, NW Turkey. *Cretac. Res.* 52, 251–267. <https://doi.org/10.1016/j.cretres.2014.07.011>

Anthonissen, E.D., Ogg, J.G., 2012. Cenozoic and Cretaceous Biochronology of Planktonic Foraminifera and Calcareous Nannofossils, in: Gradstein, F.M., Ogg, J.G., Schmitz, M.D., Ogg, G.M. (Eds.), *The Geologic Time Scale 2012*. Elsevier, Amsterdam, The Netherlands, pp. 1083–1127. <https://doi.org/10.1016/B978-0-444-59425-9.15003-6>

Baldauf, J.G., Barron, J.A., 1991. Diatom Biostratigraphy: Kerguelen Plateau and Prydz Bay Regions of the Southern Ocean, in: Barron, J.A., Larsen, B. (Eds.), *Proceedings of the Ocean Drilling Program, Scientific Results*, Vol. 119. Ocean Drilling Program, College Station, TX, USA, pp. 547–598. <https://doi.org/10.2973/odp.proc.sr.119.135.1991>

Barron, J.A., 1983. Latest Oligocene through early middle Miocene diatom biostratigraphy of the eastern tropical Pacific. *Mar. Micropaleontol.* 7, 487–515. [https://doi.org/10.1016/0377-8398\(83\)90012-9](https://doi.org/10.1016/0377-8398(83)90012-9)

Barron, J.A., 1985a. Late Eocene to Holocene Diatom Biostratigraphy of the Equatorial Pacific Ocean, Deep Sea Drilling Project Leg 85, in: Mayer, L., Theyer, F. (Eds.), *Initial Reports of the Deep Sea Drilling Project*, Vol. 85. U.S. Government Printing Office, Washington, D.C., USA, pp. 413–456. <https://doi.org/10.2973/dsdp.proc.85.108.1985>

Barron, J.A., 1985b. Miocene to Holocene planktic diatoms, in: Bolli, H.M., Saunders, J.B., Perch-Nielsen, K. (Eds.), *Plankton Stratigraphy*, vol. 2. Cambridge University Press, Cambridge, UK, pp. 763–809.

Barron, J.A., 1992. Neogene diatom datum levels in the Equatorial and North Pacific, in: Ishizaki, K., Saito, T. (Eds.), *Centenary of Japanese Micropaleontology*. Terra Scientific Publishing Company, Tokyo, Japan, pp. 413–425.

Barron, J.A., 2003. Planktonic marine diatom record of the past 18 m.y.: Appearances and extinctions in the Pacific and Southern Oceans. *Diatom Res.* 18, 203–224. <https://doi.org/10.1080/0269249X.2003.9705588>

Barron, J.A., 2005. Diatom biochronology for the Early Miocene of the Equatorial Pacific. *Stratigraphy* 2, 281–309.

Barron, J.A., Browning, J., Sugarman, P., Miller, K.G., 2013. Refinement of late-Early and Middle Miocene diatom biostratigraphy for the East Coast of the United States. *Geosphere* 9, 1286–1302. <https://doi.org/10.1130/GES00864.1>

Barron, J.A., Gladenkov, A.Y., 1995. Early Miocene to Pleistocene Diatom Stratigraphy of Leg 145, in: Rea, D.K., Basov, I.A., Scholl, D.W., Allan, J.F. (Eds.), *Proceedings of the Ocean Drilling Program, Scientific Results*, Vol. 145. Ocean Drilling Program, College Station, TX, USA, pp. 3–19. <https://doi.org/10.2973/odp.proc.sr.145.101.1995>

Barron, J.A., Keller, G., Dunn, D.A., 1985a. A multiple microfossil biochronology for the Miocene, in: Kennett, J.P. (Ed.), *The Miocene Ocean: Paleoceanography and Biogeography*, Memoir 163. The Geological Society of America, Boulder, CO, USA, pp. 21–36.

Barron, J.A., Nigrini, C.A., Pujos, A., Saito, T., Theyer, F., Thomas, E., Weinreich, N., 1985b. Synthesis of Biostratigraphy, Central Equatorial Pacific, Deep Sea Drilling Project Leg 85: Refinement of Oligocene to Quaternary Biochronology, in:

- Mayer, L., Theyer, F. (Eds.), Initial Reports of the Deep Sea Drilling Project, Vol. 85. U.S. Government Printing Office, 70 Washington, D.C., USA, pp. 905–934. <https://doi.org/10.2973/dsdp.proc.85.130.1985>
- Berggren, W.A., Kent, D. V., Flynn, J.J., Van Couvering, J.A., 1985. Cenozoic geochronology. *Geol. Soc. Am. Bull.* 96, 1407–1418. [https://doi.org/10.1130/0016-7606\(1985\)96<1407:CG>2.0.CO;2](https://doi.org/10.1130/0016-7606(1985)96<1407:CG>2.0.CO;2)
- Berggren, W.A., Kent, D. V., Swisher, C.C.I., Aubry, M.-P., 1995. A Revised Cenozoic Geochronology and Chronostratigraphy, in: Berggren, W.A., Kent, D.V., Aubry, M.-P., Hardenbol, J. (Eds.), *Geochronology, Time Scales, and Global Stratigraphic Correlation*, SEPM Special Publication No. 54. SEPM (Society for Sedimentary Geology), Tulsa, OK, USA, pp. 129–212. <https://doi.org/10.2110/pec.95.04.0129>
- Biffi, U., Manum, S.B., 1988. Late Eocene-Early Miocene dinoflagellate cyst stratigraphy from the Marche Region (Central Italy). *Boll. della Soc. Paleontol. Ital.* 27, 163–212.
- Bijl, P.K., Houben, A.J.P., Bruls, A., Pross, J., Sangiorgi, F., 2018. Stratigraphic calibration of Oligocene–Miocene organic-walled dinoflagellate cysts from offshore Wilkes Land, East Antarctica, and a zonation proposal. *J. Micropalaeontology* 37, 80 105–138. <https://doi.org/10.5194/jm-37-105-2018>
- Bijl, P.K., Sluijs, A., Brinkhuis, H., 2013. A magneto- and chemostratigraphically calibrated dinoflagellate cyst zonation of the early Palaeogene South Pacific Ocean. *Earth-Science Rev.* 124, 1–31. <https://doi.org/10.1016/j.earscirev.2013.04.010>
- Bleil, U., 1989. Magnetostratigraphy of Neogene and Quaternary sediment series from the Norwegian Sea: Ocean Drilling 85 Program, Leg 104, in: Eldholm, O., Thiede, J., Taylor, E. (Eds.), *Proceedings of the Ocean Drilling Program, Scientific Results*, Vol. 104, *Proceedings of the Ocean Drilling Program*. Ocean Drilling Program, College Station, TX, USA, pp. 829–901. <https://doi.org/10.2973/odp.proc.sr.104.1989>
- Bohaty, S.M., Wise, S.W.J., Duncan, R.A., Moore, C.L., Wallace, P.J., 2003. Neogene Diatom Biostratigraphy, Tephra Stratigraphy, and Chronology of ODP Hole 1138A, Kerguelen Plateau, in: Frey, F.A., Coffin, M.F., Wallace, P.J., Quilty, 90 P.G. (Eds.), *Proceedings of the Ocean Drilling Program, Scientific Results*, Vol. 183. Ocean Drilling Program, College Station, TX, USA, pp. 1–53. <https://doi.org/10.2973/odp.proc.sr.183.016.2003>
- Brinkhuis, H., 1994. Late Eocene to Early Oligocene dinoflagellate cysts from the Priabonian type-area (Northeast Italy): biostratigraphy and paleoenvironmental interpretation. *Palaeogeogr. Palaeoclimatol. Palaeoecol.* 107, 121–163. [https://doi.org/10.1016/0031-0182\(94\)90168-6](https://doi.org/10.1016/0031-0182(94)90168-6)
- Brinkhuis, H., Biffi, U., 1993. Dinoflagellate cyst stratigraphy of the Eocene/Oligocene transition in central Italy. *Mar. Micropaleontol.* 22, 131–183. [https://doi.org/10.1016/0377-8398\(93\)90007-K](https://doi.org/10.1016/0377-8398(93)90007-K)
- Brinkhuis, H., Munsterman, D.K., Sengers, S., Sluijs, A., Warnaar, J., Williams, G.L., 2003. Late Eocene–Quaternary Dinoflagellate Cysts from ODP Site 1168, off Western Tasmania, in: Exxon, N.F., Kennett, J.P., Malone, M.J. (Eds.), *Proceedings of the Ocean Drilling Program, Scientific Results*, Vol. 189. Ocean Drilling Program, College Station, TX, 100 USA, pp. 1–36. <https://doi.org/10.2973/odp.proc.sr.189.105.2003>
- Brown, S., Downie, C., 1984. Dinoflagellate Cyst Biostratigraphy of Late Paleocene and Early Eocene Sediments from Holes 552, 553A, and 555, Leg 81, Deep Sea Drilling Project (Rockall Plateau), in: Roberts, D.G., Schnitker, D. (Eds.),

- Initial Reports of the Deep Sea Drilling Project, Vol. 81. U.S. Government Printing Office, Washington, D.C., USA, pp. 565–579. <https://doi.org/10.2973/dsdp.proc.81.113.1984>
- 105 Brown, S., Downie, C., 1985. Dinoflagellate Cyst Stratigraphy of Paleocene to Miocene Sediments from the Goban Spur (Sites 548-550, Leg 80), in: de Graciansky, P.C., Poag, C.W. (Eds.), Initial Reports of the Deep Sea Drilling Project, Vol. 80. U.S. Government Printing Office, Washington, D.C., USA, pp. 643–651. <https://doi.org/10.2973/dsdp.proc.80.120.1985>
- Bujak, J.P., Matsuoka, K., 1986. Late Cenozoic dinoflagellate cyst zonation in the Western and Northern Pacific, in: Wrenn, J.H., Duffield, S.L., Stein, J.A. (Eds.), Papers from the First Symposium on Neogene Dinoflagellate Cyst Biostratigraphy, 110 AASP Contributions Series, Vol. 17. American Association of Stratigraphic Palynologists Foundation, Dallas, TX, USA, pp. 7–25.
- Burckle, L.H., 1972. Late Cenozoic planktonic diatom zones from the eastern equatorial Pacific, in: Simonsen, R. (Ed.), Proceedings of the First Symposium on Recent and Fossil Marine Diatoms, Bremerhaven, September 21-26, 1970, Beihefte Zur Nova Hedwigia, Vol. 39. pp. 217–246.
- 115 Burckle, L.H., 1978. Early Miocene to Pliocene diatom levels for the equatorial Pacific, in: Proceedings of the Second Working Group Meeting on Biostratigraphic Datum-Planes of the Pacific Neogene, IGCP Project 114, Bandung, May 30-June 1, 1977, Special Publications, Vol. 1. Geological Research and Development Centre, Bandung, Republic of Indonesia, pp. 25–44.
- Censarek, B., Gersonde, R., 2002. Miocene diatom biostratigraphy at ODP sites 689, 690, 1088, 1092 (Atlantic sector of the 120 Southern Ocean). *Mar. Micropaleontol.* 45, 309–356. [https://doi.org/10.1016/S0377-8398\(02\)00034-8](https://doi.org/10.1016/S0377-8398(02)00034-8)
- Chaisson, W.P., Pearson, P.N., 1997. Planktonic foraminifer biostratigraphy at Site 925: middle Miocene–Pleistocene, in: Shackleton, N.J., Curry, W.B., Richter, C., Bralower, T.J. (Eds.), Proceedings of the Ocean Drilling Program, Scientific Results, Vol. 154. Ocean Drilling Program, College Station, TX, USA, pp. 3–31. <https://doi.org/10.2973/odp.proc.sr.154.104.1997>
- 125 Ciesielski, P.F., Case, S.M., 1989. Neogene Paleoceanography of the Norwegian Sea Based Upon Silicoflagellate Assemblage Changes in ODP Leg 104 Sedimentary Sequences, in: Eldholm, O., Thiede, J., Taylor, E. (Eds.), Proceedings of the Ocean Drilling Program, Scientific Results, Vol. 104. Ocean Drilling Program, College Station, TX, USA, pp. 527–541. <https://doi.org/10.2973/odp.proc.sr.104.166.1989>
- Ciesielski, P.F., 1983. The Neogene and Quaternary Diatom Biostratigraphy of Subantarctic Sediments, Deep Sea Drilling 130 Project Leg 71, in: Ludwig, W.J., Krasheninnikov, V.A. (Eds.), Initial Reports of the Deep Sea Drilling Project, Vol. 71. U.S. Government Printing Office, Washington, D.C., USA, pp. 635–665. <https://doi.org/10.2973/dsdp.proc.71.125.1983>
- Cody, R.D., Levy, R.H., Harwood, D.M., Sadler, P.M., 2008. Thinking outside the zone: High-resolution quantitative diatom biochronology for the Antarctic Neogene. *Palaeogeogr. Palaeoclimatol. Palaeoecol.* 260, 92–121. <https://doi.org/10.1016/j.palaeo.2007.08.020>

- 135 Costa, L.I., Downie, C., 1979. Cenozoic Dinocyst Stratigraphy of Sites 403 to 406 (Rockall Plateau), IPOD, Leg 48, in: Montadert, L., Roberts, D.G. (Eds.), Initial Reports of the Deep Sea Drilling Project, Vol. 48. U.S. Government Printing Office, Washington, D.C., USA, pp. 513–529. <https://doi.org/10.2973/dsdp.proc.48.121.1979>
- De Schepper, S., Head, M.J., 2009. Pliocene and Pleistocene Dinoflagellate Cyst and Acritharchs Zonation of DSDP Hole 610a, Eastern North Atlantic. *Palynology* 33, 179–218. <https://doi.org/10.2113/gspalynol.33.1.179>
- 140 de Vernal, A., Londeix, L., Mudie, P.J., Harland, R., Morzadec-Kerfourn, M.T., Turon, J.-L., Wrenn, J.H., 1992. Quaternary organic-walled dinoflagellate cysts of the North Atlantic Ocean and adjacent seas: ecostratigraphy and biostratigraphy, in: Head, M.J., Wrenn, J.H. (Eds.), Neogene and Quaternary Dinoflagellate Cysts and Acritharchs. American Association of Stratigraphic Palynologists Foundation, Dallas, TX, USA, pp. 289–329.
- de Vernal, A., Mudie, P.J., 1989. Late Pliocene to Holocene Palynostratigraphy at ODP Site 645, Baffin Bay, in: Srivastava, 145 S.P., Arthur, M., Clement, B. (Eds.), Proceedings of the Ocean Drilling Program, Scientific Results, Vol. 105. Ocean Drilling Program, College Station, TX, USA, pp. 387–399. <https://doi.org/10.2973/odp.proc.sr.105.133.1989>
- de Verteuil, L., Norris, G., 1992. Miocene protoperidiniacean dinoflagellate cysts from the Maryland and Virginia coastal plain, in: Head, M.J., Wrenn, J.H. (Eds.), Neogene and Quaternary Dinoflagellate Cysts and Acritharchs. American Association of Stratigraphic Palynologists Foundation, Dallas, TX, USA, pp. 391–431.
- 150 de Verteuil, L., Norris, G., 1996. Miocene Dinoflagellate Stratigraphy and Systematics of Maryland and Virginia. *Micropaleontology* 42 Suppl., 186. <https://doi.org/10.2307/1485926>
- Duffield, S.L., Stein, J.A., 1986. Peridiniacean-dominated cyst assemblage from the Miocene of the Gulf of Mexico shelf, offshore Louisiana, in: Wrenn, J.H., Duffield, Susan L., Stein, Jeffrey A. (Eds.), Papers from the First Symposium on Neogene Dinoflagellate Cyst Biostratigraphy, AASP Contributions Series, Vol. 17. American Association of Stratigraphic 155 Palynologists Foundation, Dallas, TX, USA, pp. 27–45.
- Dybkjær, K., Piasecki, S., 2010. Neogene dinocyst zonation for the eastern North Sea Basin, Denmark. *Rev. Palaeobot. Palynol.* 161, 1–29. <https://doi.org/10.1016/j.revpalbo.2010.02.005>
- Edwards, L.E., 1984. Miocene Dinocysts from Deep Sea Drilling Project Leg 81, Rockall Plateau, Eastern North Atlantic Ocean, in: Roberts, D.G., Schnitker, D. (Eds.), Initial Reports of the Deep Sea Drilling Project, Vol. 81. U.S. Government 160 Printing Office, Washington, D.C., USA, pp. 581–594. <https://doi.org/10.2973/dsdp.proc.81.114.1984>
- Egger, L.M., Śliwińska, K.K., van Peer, T.E., Liebrand, D., Lippert, P.C., Friedrich, O., Wilson, P.A., Norris, R.D., Pross, J., 2016. Magnetostratigraphically-calibrated dinoflagellate cyst bioevents for the uppermost Eocene to lowermost Miocene of the western North Atlantic (IODP Expedition 342, Paleogene Newfoundland sediment drifts). *Rev. Palaeobot. Palynol.* 234, 159–185. <https://doi.org/10.1016/j.revpalbo.2016.08.002>
- 165 Eldrett, J.S., Harding, I.C., 2009. Palynological analyses of Eocene to Oligocene sediments from DSDP Site 338, Outer Voring Plateau. *Mar. Micropaleontol.* 73, 226–240. <https://doi.org/10.1016/j.marmicro.2009.10.004>

- Eldrett, J.S., Harding, I.C., Firth, J. V., Roberts, A.P., 2004. Magnetostratigraphic calibration of Eocene–Oligocene dinoflagellate cyst biostratigraphy from the Norwegian–Greenland Sea. *Mar. Geol.* 204, 91–127. [https://doi.org/10.1016/S0025-3227\(03\)00357-8](https://doi.org/10.1016/S0025-3227(03)00357-8)
- 170 Fensome, R., Crux, J., Gard, G., MacRae, A., Williams, G., Thomas, F., Fiorini, F., Wach, G., 2008. The last 100 million years on the Scotian Margin, offshore eastern Canada: an event-stratigraphic scheme emphasizing biostratigraphic data. *Atl. Geol.* 44, 93–126. <https://doi.org/10.4138/6506>
- Firth, J.V., 1996. Upper Middle Eocene to Oligocene Dinoflagellate Biostratigraphy and Assemblage Variations in Hole 913B, Greenland Sea, in: Thiede, J., Myhre, A.M., Firth, J.V., Johnson, G.L., Ruddiman, W.F. (Eds.), *Proceedings of the 175 Ocean Drilling Program, Scientific Results*, Vol. 151. Ocean Drilling Program, College Station, TX, USA, pp. 203–242. <https://doi.org/10.2973/odp.proc.sr.151.105.1996>
- Gladenkov, A.Y., Barron, J.A., 1995. Oligocene and Early Middle Miocene Diatom Biostratigraphy of Hole 884B, in: Rea, D.K., Basov, I.A., Scholl, D.W., Allan, J.F. (Eds.), *Proceedings of the Ocean Drilling Program, Scientific Results*, Vol. 145. Ocean Drilling Program, College Station, TX, USA, pp. 21–41. <https://doi.org/10.2973/odp.proc.sr.145.105.1995>
- 180 Goll, R.M., 1989. A Synthesis of Norwegian Sea Biostratigraphies: ODP Leg 104 on the Vørung Plateau, in: Eldholm, O., Thiede, J., Taylor, E. (Eds.), *Proceedings of the Ocean Drilling Program, Scientific Results*, Vol. 104. Ocean Drilling Program, College Station, TX, USA, pp. 777–826. <https://doi.org/10.2973/odp.proc.sr.104.203.1989>
- Goll, R.M., Bjørklund, K.R., 1989. A New Radiolarian Biostratigraphy for the Neogene of the Norwegian Sea: ODP Leg 104, in: Eldholm, O., Thiede, J., Taylor, E. (Eds.), *Proceedings of the Ocean Drilling Program, Scientific Results*, Vol. 104. 185 Ocean Drilling Program, College Station, TX, USA, pp. 697–737. <https://doi.org/10.2973/odp.proc.sr.104.205.1989>
- Gradstein, F.M., Kristiansen, I.L., Loemo, L., Kaminski, M.A., 1992. Cenozoic Foraminiferal and Dinoflagellate Cyst Biostratigraphy of the Central North Sea. *Micropaleontology* 38, 101–137. <https://doi.org/10.2307/1485991>
- Gradstein, F.M., Ogg, J.G., Schmitz, M.D., Ogg, G.M., 2012. *The Geologic Time Scale 2012*. Elsevier, Amsterdam, The Netherlands. <https://doi.org/10.1016/C2011-1-08249-8>
- 190 Gradstein, F.M., Ogg, J.G., Smith, A.G., 2004. *A Geologic Time Scale 2004*. Cambridge University Press, Cambridge, UK. <https://doi.org/10.1017/CBO9780511536045>
- Harwood, D.M., Maruyama, T., 1992. Middle Eocene to Pleistocene Diatom Biostratigraphy of Southern Ocean Sediments from the Kerguelen Plateau, Leg 120, in: Wise, S.W.J., Schlich, R. (Eds.), *Proceedings of the Ocean Drilling Program, Scientific Results*, Vol. 120. Ocean Drilling Program, College Station, TX, USA, pp. 683–733. 195 <https://doi.org/10.2973/odp.proc.sr.120.160.1992>
- Head, M.J., 1993. Dinoflagellates, Sporomorphs, and Other Palynomorphs from the Upper Pliocene St. Erth Beds of Cornwall, Southwestern England. *J. Paleontol.*, The Paleontological Society Memoir 31, 67 Suppl., 1–62. <https://doi.org/10.1017/S0022336000061126>
- Head, M.J., 1994. Morphology and Paleoenvironmental Significance of the Cenozoic Dinoflagellate Genera *Tectatodinium* 200 and *Habibacysta*. *Micropaleontology* 40, 289–321. <https://doi.org/10.2307/1485937>

- Head, M.J., 1998. Marine environmental change in the Pliocene and early Pleistocene of eastern England: the dinoflagellate evidence reviewed, in: van Kolfschoten, T., Gibbard, P.L. (Eds.), *The Dawn of the Quaternary*, Mededelingen Nederlands Instituut Voor Toegepaste Geowetenschappen TNO, Vol. 60. pp. 199–226.
- Head, M.J., Norris, G., 1989. Palynology and Dinocyst Stratigraphy of the Eocene and Oligocene in ODP Leg 105, Hole 205 647A, Labrador Sea, in: Srivastava, S.P., Arthur, M.A., Clement, B.M. (Eds.), *Proceedings of the Ocean Drilling Program, Scientific Results*, Vol. 105. Ocean Drilling Program, College Station, TX, USA, pp. 515–550. <https://doi.org/10.2973/odp.proc.sr.105.178.1989>
- Head, M.J., Norris, G., Mudie, P.J., 1989a. Palynology and Dinocyst Stratigraphy of the Upper Miocene and Lowermost Pliocene, ODP Leg 105, Site 646, Labrador Sea, in: Srivastava, S.P., Arthur, M., Clement, B. (Eds.), *Proceedings of the 210 Ocean Drilling Program, Scientific Results*, Vol. 105. Ocean Drilling Program, College Station, TX, USA, pp. 423–451. <https://doi.org/10.2973/odp.proc.sr.105.135.1989>
- Head, M.J., Norris, G., Mudie, P.J., 1989b. New Species of Dinocysts and a New Species of Acritarch from the Upper Miocene and Lowermost Pliocene, ODP Leg 105, Site 646, Labrador Sea, in: Srivastava, S.P., Arthur, M., Clement, B. (Eds.), *Proceedings of the Ocean Drilling Program, Scientific Results*, Vol. 105. Ocean Drilling Program, College Station, 215 TX, USA, pp. 453–466. <https://doi.org/10.2973/odp.proc.sr.105.136.1989>
- Head, M.J., Wrenn, J.H., 1992. Neogene and Quaternary Dinoflagellate cysts and Acritarchs. American Association of Stratigraphic Palynologists Foundation, Dallas, TX, USA.
- Heilmann-Clausen, C., Costa, L.I., 1989. Dinoflagellate zonation of the uppermost Paleocene? to Lower Miocene in the Wursterheide research well, NW Germany. *Geol. Jahrbuch*, R. A 111, 431–521.
- Hilgen, F.J., Krijgsman, W., Raffi, I., Turco, E., Zachariasse, W.J., 2000. Integrated stratigraphy and astronomical calibration of the Serravallian/Tortonian boundary section at Monte Gibliscemi (Sicily, Italy). *Mar. Micropaleontol.* 38, 181–220. [https://doi.org/10.1016/S0377-8398\(00\)00008-6](https://doi.org/10.1016/S0377-8398(00)00008-6)
- Jan du Chêne, R., 1977. Étude palynologique du Miocene supérieur Andalou (Espagne). *Rev. Española Micropaleontol.* 9, 97–114.
- Köthe, A., 2012. A revised Cenozoic dinoflagellate cyst and calcareous nannoplankton zonation for the German sector of the southeastern North Sea Basin. *Newsletters Stratigr.* 45, 189–220. <https://doi.org/10.1127/0078-0421/2012/0021>
- Kuhlmann, G., Langereis, C.G., Munsterman, D., van Leeuwen, R.-J., Verreussel, R., Meulenkamp, J.E., Wong, T.E., 2006. Integrated chronostratigraphy of the Pliocene-Pleistocene interval and its relation to the regional stratigraphical stages in the southern North Sea region. *Netherlands J. Geosci. - Geol. en Mijnb.* 85, 19–35. <https://doi.org/10.1017/S0016774600021405>
- Laskar, J., Joutel, F., Boudin, F., 1993. Orbital, precessional, and insolation quantities for the Earth from -20 Myr to +10 Myr. *Astron. Astrophys.* 270, 522–533.
- Lazarus, D., Barron, J.A., Renaudie, J., Diver, P., Türke, A., 2014. Cenozoic Planktonic Marine Diatom Diversity and Correlation to Climate Change. *PLoS One* 9, e84857. <https://doi.org/10.1371/journal.pone.0084857>

- Lirer, F., Caruso, A., Foresi, L.M., Sprovieri, M., Bonomo, S., Di Stefano, A., Di Stefano, E., Iaccarino, S.M., Salvatorini, G., Sprovieri, R., Mazzola, S., 2002. Astrochronological calibration of the upper Serravallian/lower Tortonian sedimentary sequence at Tremiti Islands (Adriatic sea, Southern Italy). *Riv. Ital. di Paleontol. e Stratigr.* 108, 241–256.
- Londeix, L., Jan Du Chêne, R., 1998. Burdigalian dinocyst stratigraphy of the stratotypic area (Bordeaux, France). *Geobios* 30, 283–294. [https://doi.org/10.1016/S0016-6995\(98\)80012-0](https://doi.org/10.1016/S0016-6995(98)80012-0)
- Lourens, L.J., Hilgen, F.J., Laskar, J., Shackleton, N.J., Wilson, D., 2004. The Neogene Period, in: Gradstein, F.M., Ogg, J.G., Smith, A.G. (Eds.), *A Geologic Time Scale 2004*. Cambridge University Press, Cambridge, UK, pp. 409–440.
- Louwye, S., Foubert, A., Mertens, K.N., Van Rooij, D., the IODP Expedition 307 scientific party, 2008. Integrated stratigraphy and palaeoecology of the Lower and Middle Miocene of the Porcupine Basin. *Geol. Mag.* 145, 321–344. <https://doi.org/10.1017/S0016756807004244>
- Manum, S.B., Boulter, M.C., Gunnarsdottir, H., Rangnes, K., Scholze, A., 1989. Eocene to Miocene Palynology of the Norwegian Sea (ODP Leg 104), in: Eldholm, O., Thiede, J., Taylor, E. (Eds.), *Proceedings of the Ocean Drilling Program, Scientific Results, Vol. 104. Ocean Drilling Program, College Station, TX, USA*, pp. 611–662. <https://doi.org/10.2973/odp.proc.sr.104.176.1989>
- Manum, S.B., 1976. Dinocysts in Tertiary Norwegian-Greenland Sea Sediments (Deep Sea Drilling Project Leg 38), with Observations on Palynomorphs and Palynodebris in Relation to Environment, in: Talwani, M., Udintsev, G. (Eds.), *Initial Reports of the Deep Sea Drilling Project, Vol. 38. U.S. Government Printing Office, Washington, D.C., USA*, pp. 897–919. <https://doi.org/10.2973/dsdp.proc.38.129.1976>
- McMinn, A., 1992. Neogene Dinoflagellate Distribution in the Eastern Indian Ocean from Leg 123, Site 765, in: Gradstein, F.M., Ludden, J.N. (Eds.), *Proceedings of the Ocean Drilling Program, Scientific Results, Vol. 123. Ocean Drilling Program, College Station, TX, USA*, pp. 429–441. <https://doi.org/10.2973/odp.proc.sr.123.120.1992>
- McMinn, A., 1993. Neogene Dinoflagellate Cyst Biostratigraphy from Sites 815 and 823, Leg 133, Northeast Australian Margin, in: McKenzie, J.A., Davies, P.J., Palmer-Julson, A. (Eds.), *Proceedings of the Ocean Drilling Program, Scientific Results, Vol. 133. Ocean Drilling Program, College Station, TX, USA*, pp. 97–105. <https://doi.org/10.2973/odp.proc.sr.133.219.1993>
- Mertens, K.N., Takano, Y., Head, M.J., Matsuoka, K., 2014. Living fossils in the Indo-Pacific warm pool: A refuge for thermophilic dinoflagellates during glaciations. *Geology* 42, 531–534. <https://doi.org/10.1130/G35456.1>
- Miller, K.G., Aubry, M.-P., Khan, M.J., Melillo, A.J., Kent, D. V., Berggren, W.A., 1985. Oligocene-Miocene biostratigraphy, magnetostratigraphy, and isotopic stratigraphy of the western North Atlantic. *Geology* 13, 257–261. [https://doi.org/10.1130/0091-7613\(1985\)13<257:OBMAIS>2.0.CO;2](https://doi.org/10.1130/0091-7613(1985)13<257:OBMAIS>2.0.CO;2)
- Montanari, A., Bice, D.M., Capo, R., Coccioni, R., Deino, A., DePaolo, D.J., Emmanuel, L., Monechi, S., Renard, M., Zevenboom, D., 1997. Integrated stratigraphy of the Chattian to mid-Burdigalian pelagic sequence of the Contessa valley (Gubbio, Italy), in: Montanari, A., Odin, G.S., Coccioni, Rodolfo (Eds.), *Miocene Stratigraphy: An Integrated Approach, Developments in Palaeontology and Stratigraphy*, Vol. 15. Elsevier, Amsterdam, The Netherlands, pp. 249–277.

- Morgenroth, P., 1966. Mikrofossilien und Konkretionen des nordwesteuropäischen Untereozäns. Palaeontogr. Abteilung B 119, 1–53.
- 270 Mudge, D.C., Bujak, J.P., 1996. An integrated stratigraphy for the Paleocene and Eocene of the North Sea, in: Knox, R.W.O., Corfield, R.M., Dunay, R.E. (Eds.), Correlation of the Early Paleogene in Northwest Europe, Special Publications, Vol. 101. Geological Society, London, UK, pp. 91–113. <https://doi.org/10.1144/GSL.SP.1996.101.01.06>
- Mudie, P.J., 1987. Palynology and Dinoflagellate Biostratigraphy of Deep Sea Drilling Project Leg 94, Sites 607 and 611, North Atlantic Ocean, in: Ruddiman, W.F., Kidd, R.B., Thomas, E. (Eds.), Initial Reports of the Deep Sea Drilling Project, 275 Vol. 94. U.S. Government Printing Office, Washington, D.C., USA, pp. 785–812. <https://doi.org/10.2973/dsdp.proc.94.118.1987>
- Mudie, P.J., 1989. Palynology and Dinocyst Biostratigraphy of the Late Miocene to Pleistocene, Norwegian Sea: ODP Leg 104, Sites 642 to 644, in: Eldholm, O., Thiede, J., Taylor, E. (Eds.), Proceedings of the Ocean Drilling Program, Scientific Results, Vol. 104. Ocean Drilling Program, College Station, TX, USA, pp. 587–610. 280 <https://doi.org/10.2973/odp.proc.sr.104.174.1989>
- Nigrini, C., Sanfilippo, A., Moore, T.J.J., 2005. Cenozoic Radiolarian Biostratigraphy: A Magnetobiostratigraphic Chronology of Cenozoic Sequences from ODP Sites 1218, 1219, and 1220, Equatorial Pacific, in: Wilson, P.A., Lyle, M., Firth, J. V. (Eds.), Proceedings of the Ocean Drilling Program, Scientific Results, Vol. 199. Ocean Drilling Program, College Station, TX, USA, pp. 1–76. <https://doi.org/10.2973/odp.proc.sr.199.225.2006>
- 285 Olde, K., Jarvis, I., Pearce, M., Uličný, D., Tocher, B., Trabucho-Alexandre, J., Gröcke, D., 2015. A revised northern European Turonian (Upper Cretaceous) dinoflagellate cyst biostratigraphy: Integrating palynology and carbon isotope events. Rev. Palaeobot. Palynol. 213, 1–16. <https://doi.org/10.1016/j.revpalbo.2014.10.006>
- Pälike, H., Lyle, M., Nishi, H., Raffi, I., Gamage, K., Klaus, A., the Expedition 320/321 Scientists, 2010. Proceedings of the Integrated Ocean Drilling Program, vol. 320/321. Integrated Ocean Drilling Program Management International, Inc., 290 Tokyo, Japan.
- Piasecki, S., 1980. Dinoflagellate cyst stratigraphy of the Miocene Hodde and Gram formations, Denmark. Bull. Geol. Soc. Denmark 29, 53–76.
- Piasecki, S., 2003. Neogene dinoflagellate cysts from Davis Strait, offshore West Greenland. Mar. Pet. Geol. 20, 1075–1088. [https://doi.org/10.1016/S0264-8172\(02\)00089-2](https://doi.org/10.1016/S0264-8172(02)00089-2)
- 295 Powell, A.J., 1986a. Latest Palaeogene and earliest Neogene dinoflagellate cysts from the Lemme section, northwest Italy, in: Wrenn, J.H., Duffield, S.L., Stein, J.A. (Eds.), Papers from the First Symposium on Neogene Dinoflagellate Cyst Biostratigraphy, AASP Contributions Series, Vol. 17. American Association of Stratigraphic Palynologists Foundation, Dallas, TX, USA, pp. 83–104.
- Powell, A.J., 1986b. A dinoflagellate cyst biozonation for the late Oligocene to middle Miocene succession of the Langhe 300 region, northwest Italy, in: Wrenn, J.H., Duffield, S.L., Stein, J.A. (Eds.), Papers from the First Symposium on Neogene

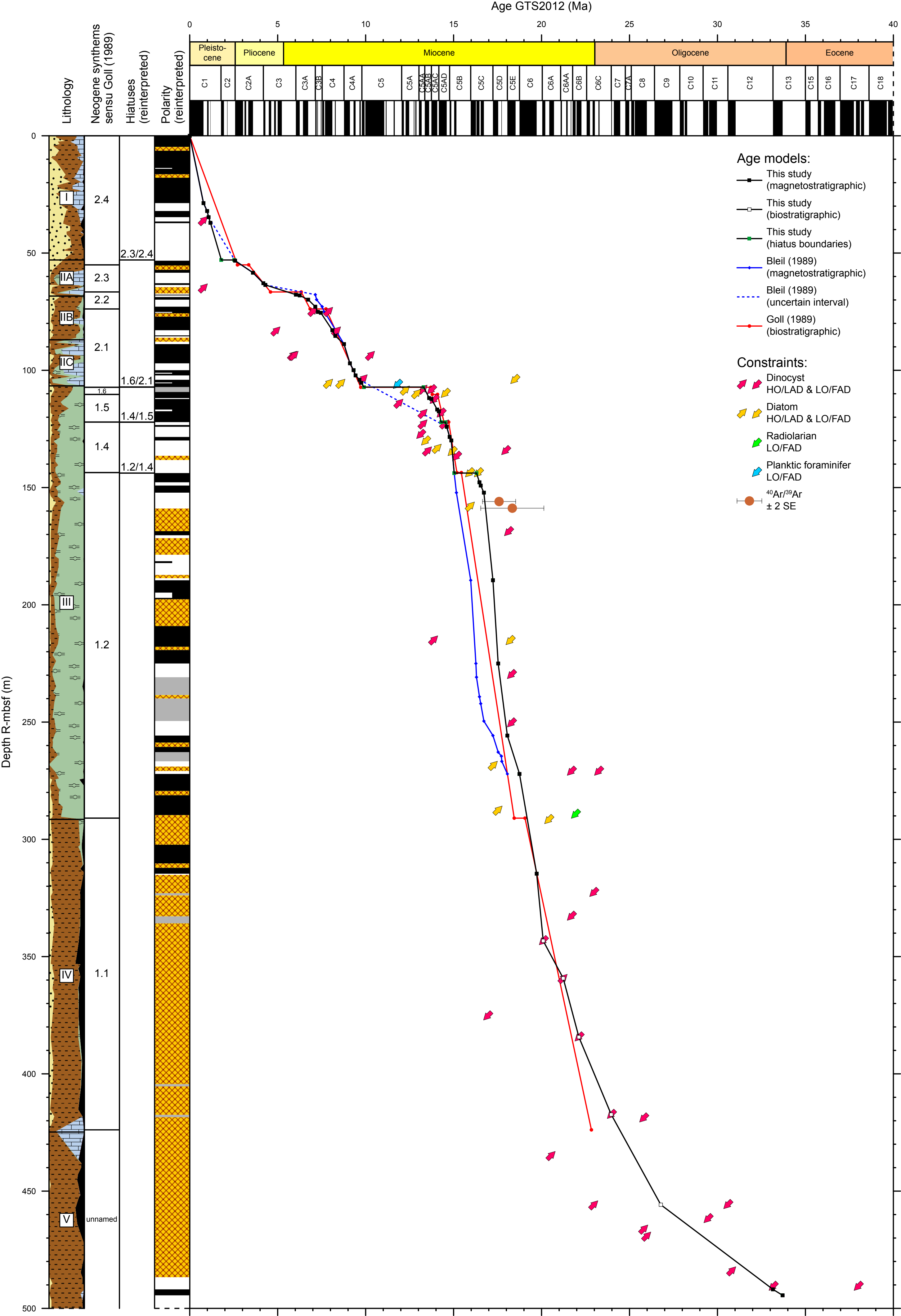
- Dinoflagellate Cyst Biostratigraphy, AASP Contributions Series, Vol. 17. American Association of Stratigraphic Palynologists Foundation, Dallas, TX, USA, pp. 105–128.
- Powell, A.J., 1992. Dinoflagellate cysts of the Tertiary System, in: Powell, A.J. (Ed.), A Stratigraphic Index of Dinoflagellate Cysts, British Micropalaeontological Society Publication Series. Chapman and Hall, London, UK, pp. 155–251.
- 305 Prince, I.M., Jarvis, I., Pearce, M.A., Tocher, B.A., 2008. Dinoflagellate cyst biostratigraphy of the Coniacian–Santonian (Upper Cretaceous): New data from the English Chalk. *Rev. Palaeobot. Palynol.* 150, 59–96. <https://doi.org/10.1016/j.revpalbo.2008.01.005>
- Pross, J., Houben, A.J.P., van Simaeys, S., Williams, G.L., Kotthoff, U., Coccioni, R., Wilpshaar, M., Brinkhuis, H., 2010.  
310 Umbria–Marche revisited: A refined magnetostratigraphic calibration of dinoflagellate cyst events for the Oligocene of the Western Tethys. *Rev. Palaeobot. Palynol.* 158, 213–235. <https://doi.org/10.1016/j.revpalbo.2009.09.002>
- Quaijtaal, W., Donders, T.H., Persico, D., Louwye, S., 2014. Characterising the middle Miocene Mi-events in the Eastern North Atlantic realm: A first high-resolution marine palynological record from the Porcupine Basin. *Palaeogeogr. Palaeoclimatol. Palaeoecol.* 399, 140–159. <https://doi.org/10.1016/j.palaeo.2014.02.017>
- 315 Quaijtaal, W., Mertens, K.N., Louwye, S., 2015. Some new acritarch species from the lower and middle Miocene of the Porcupine Basin, North Atlantic Ocean: biostratigraphy and palaeoecology. *Palynology* 39, 37–55. <https://doi.org/10.1080/01916122.2014.933749>
- Schreck, M., Matthiessen, J., 2014. *Batiacasphaera bergenensis* and *Lavradosphaera elongata* — New dinoflagellate cyst and acritarch species from the Miocene of the Iceland Sea (ODP Hole 907A). *Rev. Palaeobot. Palynol.* 211, 97–106.  
320 <https://doi.org/10.1016/j.revpalbo.2014.07.002>
- Schreck, M., Matthiessen, J., Head, M.J., 2012. A magnetostratigraphic calibration of Middle Miocene through Pliocene dinoflagellate cyst and acritarch events in the Iceland Sea (Ocean Drilling Program Hole 907A). *Rev. Palaeobot. Palynol.* 187, 66–94. <https://doi.org/10.1016/j.revpalbo.2012.08.006>
- Shackleton, N.J., Baldauf, J.G., Flores, J.-A., Iwai, M., Moore Jr., T.C., Raffi, I., Vincent, E., 1995. Biostratigraphic  
325 Summary for Leg 138, in: Pisias, N.G., Mayer, L.A., Janecek, T.R., Palmer-Julson, A., van Andel, T.H. (Eds.), Proceedings of the Ocean Drilling Program, Scientific Results, Vol. 138. Ocean Drilling Program, College Station, TX, USA, pp. 517–536. <https://doi.org/10.2973/odp.proc.sr.138.127.1995>
- Shipboard Scientific Party, 1987. Site 643: Norwegian Sea, in: Eldholm, O., Thiede, J., Taylor, E. (Eds.), Proceedings of the Ocean Drilling Program, Initial Reports, Vol. 104. Ocean Drilling Program, College Station, TX, USA, pp. 455–615.  
330 <https://doi.org/10.2973/odp.proc.ir.104.105.1987>
- Śliwińska, K.K., Abrahamsen, N., Beyer, C., Brünings-Hansen, T., Thomsen, E., Ulleberg, K., Heilmann-Clausen, C., 2012. Bio- and magnetostratigraphy of Rupelian–mid Chattian deposits from the Danish land area. *Rev. Palaeobot. Palynol.* 172, 48–69. <https://doi.org/10.1016/j.revpalbo.2012.01.008>

- Soliman, A., Ćorić, S., Head, M.J., Piller, W.E., El Beialy, S.Y., 2012. Lower and Middle Miocene biostratigraphy, Gulf of 335 Suez, Egypt based on dinoflagellate cysts and calcareous nannofossils. *Palynology* 36, 38–79.  
<https://doi.org/10.1080/01916122.2011.633632>
- Strauss, C., Lund, J.J., 1992. A Middle Miocene dinoflagellate cyst microflora from Papendorf near Hamburg, Germany. *Mitteilungen Geol. Inst. der Univ. Hambg.* 73, 159–189.
- Tocher, B.A., Jarvis, I., 1994. Dinoflagellate cyst distribution and stratigraphy of the lower-middle Cenomanian (Upper 340 Cretaceous) at Fumichon, Normandy, northern France. *Rev. Micropaléontologie* 37, 223–232.
- Tocher, B.A., Jarvis, I., 1996. Dinoflagellate cyst distributions and the Albian–Cenomanian boundary (mid-Cretaceous) at Cordebugle, NW France and Lewes, southern England. *J. Micropalaeontology* 15, 55–67. <https://doi.org/10.1144/jm.15.1.55>
- van Mourik, C.A., Brinkhuis, H., 2005. The Massignano Eocene-Oligocene golden spike section. *Stratigraphy* 2, 13–30.
- van Mourik, C.A., Brinkhuis, H., Williams, G.L., 2001. Mid- to Late Eocene organic-walled dinoflagellate cysts from ODP 345 Leg 171B, offshore Florida, in: Kroon, D., Norris, R.D., Klaus, A. (Eds.), *Western North Atlantic Palaeogene and Cretaceous Palaeoceanography, Special Publications*, Vol. 183. Geological Society, London, UK, pp. 225–251.  
<https://doi.org/10.1144/GSL.SP.2001.183.01.11>
- Van Simaeys, S., De Man, E., Vandenberghe, N., Brinkhuis, H., Steurbaut, E., 2004. Stratigraphic and palaeoenvironmental analysis of the Rupelian-Chattian transition in the type region: Evidence from dinoflagellate cysts, foraminifera and 350 calcareous nannofossils. *Palaeogeogr. Palaeoclimatol. Palaeoecol.* 208, 31–58. <https://doi.org/10.1016/j.palaeo.2004.02.029>
- Versteegh, G.J.M., Zevenboom, D., 1995. New genera and species of dinoflagellate cysts from the Mediterranean Neogene. *Rev. Palaeobot. Palynol.* 85, 213–229. [https://doi.org/10.1016/0034-6667\(94\)00127-6](https://doi.org/10.1016/0034-6667(94)00127-6)
- Williams, G.L., Fensome, R.A., MacRae, R.A., 2017. The Lentin and Williams index of fossil dinoflagellates 2017 edition. *Am. Assoc. Stratigr. Palynol. Contrib. Ser.* 48.
- Williams, G.L., Manum, S.B., 1999. Oligocene–early Miocene dinocyst stratigraphy of Hole 985A (Norwegian Sea), in: 355 Raymo, M.E., Jansen, E., Blum, P., Herbert, T.D. (Eds.), *Proceedings of the Ocean Drilling Program, Scientific Results*, Vol. 162. Ocean Drilling Program, College Station, TX, USA, pp. 99–109. <https://doi.org/10.2973/odp.proc.sr.162.030.1999>
- Williams, G.L., Stover, L.E., Kidson, E.J., 1993. Morphology and stratigraphic ranges of selected Mesozoic-Cenozoic dinoflagellate taxa in the Northern Hemisphere, Paper 92-10. Geological Survey of Canada, Ottawa, Canada.
- Wilpshaar, M., Santarelli, A., Brinkhuis, H., Visscher, H., 1996. Dinoflagellate cysts and mid-Oligocene chronostratigraphy 360 in the central Mediterranean region. *J. Geol. Soc. London.* 153, 553–561. <https://doi.org/10.1144/gsjgs.153.4.0553>
- Wrenn, J.H., Kokinos, J.P., 1986. Preliminary comments on Miocene through Pleistocene dinoflagellate cysts from De Soto Canyon, Gulf of Mexico, in: Wrenn, John H., Duffield, S.L., Stein, J.A. (Eds.), *Papers from the First Symposium on Neogene Dinoflagellate Cyst Biostratigraphy, AASP Contributions Series*, Vol. 17. American Association of Stratigraphic 365 Palynologists Foundation, Dallas, TX, USA, pp. 169–225.

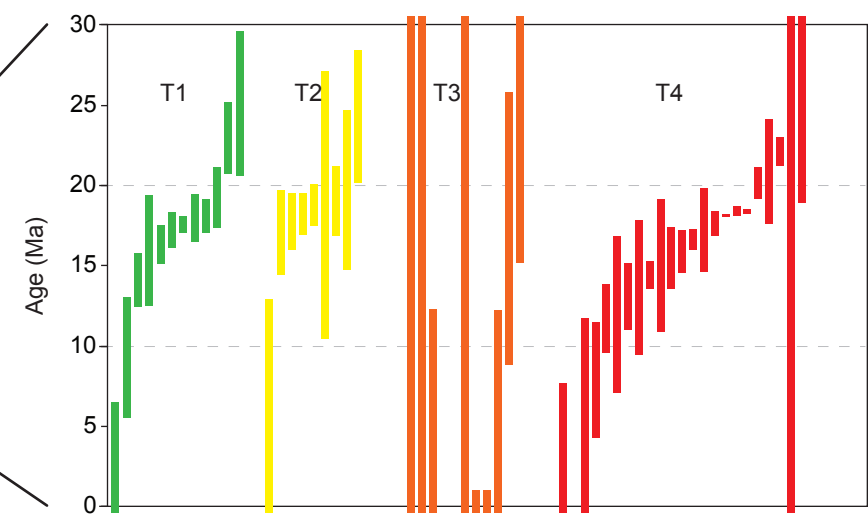
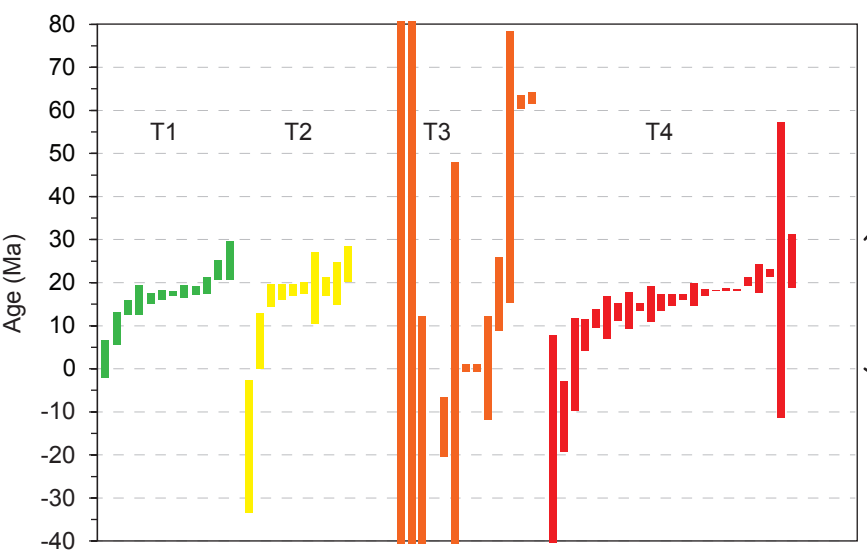
Yanagisawa, Y., Akiba, F., 1998. Refined Neogene diatom biostratigraphy for the northwest Pacific around Japan, with an introduction of code numbers for selected diatom biohorizons. *J. Geol. Soc. Japan* 104, 395–414.  
<https://doi.org/10.5575/geosoc.104.395>

Zegarra, M., Helenes, J., 2011. Changes in Miocene through Pleistocene dinoflagellates from the Eastern Equatorial Pacific  
370 (ODP Site 1039), in relation to primary productivity. *Mar. Micropaleontol.* 81, 107–121.  
<https://doi.org/10.1016/j.marmicro.2011.09.005>

Zevenboom, D., 1995. Dinoflagellate cysts from the Mediterranean Late Oligocene and Miocene. Utrecht University.



## Age calculations where negative intensities are allowed



## Age calculations where negative intensities are set to zero

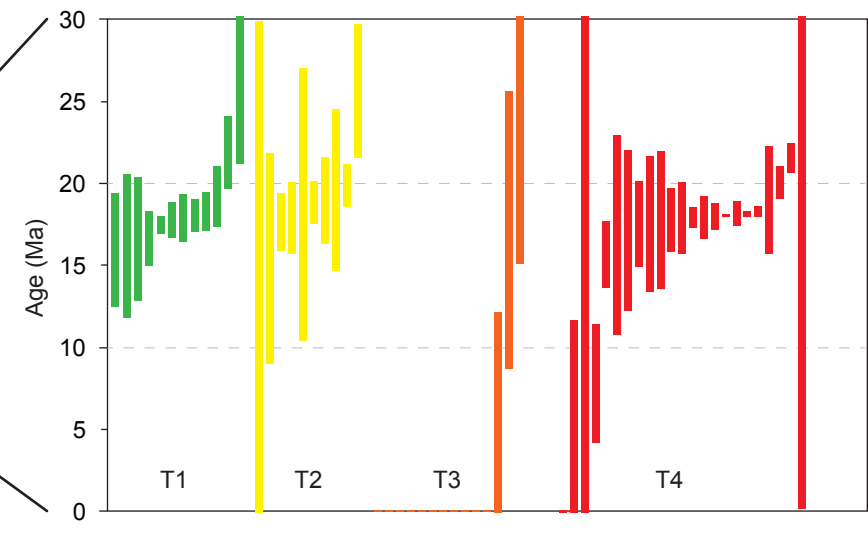


TABLE S1

200,44	213,76	22X	4	64	D	5	70	25	3,00	0,00	0,00	25,00	0,00	0,00	0,00	0,00	0,00	0,00	0,00	0,00	0,00	0,00	40,00	5,00	25,00	2,00	0,00	3,00	25,00	72,00	0,00	0,00	0,00		
203,43	216,75	22X	6	63	D	10	65	25	5,05	0,00	0,00	20,20	0,00	0,00	0,00	0,00	0,00	0,00	0,00	0,00	0,00	0,00	50,51	1,01	20,20	3,03	0,00	5,05	20,20	74,75	0,00	0,00	0,00		
204,48	217,80	22X	7	18	M	80	20	0,00	0,00	0,00	10,00	0,00	0,00	0,00	0,00	0,00	0,00	0,00	0,00	0,00	0,00	0,00	45,00	1,00	40,00	4,00	0,00	0,00	10,00	90,00	0,00	0,00	0,00		
205,40	219,22	23X	1	30	M	5	75	20	3,00	0,00	0,00	15,00	0,00	0,00	0,00	0,00	0,00	0,00	0,00	0,00	0,00	0,00	35,00	1,00	25,00	1,00	0,00	3,00	15,00	62,00	0,00	0,00	20,00		
207,60	221,42	23X	2	100	D	80	20	0,00	0,00	0,00	10,00	0,00	0,00	0,00	0,00	0,00	0,00	0,00	0,00	0,00	0,00	0,00	50,00	8,00	30,00	2,00	0,00	0,00	10,00	90,00	0,00	0,00	0,00		
210,12	223,94	23X	4	52	D	70	30	0,00	0,00	0,00	20,00	0,00	0,00	0,00	0,00	0,00	0,00	0,00	0,00	0,00	0,00	0,00	40,00	5,00	30,00	5,00	0,00	0,00	20,00	80,00	0,00	0,00	0,00		
213,38	227,20	23X	6	78	D	80	20	0,00	0,00	0,00	10,00	0,00	0,00	0,00	0,00	0,00	0,00	0,00	0,00	0,00	0,00	0,00	50,00	5,00	30,00	5,00	0,00	0,00	10,00	90,00	0,00	0,00	0,00		
213,48	227,30	23X	6	88	M	80	20	0,00	0,00	0,00	20,00	0,00	0,00	0,00	0,00	0,00	0,00	0,00	0,00	0,00	0,00	0,00	30,00	2,00	40,00	8,00	0,00	0,00	20,00	80,00	0,00	0,00	0,00		
215,70	230,04	24X	1	80	D	5	80	15	0,00	0,00	0,00	10,00	0,00	0,00	0,00	0,00	0,00	0,00	0,00	0,00	0,00	0,00	50,00	3,00	35,00	2,00	0,00	0,00	10,00	90,00	0,00	0,00	0,00		
218,00	232,42	24X	3	18	M	30	60	10	0,00	0,00	0,00	5,00	60,00	0,00	0,00	0,00	0,00	0,00	0,00	0,00	0,00	0,00	0,00	20,00	0,00	15,00	0,00	0,00	0,00	5,00	35,00	0,00	0,00	0,00	
220,50	234,84	24X	4	110	D	70	30	0,00	0,00	0,00	20,00	5,00	0,00	0,00	0,00	0,00	0,00	0,00	0,00	0,00	0,00	0,00	40,00	3,00	30,00	2,00	0,00	0,00	20,00	75,00	0,00	0,00	5,00		
223,13	237,47	24X	6	73	D	10	80	10	0,00	0,00	0,00	11,11	1,11	0,00	0,00	0,00	0,00	0,00	0,00	0,00	0,00	0,00	0,00	55,56	2,22	27,78	2,22	0,00	0,00	11,11	87,78	0,00	0,00	1,11	
224,28	238,62	24X	7	38	D	75	25	0,00	0,00	0,00	20,00	1,00	0,00	0,00	0,00	0,00	0,00	0,00	0,00	0,00	0,00	0,00	35,00	1,00	40,00	3,00	0,00	0,00	20,00	79,00	0,00	0,00	1,00		
226,70	241,54	25X	2	50	D	15	60	20	0,00	0,00	0,00	15,00	2,00	0,00	0,00	0,00	0,00	0,00	0,00	0,00	0,00	0,00	0,00	50,00	5,00	25,00	3,00	0,00	0,00	15,00	83,00	0,00	0,00	2,00	
229,63	244,49	25X	4	45	M	5	60	30	0,00	0,00	0,00	25,00	0,00	0,00	0,00	0,00	0,00	0,00	0,00	0,00	0,00	0,00	40,00	1,00	25,00	4,00	0,00	0,00	25,00	70,00	0,00	0,00	5,00		
233,20	248,04	25X	6	100	D	20	65	15	0,00	0,00	0,00	10,00	0,00	0,00	0,00	0,00	0,00	0,00	0,00	0,00	0,00	0,00	60,00	2,00	25,00	3,00	0,00	0,00	10,00	90,00	0,00	0,00	0,00		
233,60	248,44	25X	6	140	D	15	60	20	0,00	0,00	0,00	15,00	1,00	0,00	0,00	0,00	0,00	0,00	0,00	0,00	0,00	0,00	50,00	3,00	30,00	2,00	0,00	0,00	15,00	84,00	0,00	0,00	1,00		
234,21	249,15	25X	CC	12	M	60	30	10	0,00	0,00	0,00	5,00	60,00	0,00	0,00	0,00	0,00	0,00	0,00	0,00	0,00	0,00	0,00	25,00	0,00	20,00	0,00	0,00	0,00	5,00	45,00	0,00	0,00	50,00	
237,68	253,07	26X	3	18	M	95	5	0,00	0,00	0,00	0,00	0,00	0,00	0,00	0,00	0,00	0,00	0,00	0,00	0,00	0,00	0,00	0,00	0,00	0,00	0,00	0,00	0,00	0,00	0,00	0,00	0,00	0,00	0,00	0,00
238,49	253,88	26X	3	99	D	20	60	20	0,00	0,00	0,00	20,00	0,00	0,00	0,00	0,00	0,00	0,00	0,00	0,00	0,00	0,00	45,00	1,00	30,00	4,00	0,00	0,00	20,00	80,00	0,00	0,00	0,00		
240,19	255,58	26X	4	119	M	50	25	20	0,00	0,00	0,00	25,00	4,00	0,00	0,00	0,00	0,00	0,00	0,00	0,00	0,00	0,00	20,00	0,00	15,00	0,00	0,00	0,00	25,00	35,00	0,00	0,00	40,00		
242,35	257,74	26X	6	35	D	5	85	10	0,00	0,00	0,00	10,00	0,00	0,00	0,00	0,00	0,00	0,00	0,00	0,00	0,00	0,00	40,00	0,00	45,00	5,00	0,00	0,00	10,00	90,00	0,00	0,00	3,00		
243,17	258,56	26X	6	117	M	60	35	5	0,00	0,00	0,00	5,00	90,00	0,00	0,00	0,00	0,00	0,00	0,00	0,00	0,00	0,00	0,00	0,00	0,00	0,00	0,00	0,00	0,00	0,00	95,00	0,00	0,00	0,00	
244,88	260,80	27X	1	59	D	10	80	10	0,00	0,00	0,00	10,00	0,00	0,00	0,00	0,00	0,00	0,00	0,00	0,00	0,00	0,00	55,00	2,00	30,00	3,00	0,00	0,00	10,00	90,00	0,00	0,00	0,00		
248,16	264,07	27X	3	86	D	70	30	0,00	0,00	0,00	25,00	1,00	0,00	0,00	0,00	0,00	0,00	0,00	0,00	0,00	0,00	0,00	30,00	1,00	40,00	3,00	0,00	0,00	25,00	74,00	0,00	0,00	1,00		
252,20	268,11	27X	6	40	D	70	30	0,00	0,00	0,00	0,00	0,00	0,00	0,00	0,00	0,00	0,00	0,00	0,00	0,00	40,00	4,53	27,67	2,67	0,00	0,00	0,00	0,00	0,00	0,00	0,00	0,00	0,00	0,00	
252,78	268,69	27X	6	98	M	80	20	0,00	0,00	0,00	0,00	0,00	0,00	0,00	0,00	0,00	0,00	0,00	0,00	0,00	50,00	6,25	37,50	6,25	0,00	0,00	0,00	0,00	0,00	0,00	0,00	0,00	0,00	0,00	
256,45	271,06	28X	4	55	D	15	65	20	2,00	0,00	0,00	15,00	3,00	0,00	0,00	0,00	0,00	0,00	0,00	0,00	0,00	0,00	59,41	4,95	1,98	0,00	0,00	0,00	2,00	85,00	0,00	0,00	0,00		
257,05	273,49	28X	2	148	M	0	0	0,00	0,00	0,00	20,00	50,00	0,00	0,00	0,00	0,00	0,00	0,00	0,00	0,00	0,00	0,00	0,00	0,00	0,00	0,00	0,00	0,00	0,00	0,00	0,00	0,00	0,00		
257,60	274,01	28X	3	50	D	15	55	30	3,00	0,00	0,00	25,00	0,00	0,00	0,00	0,00	0,00	0,00	0,00	0,00	0,00	0,00	50,00	2,00	20,00	2,00	0,00	0,00	25,00	72,00	0,00	0,00	0,00		
258,00	274,47	28X	3	96	D	20	70	10	9,09	0,00	0,00	9,13	64	0,00	0,00	0,00	0,00	0,00	0,00	0,00	0,00	0,00	0,00	45,45	0,00	22,73	0,00	0,00	0,00	9,09	68,18	0,00	0,00	13,64	
260,88	277,29	28X	5	78	D	5	70	25	3,00	0,00	0,00	20,00	0,00	0,00	0,00	0,00	0,00	0,00	0,00	0,00	0,00	0,00	40,00	2,00	35,00	0,00	0,00	0,00	20,00	77,00	0,00	0,00	0,00		
262,58	278,99	28X	6	98	D	10	60	30	5,00	0,00	0,00	25,00	0,00	0,00	0,00	0,00	0,00	0,00	0,00	0,00	0,00	0,00	50,00	10,00	5,00	0,00	0,00	0,00	25,00	70,00	0,00	0,00	0,00		
263,29	279,70	28X	7	19	D	15	55	30	7,00	0,00	0,00	21,00	0,00	0,00	0,00	0,00	0,00	0,00	0,00	0,00	0,00	0,00	55,00	10,00	5,00	0,00	0,00	0,00	21,00	72,00	0,00	0,00	0,00		
264,60	281,51	29X	1	70	D	15	60	25	4,95	0,00	0,00	22,77	0,99	0,00	0,00	0,00	0,00	0,00	0,00	0,00	0,00	0,00	59,41	4,95	1,98	0,00	0,00	0,00	22,77						



TABLE S2

Core	Core top (mbsf)	Drilled length (m)	Core recovery (m)	Core recovery (%)	Individual offset (m)	Cumulative offset (m)	Core top (R-mbsf)
1H	0,00	5,30	5,25	99,06	0,00	0,00	0,00
2H	5,30	9,50	9,81	103,26	0,50	0,50	5,80
3H	14,80	9,50	9,83	103,47	0,81	1,31	16,11
4H	24,30	9,50	9,91	104,32	0,83	2,14	26,44
5H	33,80	9,50	9,43	99,26	0,91	3,05	36,85
6H	43,30	9,50	8,74	92,00	0,50	3,55	46,85
7H	52,80	9,50	8,15	85,79	0,50	4,05	56,85
8H	62,30	9,50	9,47	99,68	0,50	4,55	66,85
9H	71,80	9,50	9,91	104,32	0,50	5,05	76,85
10H	81,30	9,50	9,52	100,21	0,91	5,96	87,26
11H	90,80	9,50	9,90	104,21	0,52	6,48	97,28
12H	100,30	9,50	9,30	97,89	0,90	7,38	107,68
13H	109,80	9,50	9,82	103,37	0,50	7,88	117,68
14H	119,30	9,50	9,13	96,11	0,82	8,70	128,00
15H	128,80	9,50	9,42	99,16	0,50	9,20	138,00
16H	138,30	9,50	9,88	104,00	0,50	9,70	148,00
17X	147,80	9,50	0,67	7,05	0,88	10,58	158,38
18X	157,30	9,50	3,62	38,11	0,50	11,08	168,38
19X	166,80	9,50	9,49	99,89	0,50	11,58	178,38
20X	176,30	9,50	9,74	102,53	0,50	12,08	188,38
21X	185,80	9,50	5,28	55,58	0,74	12,82	198,62
22X	195,30	9,80	9,75	99,49	0,50	13,32	208,62
23X	205,10	9,80	9,82	100,20	0,50	13,82	218,92
24X	214,90	9,80	9,78	99,80	0,52	14,34	229,24
25X	224,70	9,80	9,85	100,51	0,50	14,84	239,54
26X	234,50	9,80	9,82	100,20	0,55	15,39	249,89
27X	244,30	9,80	9,71	99,08	0,52	15,91	260,21
28X	254,10	9,80	9,77	99,69	0,50	16,41	270,51
29X	263,90	9,80	9,82	100,20	0,50	16,91	280,81
30X	273,70	9,80	0,55	5,61	0,52	17,43	291,13
31X	283,50	9,80	9,84	100,41	0,50	17,93	301,43
32X	293,30	9,80	4,88	49,80	0,54	18,47	311,77
33X	303,10	9,80	4,88	49,80	0,50	18,97	322,07
34X	312,90	9,80	4,02	41,02	0,50	19,47	332,37
35X	322,70	9,80	3,79	38,67	0,50	19,97	342,67
36X	332,50	9,80	8,82	90,00	0,50	20,47	352,97
37X	342,30	9,80	6,17	62,96	0,50	20,97	363,27
38X	352,10	9,70	3,65	37,63	0,50	21,47	373,57
39X	361,80	9,60	3,65	38,02	0,50	21,97	383,77
40X	371,40	9,70	1,07	11,03	0,50	22,47	393,87
41X	381,10	9,60	1,83	19,06	0,50	22,97	404,07
42X	390,70	9,70	5,29	54,54	0,50	23,47	414,17
43X	400,40	9,60	0,41	4,27	0,50	23,97	424,37
44X	410,00	9,70	9,82	101,24	0,50	24,47	434,47
45X	419,70	9,70	8,93	92,06	0,62	25,09	444,79
46X	429,40	9,70	9,75	100,52	0,50	25,59	454,99
47X	439,10	9,60	9,80	102,08	0,55	26,14	465,24
48X	448,70	9,70	9,82	101,24	0,70	26,84	475,54
49X	458,40	9,70	9,74	100,41	0,62	27,46	485,86
50X	468,10	9,60	1,23	12,81	0,54	28,00	496,10
51X	477,70	9,60	9,79	101,98	0,50	28,50	506,20
52X	487,30	9,70	9,85	101,55	0,69	29,19	516,49
53X	497,00	9,70	9,20	94,85	0,65	29,84	526,84
54X	506,70	9,70	9,83	101,34	0,50	30,34	537,04
55X	516,40	9,60	9,82	102,29	0,63	30,97	547,37
56X	526,00	9,60	9,69	100,94	0,72	31,69	557,69
57X	535,60	9,60	9,64	100,42	0,59	32,28	567,88
59X	545,20	9,70	1,45	14,95	0,54	32,82	578,02
60X	554,90	6,30	3,73	59,21	0,50	33,32	588,22
61X	561,20	2,50	1,75	70,00	0,50	33,82	595,02
62X	563,70	1,50	1,71	114,00	0,50	34,32	598,02

TABLE S3

Top depth (mbsf)	Top depth (R-mbsf)	Core	Section	Half	Interval (cm)	Sample size (g)
100,920	108,300	12H	1	W	62-64	1,08
103,920	111,300	12H	3	W	62-64	1,11
110,440	118,320	13H	1	W	64-66	1,07
114,920	122,800	13H	4	W	62-64	1,07
119,980	128,680	14H	1	W	68-70	1,04
129,480	138,680	15H	1	W	68-70	1,03
135,480	144,680	15H	5	W	68-70	1,07
138,900	148,600	16H	1	W	60-62	1,08
148,240	158,820	17X	1	W	44-46	1,02
157,780	168,860	18X	1	W	48-50	1,05
167,300	178,880	19X	1	W	50-52	1,06
176,720	188,800	20X	1	W	42-44	1,11
186,340	199,160	21X	1	W	54-56	1,04
195,850	209,170	22X	1	W	55-57	1,10
205,650	219,470	23X	1	W	55-57	1,06
215,450	229,790	24X	1	W	55-57	1,05
225,220	240,060	25X	1	W	52-54	1,05
235,020	250,410	26X	1	W	52-54	0,99
244,890	260,800	27X	1	W	59-61	1,03
254,620	271,030	28X	1	W	52-54	1,06
264,400	281,310	29X	1	W	50-52	1,00
273,800	291,230	30X	CC	W	10-12	1,03
284,050	301,980	31X	1	W	55-57	1,05
293,800	312,270	32X	1	W	50-52	1,11
303,725	322,695	33X	1	W	62.5-64.5	1,05
313,375	332,845	34X	1	W	47.5-49.5	1,13
323,320	343,290	35X	1	W	62-64	1,14
333,090	353,560	36X	1	W	59-61	1,09
342,870	363,840	37X	1	W	57-59	1,07
352,650	374,120	38X	1	W	55-57	1,14
362,350	384,320	39X	1	W	55-57	1,08

TABLE S4

Top depth (mbsf)	Top depth (R-mbsf)	Core	Section	Half	Interval (cm)	Volume (cc)	Selected for Ar/Ar analysis	Macroscopic description
99,890	106,370	11H	7	W	9-10	5		Discrete layer ~1 cm thick
103,910	111,290	12H	3	W	61-62	5		Lens
110,040	117,920	13H	1	W	24-26	5		Lenses
125,070	133,770	14H	4	W	127-129	5		Lens with thickness varying between 4 cm on one side and pinching out on other side.
125,260	133,960	14H	4	W	146-147	5		Not a very distinct layer, but more dispersed in sediment. Secondary gypsum crystals might indicate volcanic material.
134,745	143,945	15H	4	W	144.5-145.5	5		Volcanic ash
139,640	149,340	16H	1	W	134-135	5		Discrete ash layer, 2-7 mm thick. Crystals visible with hand lens.
140,005	149,705	16H	2	W	20.5-21.5	5		Discrete layer ~1 cm thick
146,260	155,960	16H	6	W	46-48	5	X	Thick relatively coarse ash
148,210	158,790	17X	1	W	41-43.5	5	X	Ash interval
160,040	171,120	18X	2	W	124-126	5		Disseminated layer
170,730	182,310	19X	3	W	93-96	5		Discrete layer ~4 cm thick
172,465	184,045	19X	4	W	116.5-117.5	5		
196,655	209,975	22X	1	W	135.5-137.5	5		
199,580	212,900	22X	3	W	128-130	5	X	Dark grey ash ~2 cm thick
218,080	232,420	24X	3	W	18-19	5		Discrete but not continuous layer
237,420	252,810	26X	2	W	142-143	5		Dispersed ash?
257,080	273,490	28X	2	W	148-150	5	X	Discrete ash

TABLE S5

<b>Detector</b>	<b>H2</b>	<b>H1</b>	<b>AX</b>	<b>L1</b>	<b>L2</b>	<b>L3</b>
<b>Amplifier</b>	$10^{12} \Omega$	$10^{13} \Omega$	$10^{13} \Omega$	$10^{13} \Omega$	CDD	CDD
<b>Isotope -&gt;1000fA <math>^{40}\text{Ar}</math></b>	$^{40}\text{Ar}$	$^{39}\text{Ar}$	$^{38}\text{Ar}$	$^{37}\text{Ar}$	$^{36}\text{Ar}$	
<b>Isotope -&lt;1000fA <math>^{40}\text{Ar}</math></b>		$^{40}\text{Ar}$	$^{39}\text{Ar}$	$^{38}\text{Ar}$	$^{37}\text{Ar}$	$^{36}\text{Ar}$





TABLES

Species reported by:	Category	Species/taxon	Consisting of/synonymized with:	Based on:	Also included in:	Stratigraphic notes
Ma	species	<i>Achillesodium biformoides</i>				
Ma	species	<i>Thalassiphora pelagica</i>				
Ma	spp.	<i>Achomosphaera</i> spp. (pars.)				
TS, Ma, Mu	spp.	<i>Palaeocystodinium</i> spp.	Grouped records of <i>P. golowense</i> , <i>P.</i> sp. 1, <i>P.</i> sp. 2, <i>P.</i> sp. 3, <i>P.</i> sp. A of Costa and Downie (1979).	Dinofla3 (Williams et al., 2017)		
TS, Ma, Mu	species	<i>Palaeocystodinium golowense</i>			<i>Palaeocystodinium</i> spp.	
TS, Ma	spp.	<i>Operculodinium</i> spp. (pars.)				
TS, Ma	species	<i>Spiniferites pseudofurcatus</i>				
TS, Ma, Mu	spp.	<i>Impagidinium</i> spp. (pars.)				
TS, Ma, Mu	spp.	<i>Spiniferites</i> spp. (pars.)				
Ma	species	<i>Deflandrea phosphoritica</i>				
Ma	spp.	<i>Glyphyrocysta</i> spp. (pars.)				
Ma	species	<i>Licracysta semicirculata</i>	Ma: <i>Glyphyrocysta intricata</i>	Ma: <i>Glyphyrocysta intricata</i>		
TS, Ma, Mu	species	<i>Cleistosphaeridium placacanthum</i>	Ma, Mu: <i>Systematophora placacantha</i>	Dinofla3 (Williams et al., 2017)		
TS, Ma, Mu	species	<i>Nematosphaeropsis labyrinthus</i>				
TS, Ma	species	<i>Apteoiodinium austriense</i>				
TS, Ma, Mu	species	<i>Lingulodinium machaerophorum</i>				
Ma	species	<i>Pentadinium laticinctum laticinctum</i>				
TS, Ma	species	<i>Impagidinium velorum</i>				
TS, Ma	species	<i>Spiniferites rarus</i>				
TS, Ma	species	<i>Dinopterygium cladooides</i> sensu Morgenroth (1966)				
TS, Ma	species	<i>Cordosphaeridium cantharellus</i>				
Ma	species	<i>Enneadiscostauca</i>	Ma: <i>Areosphaeridium arcuatum</i>	Dinofla3 (Williams et al., 2017)		
Ma	species	<i>Distatodinium "craterum"</i>	Grouped records of <i>D. paradoxum</i> , <i>D. "craterum"</i> .	Dinofla3 (Williams et al., 2017)	<i>Distatodinium paradoxum</i> (s.l.)	
TS, Ma	species	<i>Distatodinium paradoxum</i> (s.l.)				
Ma	species	<i>Chiropertidium lobospinosum</i>				
TS, Ma	species	<i>Heterula/cacysta campanula</i>				
TS, Ma	species	<i>Spiniferites hyperacanthus</i>				
TS, Ma, Mu	spp.	<i>Impletosphaeridium</i> spp.				
TS, Ma	species	<i>Batiacosphaera micropapillata</i>				
TS, Ma, Mu	species	<i>Reticulatosphaera actinocoronata</i>	Ma: <i>Areosphaeridium actinocoronatum</i>	Dinofla3 (Williams et al., 2017)		
Ma	species	<i>Chiropertidium partispinatum</i>	Grouped records of <i>C. partispinatum</i> , <i>C. mespilum</i> .	Dinofla3 (Williams et al., 2017)	<i>Chiropertidium galea</i> (s.l.)	
Ma	species	<i>Chiropertidium galea</i> (s.l.)				
TS, Ma	species	<i>Impagidinium aculeatum</i>				
Ma	species	<i>Pentadinium laticinctum granulatum</i>				
TS, Ma	species	<i>Leptodinium italicum</i>	Ma: <i>Impagidinium</i> sp. 1			
TS, Ma	species	<i>Distatodinium paradoxum</i> (s.s.)			<i>Distatodinium paradoxum</i> (s.l.)	
TS, Ma	species	<i>Homotryblium floripes</i>				
TS, Ma	species	<i>Minisphaeridium latirictum</i>	Ma: <i>Hystrichosphaeridium latirictum</i> & Dinocyst II of Manum (1976)			
TS, Ma, Mu	species	<i>Hystrichokolpoma rigaudiae</i>				
TS, Ma	species	<i>Hystrichokolpoma cinctum</i>				
TS, Ma, Mu	species	<i>Apteoiodinium spiridooides</i>	Ma, Mu: <i>Emsländia spiridooides</i>	Dinofla3 (Williams et al., 2017)		
TS, Ma, Mu	species	<i>Operculodinium centrocarpum</i>				
Ma	species	<i>Chiropertidium mespilum</i>			<i>Chiropertidium galea</i> (s.l.)	
TS, Ma	species	<i>Caligodinium amicum</i>				
TS, Ma, Mu	species	<i>Invertocysta tabulata</i>				
TS, Ma, Mu	species	<i>Operculodinium janduchenei</i>	Ma: <i>Operculodinium</i> sp. 1; Mu: <i>Operculodinium</i> sp. Jan du Chêne (1977).			
Ma	species	<i>Dapsilidinium pseudocolligerum</i>				
TS, Ma	species	<i>Impagidinium pallidum</i>	Grouped records of <i>D. pastielsii</i> and <i>D. pseudocolligerum</i> .		<i>Dapsilidinium pastielsii</i> (s.l.)	
TS, Ma, Mu	species	<i>Dapsilidinium pastielsii</i> (s.l.)				
TS, Ma	species	<i>Batiacosphaera baculata</i> sensu Manum et al. (1989)				
TS, Ma	species	<i>Batiacosphaera hirsuta</i>				
TS	species	<i>Xandarodinium xanthum</i>				
TS, Ma	species	<i>Evittosphaerula paratabulata</i>				
TS, Ma	spp.	<i>Hystrichosphaeridium</i> ? spp.				
TS	species	<i>Cleistosphaeridium ancyrum</i>	Probably included in <i>C. placacanthum</i> by Manum et al. (1989) and Mudie (1989).			
TS	species	<i>Solenopeltix brevipinosa</i>				
TS	spp.	<i>Cleistosphaeridium</i> spp. (pars.)				
TS	spp.	<i>Dinocyst</i> spp. (pars.)				
TS	spp.	<i>Spiniferites</i> / <i>Achomosphaera</i> spp. (pars.)				
TS, Ma	species	<i>Lejeune cysta fallax</i>				
TS, Ma, Mu	species	<i>Batiacosphaera sphaerica</i>				
TS, Ma, Mu	species	<i>Tuberculodinium vancampae</i>				
TS, Ma, Mu	species	<i>Dapsilidinium pastielsii</i> (s.s.)			<i>Dapsilidinium pastielsii</i> (s.l.)	
TS, Ma, Mu	species	<i>Operculodinium piaseckii</i>	Ma, Mu: <i>Operculodinium</i> sp. of Piasecki (1980)			
TS	spp.	<i>Arcticacysta</i> ? spp.				
TS, Ma, Mu	species	<i>Operculodinium piaseckii</i>				
TS	spp.	<i>Arcticacysta</i> ? spp.				

TS	spp.	<i>Lejeuneicysta</i> spp. (pars.)				
TS, Ma	species	<i>Impagidinium japonicum</i>				
TS, Mu,	species	<i>Tectatodinium pellitum</i> (s.l.)	Grouped records of <i>T. pellitum</i> (s.s.) (specimens of Mudie (1989) with question mark) and <i>T. sp.</i> of Piasek (1980) sensu Mudie (1989) (with question mark).	Grouped following questionable synonymy of <i>T. sp.</i> sp. of Piasek (1980) sensu Mudie (1989) according to amended species description (Head, 1994).		
TS, Mu,	species	<i>Tectatodinium pellitum</i> (s.s.)		Synonymy of <i>T. sp.</i> 2 based on species description of <i>T. grande</i> (Williams et al., 1993), which is considered a junior synonym of <i>T. pellitum</i> (Head, 1994). <i>T. pellitum</i> of Mudie (1989) at ODP Site 642 is not <i>T. pellitum</i> , but possibly <i>Habibacysta tectata</i> (See Head, 1994). However, <i>T. pellitum</i> has been confirmed from the Pliocene of ODP Site 644 in samples of Mudie (1989) by Head (1994). Therefore uncertainty remains about specimens at ODP Site 643.		
TS, Mu,	species	<i>Cribroperidinium tenuitubulatum</i>			<i>Tectatodinium pellitum</i> (s.l.) / <i>Habibacysta tectata</i> (s.l.)	
TS, Ma	species	<i>Aptodinium tectatum</i>				
TS, Ma,	species	<i>Hystrichosphaeropsis obscura</i>		Includes specimens of <i>O. ?eirikianum</i> (Head and Wrenn, 1992; Head, 1993).		
Ma, Mu	species	<i>Operculodinium longispinigerum</i>				
TS	species	<i>Distatodinium "covatum"</i>				
TS	species	<i>Spiniferites mirabilis</i>				
TS, Ma,	species	<i>Pentadinium imaginatum</i>				
TS	species	<i>Lejeuneicysta hyalina</i>				
TS, Mu	species	<i>Spiniferites pachydermus</i>				
TS, Mu	species	<i>Polyphaenidium zoharyi</i>				
TS	spp.	<i>Cribroperidinium</i> spp. (pars.)				
TS	species	<i>Exochosphaeridium insigne</i>				
TS, Ma	species	<i>Impagidinium paradoxum</i>				
TS, Ma	species	<i>Impagidinium patulum</i>				
TS, Ma,	species	<i>Selenopempix rephroides</i>				
Ma	species	<i>Pterodinium cingulatum cingulatum</i>				
TS, Ma	species	<i>Impagidinium elongatum</i>	Ma: <i>I. sp.</i> 3.			
TS	spp.	<i>Corrudinium?</i> spp.				
TS	species	<i>Lejeuneicysta cinctoria</i>				
TS	species	<i>Sumatradinium soucouyaniae</i>				
TS, Ma,	species	<i>Melitasphaeridium chaonophorum</i>				
TS, Ma	species	<i>Cannospheeropsis utinensis</i>				
TS, Ma	species	<i>Lophocysta sulcolumbata</i>				
TS, Ma	species	<i>Pyxdinopsis isolata</i>	Ma: <i>Tectatodinium psilatum</i>	DinoflaJ3 (Williams et al., 2017)		
TS, Ma	species	<i>Dalela chathamensis</i>				
TS, Ma	species	<i>Nematosphaeropsis downiei</i>				
TS	species	<i>Cleistosphaeridium diversispinosum</i>		Probably included in <i>C. placacanthum</i> by Manum et al. (1989) and Mudie (1989).		
TS, Ma	species	<i>Homotrybium vallum</i>				
Ma	species	<i>Spiniferites ramosus breifurcatus</i>				
TS, Ma	species	<i>Cribroperidinium giuseppei</i>	Ma: <i>Cribroperidinium giuseppei major</i>	DinoflaJ3 (Williams et al., 2017)		
TS, Ma	species	<i>Operculodinium? placutum</i>				
TS	species	<i>Pyxdinopsis tuberculata</i>				
TS, Ma	species	<i>Cousteaudinium Aubryae</i>	Ma: Dinocyst sp. 6			
TS, Ma,	species	<i>Filisphaera filifera</i>				
TS, Ma,	species	<i>Labyrinthodinium truncatum</i> (s.l.)	Grouped records of <i>L. truncatum</i> and <i>L. cf. truncatum</i> .	Grouped following questionable synonymy according to Schreck et al. (2012).		
TS	spp.	<i>Lingulodinium</i> spp. (pars.)				
Ma, Mu	species	<i>Operculodinium crassum</i>				
TS, Ma,	species	<i>Trinavonetidium applanatum</i>	Ma: <i>T. cf. capitatus</i> ; Ma: <i>T. capitatum</i> .	DinoflaJ3 (Williams et al., 2017); Possibly junior synonym of <i>O. israelianum</i> . Here not synonymized.		
TS	species	<i>Sumatradinium hispidum</i>		DinoflaJ3 (Williams et al., 2017); Synonymy of <i>T. cf. capitatus</i> based on photographs by Manum et al. (1989).		
TS	spp.	<i>Sumatradinium</i> spp. (pars.)				
TS	species	<i>Erymnodinium detectabile</i>				
TS	spp.	<i>Pyxdinopsis</i> spp. (pars.)				
TS	species	<i>Hystrichostrogylon membraniphorum</i> (s.s.)				
TS	species	<i>Hystrichostrogylon membraniphorum</i> (s.l.)	Grouped records of <i>H. membraniphorum</i> and <i>H. cf. membraniphorum</i> .	Grouped based on photographs by Manum et al. (1989).	<i>Hystrichostrogylon membraniphorum</i> (s.l.)	
TS, Ma	species	<i>Pyxiella?</i> spp.				
TS	species	<i>Sumatradinium druggii</i>				
TS	spp.	<i>Baticapsphaera?</i> spp.				
TS	spp.	<i>Cerebrocysta</i> spp. (pars.)				
TS, Ma,	species	<i>Labyrinthodinium truncatum</i> (s.s.)			<i>Labyrinthodinium truncatum</i> (s.l.)	
TS, Ma,	species	<i>Invertocysta lacrymosa</i>				
Ma	species	<i>Nematosphaeropsis lemnickata</i>				
Ma	species	<i>Achomosphaera crassipellis</i>				
Ma	species	<i>Pyxidiella simplex</i>	Ma: <i>Tectatodinium simplex</i>	DinoflaJ3 (Williams et al., 2017)		
TS	spp.	<i>Hystrichostrogylon</i> spp. (pars.)				
TS, Mu	species	<i>Impagidinium multiplexum</i>				
TS, Ma	species	<i>Impagidinium maculatum</i>				
TS, Mu	species	<i>Habibacysta tectata</i> (s.l.)	Grouped records of <i>H. tectata</i> (s.s.), <i>Tectatodinium pellitum</i> sensu Mudie (1989) and (1989) (with question mark), Dinocyst sp. 1 (with question mark), and <i>Habibacysta?</i> cf. ( <i>tectata</i> ) (amended) description by Head (1994). <i>H. ? tectata</i> (with question mark). Note that occurrences of <i>T. pellitum</i> sensu Mudie (1989) are also included in <i>T. pellitum</i> (s.s.) with question marks.	Grouped following questionable synonymy of <i>T. pellitum</i> sensu Mudie (1989) and (1989) (with question mark), Dinocyst sp. 1 of Mudie (1989) according to (amended) description by Head (1994). <i>H. ? tectata</i> (TS) not included in <i>H. tectata</i> (s.s.), due to distinct stratigraphic range, but here included (with question mark) in <i>H. tectata</i> (s.l.).		
TS, Mu,	species	<i>Unipontidinium aquaeductus</i>	Ma, Mu: <i>Impagidinium aquaeductum</i>	DinoflaJ3 (Williams et al., 2017)		
TS, Ma,	species	<i>Cerebrocysta poulsenii</i>	Ma: Gen. et sp. indet. of Piasek (1980)	Synonymized following species description (de Verteuil and Norris, 1996).		
Mu	species	<i>Gramocysta verricula</i>	Ma: <i>Dinopterygium verriculum</i>	DinoflaJ3 (Williams et al., 2017)		
Mu	species	<i>Achomosphaera ramulifera</i>				
Mu	species	<i>Operculodinium walli</i>				

The LAD of 9.867 Ma is based on 67% in NN9 (de Verteuil and Norris, 1996), but the exact position in NN9 is unknown. 100% NN9 is 9.53 Ma (GTS2012), which is consistent with our magnetostratigraphic interpretation.

TS, Ma	species	<i>Achemosphaera andalouensis</i>			
Mu	species	<i>Selenopemphix dionaeacysta</i>			
TS	species	<i>Habibacysta tectata</i> (s.s.)			
			<i>Habibacysta tectata</i> (s.l.)		
TS, Ma	species	<i>Cerebrocysta irregularis</i>			
TS	species	<i>Batiacapsphaera bergenensis</i>			
Mu	species	<i>Impagidinium sphaericum</i>			
Mu	species	<i>Spiniferites rubinus</i>			
Mu	species	<i>Bitectatodinium tepikiense</i>			
Mu	species	<i>Amiculospaera umbracula</i>			
Mu	species	<i>Hystrichosphaerops pantaniana</i>			
Mu, Mu	species	<i>Spiniferites bentorii</i>			
Mu	species	<i>Operculodinium israelianum</i>			
Mu, Mu	species	<i>Spiniferites elongatus</i>			
Mu	species	<i>Brigantedinium simplex</i>			
Mu	species	<i>Islandinium minutum</i>			
Mu	species	<i>Scripsiella acuminata</i> cyst			
Mu	species	<i>Spiniferites scabratus</i>			
Mu	specie	<i>Ataxiodinium chaone</i>			
TS, Ma	specie	<i>Cyclopsiella lusatica</i>			
TS	specie	<i>Pusillispheara solaris</i>			
TS	specie	<i>Skolarchoritecrtarchs</i>			
TS, Ma	specie	<i>Platycystidia manumii</i>			
TS	specie	<i>Acrirarch spp.</i> (pars.)			
TS, Mu	specie	<i>Cymatosphaera ?invaginata</i>			
TS	specie	<i>Porcupinea indentata</i>			
Mu	specie	<i>Cyclopsiella elliptica</i>			
Mu	specie	<i>Palaeostomocystis</i> spp.			
Ma	open	<i>Areniana</i> sp. 1			
Ma	open	<i>Spiniferites</i> sp. 1 of Manum et al. (1989)			
Ma	open	<i>Spiniferites</i> sp. 2			
Ma	open	<i>Gelatia</i> sp. 1			
Ma	open	<i>Dinocyst</i> sp. 3 ( <i>Evittosphaerula</i> ? sp. 1)			
Ma	open	<i>Arealgera</i> sp. 1			
Ma	open	<i>Samlandia</i> sp. 1			
Ma	open	<i>Pyxidinopsis</i> sp. 1			
Ma	open	<i>Palaeocystodinium</i> sp. 1			
Ma	open	<i>Systematophora</i> ? sp. 1			
Ma	open	<i>Spiniferites</i> sp. 3			
Ma	open	<i>Palaeocystodinium</i> sp. 2			
Ma	open	<i>Batiacapsphaera</i> sp. 1			
Ma	open	<i>Impagidinium</i> sp. 2			
Ma	open	<i>Hystrichokolpoma</i> ? sp. 2			
TS, Ma	open	<i>Bitectatodinium</i> sp. 1			
Ma	open	<i>Invertocyst?</i> sp. 1			
Ma	open	<i>Palaeocystodinium</i> sp. 3			
Ma	open	<i>Hystrichosphaeridium</i> sp. 1			
Ma	open	<i>Dinocyst</i> sp. 4			
Ma	open	<i>Dinocyst</i> sp. 5			
Ma	open	<i>Pyxidiella</i> sp. 1 of Manum et al. (1989)			
Ma	open	<i>Impagidinium</i> sp. 4			
Ma	open	<i>Corradinium</i> sp. 1			
Ma	open	<i>Dinocyst</i> sp. 7			
Ma	open	<i>Operculodinium</i> sp. 2			
Ma	open	<i>Dapsilidinium</i> sp. 1			
Ma	open	<i>Lingulodinium</i> sp. 1			
Ma	open	<i>Oleistosphaeridium</i> sp. 1			
Ma	open	<i>Tectatodinium</i> sp. 3 of Manum et al. (1989)			
Ma	open	<i>Hystrichostrogylion</i> sp. 1			
Mu	open	<i>Spiniferites</i> sp. of Mudie (1989)			
Mu	open	<i>Pyxidiella</i> sp. 1 of Mudie (1989)			
Mu	open	<i>Dinocyst</i> sp. 1			
Mu	open	<i>Brigantedinium</i> sp. gp. B			
Ma	open	<i>Batiacapsphaera</i> sp. 2			
Ma	open	<i>Nematospheropsis</i> sp. 2			
Ma	open	<i>Operculodinium</i> sp. 3			
Ma	open	<i>Spiniferites</i> sp. 4			
Ma	open	<i>Labyrinthodinium</i> sp. 1			
Mu	open	<i>Tectatodinium</i> sp. 3 of Mudie (1989)			
Ma	open	<i>Achemosphaera</i> sp. 1			
Mu	open	<i>Tectatodinium</i> sp. 1			
Mu	open	<i>Brigantedinium</i> sp. A			
Mu	open	<i>Tectatodinium</i> sp. 2			
Ma	c.f.	<i>Glaphyrocysta</i> cf. <i>vicina</i>			
Ma	c.f.	<i>Spiniferites</i> cf. <i>miraibilis</i>			
Ma	c.f.	<i>Lejeuneacyta</i> cf. <i>hyalina</i>			
Ma	c.f.	<i>Hystrichosphaeridium</i> cf. <i>complanata</i>			
Ma	c.f.	<i>Labyrinthodinium</i> cf. <i>truncatum</i>			
Ma	c.f.	<i>Polyshaeridium</i> cf. <i>subtile</i>			
Mu	c.f.	<i>Thallassiphora</i> cf. <i>pansa</i>			
TS	c.f.	<i>Habibacysta</i> ? cf. <i>tectata</i>			
Ma	c.f.	<i>Hystrichostrogylion</i> cf. <i>membraniphorum</i>			
Ma	c.f.	<i>Amiculospaera</i> cf. <i>umbracula</i>			
Ma	informal species	<i>Deflandrea</i> sp. B of Powell (1986a) sensu informal species Manum et al. (1989)			
Ma	informal species	<i>Palaeocystodinium</i> sp. A of Costa and Downie (1979)			
Ma, Mu	informal species	<i>Cannospheeropsis</i> sp. A of Costa and informal species Downie (1979)			
Ma	informal species	<i>Leptodinium</i> ? sp. III of Manum (1976)			
Ma	informal species	<i>Tanyosphaeridium</i> sp. I of Manum (1976)			
Ma	informal species	<i>Problematicum</i> IV of Manum (1976)			
Ma	informal species	<i>Sumatradinium</i> ? sp. C of Powell (1986b)			
Ma	informal species	<i>Sumatradinium</i> ? sp. D of Powell (1986b)			
Ma	informal species	<i>Hystrichostrogylion</i> sp. of Edwards (1984)			
Ma	informal species	<i>Cordosphaeridium</i> sp. I of Manum (1976)			
Mu	informal species	<i>Hystrichokolpoma</i> sp. of Edwards (1984)			
Mu	informal species	<i>Tectatodinium</i> sp. of Piasecki (1980)			
TS, Ma	acritarch	Acrirarch sp. 2 (Dinocyst IV of Manum 1976)			
TS	informal acritarch	Acrirarch sp. 1 (Dinocyst III of Manum 1976)			
			Reinterpreted as acritarch		
			Reinterpreted as acritarch		

The FAD of 13.123 Ma (Dybkjær and Piasecki, 2010) suggests a younger age than our magnetostratigraphic interpretation, but the LO of *A. andalouensis* at 127.40 R-mbsf occurs in an isolated sample. Its LPO occurs at 111.30 R-mbsf and the FAD of Dybkjær and Piasecki (2010) would be closer to our age model at this depth, although an inconsistency remains.

The LAD of *C. irregularis* (10.283 Ma) has so far only been dated by Schreck et al. (2012) and may have a younger age at ODP Site 643. Following Schreck et al. (2012), we have tentatively synonymised *C. irregularis* with *Tectatodinium* sp. 4 of Manum et al. (1989). The highest confirmed species of *C. irregularis* occurs at 108.30 R-mbsf and is consistent with our magnetostratigraphic interpretation.

TABLE S8

Species reported by:	Microfoss Species	Species name in original study (if different)	Stratigraphic notes
CC	Diatom <i>Proboscia barboi</i> (Brun) Jordan and Priddle 1991	CC: <i>Rhizosolenia barboi</i>	
CC	Diatom <i>Thalassiosira grunowii</i> Akiba and Yanagisawa 1985	CC: <i>Coscinodiscus plicatus</i>	
CC	Diatom <i>Denticulopsis lauta</i>		
CC	Diatom <i>Crucidenticula nicobarica</i> (Grunow)	CC: <i>Denticulopsis nicobarica</i>	
		Akiba and Yanagisawa 1985	
CC	Diatom <i>Araniscus lewisiensis</i> (Greville)	CC: <i>Coscinodiscus lewisiensis</i>	
		Komura 1998	
CC	Diatom <i>Crucidenticula punctata</i> (Schrader)	CC: <i>Denticulopsis punctata hustedtii</i>	An FAD of 13.395 Ma (Barron Diatom Catalog in Lazarus et al. (2014)) would be younger than available age models for Hole 643A (Goll (1989), Bleil (1989) and this study) and inconsistent with other bioevents.
		Akiba and Yanagisawa 1985	
CC	Diatom <i>Cestodiscus peplum</i>		
CC	Diatom <i>Denticulopsis hyalina</i>		Barron et al. (1985a) acknowledge an imprecision of 0.1-0.3 Myr for the FAD of <i>D. hyalina</i> , which would make the FAD (14.908 Ma) consistent with our magnetostratigraphic interpretation.
SP	Diatom <i>Thalassiosira fraga</i>		The LO of <i>T. fraga</i> at 291.65 R-mbsf is close to the diagenetic opal front, so the real LO may be lower.
CC	Diatom <i>Actinocyclus ingens</i>		
CC	Diatom <i>Triceratium pileus</i>		
CC	Diatom <i>Thalassiosira spinosa</i>		
CC	Pl. <i>Neogloboquadrina acostaensis</i>		
	Foram.		
GB	Radiolar <i>Cyrtocapsella tetrapera</i>		<i>C. tetrapera</i> occurs irregularly and its LO at 289.36 R-mbsf is close to the diagenetic opal front, so the real LO may be lower.
	ian		

TABLE S9

Event Species	Age (Ma)			References	Region	Calibration (% for old isopachs)	AgeGTS2012 (Ma)	Lads.	Comments	
	Mean	Maximum	Minimum							
LAD <i>Filiophora filifera</i>	1.26	1.78	0.78	0.78	Egger et al. (2016) De Schepper and Head (2009) de Vernal and Mudie (1989) Head et al. (1989a) Head et al. (1989b) Kuhmann et al. (2006) Bujak and Matyska (1986) Zegarra and Helenes (2011) Mudie (1987)	N Atlantic N Atlantic N Atlantic Labrador Sea North Sea N Pacific C America N Atlantic	C5Cn.1n 50% 55% between C2n 100% and C1r.1n 0% NN19 45% NN12 0% NN12 0% C2n 100% Ionian 0% Serravallian 40% NN19 50%	22,66 1,39 X 1,26 X 5,59 1,14 X 1,76 X 0,78 Main 12,94 1,19 X		Local LAD?
									Large error margin	
									LAD at same, so real LAD later.	
									Large error margin	
									Local LAD?	
									Large error margin	
									Large error margin	
LAD <i>Melitasphaeridium chaoanophorum</i>	3.26	5.59	0.78	0.78	Bujak and Matyska (1986) Head et al. (1989a) Head (1998) Poulet et al. (2002) Soliman et al. (2012) McMinn (1993)	N Pacific Labrador Sea N Atlantic North Sea Egypt Australia	Ionian 0% NN12 0% C2n 60% NN19 0% NN5 0% CN11a 33%	0,78 Main 5,59 X 1,84 X 3,77 X 14,92 4,38 X		Large error margin
									Large error margin	
									Local LAD?	
									Large error margin	
									Local LAD?	
LAD <i>Labyrinthodinium truncatum</i>	7,36	8,35	5.85	5.85	de Verteuil and Norris (1996) Fensome et al. (2008) Schreck et al. (2012) Head et al. (1989a) Poulet et al. (2002) Soliman et al. (2012) McMinn (1993)	USA offshore (All) Canada offshore (All) N Atlantic Labrador Sea Ireland offshore (All) North Sea Denmark Italy N Pacific	NN11a 80% NN11d 0% 50.2% between C5n.2n 100% - C3Ar 100% NN10 100% Tortonian 80% NN11d 25% C8n.2n 25% NNS 0%	7,59 X 5,94 X 8,35 X 8,29 X 8,12 X 5,88 Main 14,92 14,92		Large error margin Dated as 8.05 Ma in Fensome et al. (2008), but not independently.
									Large error margin	
									Tortonian truncated by hiatus, so possibly older.	
									Large error margin	
									Large error margin	
									Local LAD?	
LAD <i>Hystriophospaeropsis obscura</i>	8,13	10,58	7,01	7,01	Wren and Kokinos (1986) Soliman et al. (2012) de Verteuil and Norris (1996) Fensome et al. (2008) Brown and Downie (1985) Schreck et al. (2012) Poulet et al. (2002) Dyksterhuis and Piasek (2010) Slivinskaya et al. (2012) Powell (1986a) Bujak and Matyska (1986)	USA offshore (All) Egypt USA offshore (All) Canada offshore (All) Ireland offshore (All) North Sea Denmark Italy N Pacific	N17 50% NNS 0% NN11b 80% 50.2% between NN10 0% - NN12 100% NN10 100% C5n.2n 45% NN11 30% C8n.2n 25% N4 0% Langhian 50%	7,59 X 14,91 7,01 Main 7,33 14,22 10,58 X 7,48 X 25,82 23,50 14,90		Large error margin Large error margin too large; Dated as 7.51 Ma in Fensome et al. (2008), but not independently.
									Large error margin	
									Large error margin	
									Large error margin	
									Large error margin	
									Large error margin	
									Local LAD?	
LAD <i>Operculodinium pioseckii</i>	8,13	8,35	7,90	7,90	Soliman et al. (2012) Zegarra and Helenes (2011) Piasek (2003) Schreck et al. (2012) Bijl et al. (2018)	Egypt C America Greenland N Atlantic Antarctica	NNS 10% Serravallian 25% Tortonian 85% 50.2% between C5n.2n 100% - C3Ar 100% CSAc 0%	14,77 13,27 7,90 Main 8,35 X 14,07		Local LAD? Local LAD? Tortonian truncated by hiatus, so possibly older.
									Local LAD?	
									Local LAD?	
									Local LAD?	
LAD <i>Cleistosphaeridium placacanthum</i>	10,87	13,81	4,91	4,91	Bijl et al. (2013) Soliman et al. (2012) van Mourik and Brinkhuis (2005) McMinn (1992) Mudge and Bujak (1996) Schreck et al. (2012) Zevenboom (1995) Brinkhuis and Blijf (1993) Powell (1992) de Verteuil and Norris (1996) Firth (1996) Wren and Kokinos (1986) van Mourik et al. (2001) Brown and Downie (1984)	Australia Egypt Italy Australia Australia N Atlantic Italy North Sea USA offshore (All) USA offshore (All) Ireland offshore (All) N Atlantic N Atlantic C5Ac 72%	C23n.2n 50% NNS 100% C13r 80% CN4 80% P12 67% C5n.2n 45% C4n.2n 0% P19 0% N12 90% NNS 20% NP12 100% NN11d 0% P19 0% C15n 25% C5n.2n 72%	51,40 13,53 X 33,96 13,81 X 41,40 10,58 X 8,11 X 32,10 11,95 X 13,20 X 5,94 Main 32,10 35,20 10,28 X		Possibly younger, because present in upper sample of Mazzapiedi, but absent in lowest sample Perito. Certainly between C4An 100% (8.771 Ma) and C3An 0% (6.733 Ma) or C3Bn 0% (7.212 Ma).
									Local LAD?	
									Local LAD?	
									Local LAD?	
									Local LAD?	
									Local LAD?	
									Local LAD?	
									Local LAD?	
									Local LAD?	
									Local LAD?	
LAD <i>Batiasphaera hirsuta</i>	8,35	8,35	8,35	8,35	Firth (1996) Schreck et al. (2012)	N Atlantic N Atlantic	C16n.1r 50% 50.2% between C5n.2n 100% - C3Ar 100%	35,97 8,35 Main	Local LAD? Reworked (?) fragments and specimens of <i>B. hirsuta</i> up to 4.84 Ma. Dated as 8.39 Ma by Schreck et al. (2012).	
LAD <i>Minispisoidium latirictum</i>	8,11	10,28	5,94	5,94	Bijl et al. (2013) van Mourik et al. (2001) Soliman et al. (2012) Brown and Downie (1984) Fensome et al. (2008)	Australia USA offshore (All) Egypt Ireland offshore (All) Canada offshore (All)	C18r 10% C13r 0% NNS 0% NP12 100% NN11d 0%	41,05 35,00 14,91 50,50 5,94 Main		Local LAD? Local LAD? Local LAD? Local LAD? Dated as 8.05 Ma in Fensome et al. (2008), based on occurrence at same depth as <i>HL. truncatum</i> [8.05 Ma, Williams et al. (1999), updated to GTS2004].
LAD <i>Cerebrocytta irregularis</i>	10,28	10,28	10,28	10,28	Schreck et al. (2012)	N Atlantic	CSn.2n 72%	10,28 Main		
LAD <i>Cerebrocytta poulsenii</i>	11,54	12,10	9,87	9,87	Zegarra and Helenes (2011) de Verteuil and Norris (1996) Quigley et al. (2014) Zevenboom (1995) Piasek (2003) Schreck et al. (2012)	C America Ireland offshore (All) Ireland offshore (All) N Atlantic N Atlantic N Atlantic	Langhian 75% CSAn 67% CSAn 75% C5An 100% C5An 100% CSAn 100%	14,36 9,87 Main 12,10 X 12,00 X 11,63 X 12,05 X		Local LAD? Large error margin
LAD <i>Hystrichostrogyon membraniphorum</i>	14,12	14,91	13,27	13,27	Bijl et al. (2013) Zegarra and Helenes (2011) Soliman et al. (2012) Brown and Downie (1984) Poulet et al. (2002) Olté et al. (2015) Tocher and Jarvis (1994) Prince et al. (2008) Bujak and Matyska (1986) Tocher and Jarvis (1996)	Australia C America Egypt Ireland offshore (All) North Sea North Sea France North Sea N Pacific France	C17n.3n 0% Serravallian 25% NNS 0% C4n 80% NN4 100% N11 100% UC0+ 75% Acanthoceras rhomagensis 55% Marpisites testudinarius (stems crinoid) 50% Langhian 50% Mantellites mantelli 60%	38,33 13,27 Main -14,91 14,91 X 13,41 X 13,41 X 89,82 95,74 83,75 14,90 X 99,12		Local LAD? Large error margin; Rare in core.
LAD <i>Aptedinium tectatum</i>	13,09	13,88	11,90	11,90	Powell (1992) Louwey et al. (2008) de Verteuil and Norris (1996) London and Jan Chêne (1998) Fensome et al. (2008) Soliman et al. (2012)	North Sea Ireland offshore (All) USA offshore (All) France	NN6 100% CSAn 50% NN5 75% Serravallian 25% NN5 25% NN6 0%	11,90 Main 13,49 X 13,88 X 17,59		Large error margin
LAD <i>Aptedinium spiridoides</i>	13,90	14,57	13,27	13,27	Powell (1992) Köthe (2012) Williams et al. (1993) London and Jan Chêne (1998) de Verteuil and Norris (1996) Fensome et al. (2008) Soliman et al. (2012)	North Sea Germany Northern hemisphere France USA offshore (All) USA offshore (All) Egypt	NIN 2.6% NIN 50% 40% between NNB 0% - NN10 100% NN5 25% NN5 25% NN6 0% NN5 0%	19,78 14,22 X 13,27 Main 20,55 14,57 X 13,53 X 16,43		Local LAD? Large error margin Local FAD? Local LAD? Large error margin Dated as 13.35 in Fensome et al. (2008), based on Williams et al. (1999).
FAD <i>Habibacysta tectata</i>	13,88	14,28	13,49	14,28	de Verteuil and Norris (1996) Löwye et al. (2008) Köthe (2012) Head et al. (1989a) Schreck et al. (2012)	USA offshore (All) Ireland offshore (All) Germany Labrador Sea N Atlantic	CSAn 75% CSAn 50% 40% between NNB 0% - NN10 100% NN10 <1n 0% extrapolated from overlying CSAn; CSAn -413%	13,88 X 9,85 >8,29 14,28 Main		Calibration uncertain because of uncertain magnetostratigraphy in CSACn at ODP Site 907. Downward extrapolation yields 13.885 Ma, the same as reported by Schreck et al. (2012).
LAD <i>Cribroperidinium tenuitabulatum</i>	13,93	14,90	13,27	13,27	van Mourik et al. (2001) Duffield and Stein (1986) Brinkhuis and Blijf (1993) Williams et al. (1993) Zevenboom (1995) Firth (1996) Powell (1992) Bujak and Matyska (1986)	USA offshore (All) USA offshore (All) Italy Northern hemisphere Ireland offshore (All) Germany USA offshore (All) USA offshore (All) Egypt USA offshore (All) Egypt Shukheir-1 N Pacific N Atlantic	C15n 100% N11 0% C18r 75% Serravallian 25% D20 0% NIN 30% NN10 <1n 0% N10 100% Langhian 50%	35,00 13,77 X 34,03 12,27 Main 38,62 13,77 X 14,90 X 14,50 Main 35,00 15,43 X 14,90 X 14,50 Main		Local LAD? Large error margin Local LAD? Large error margin Local LAD? Large error margin Local LAD? Large error margin Local LAD?
FAD <i>Achamospheara andalusiensis</i>	11,81	13,12	10,55	13,12	Zevenboom (1995) de Verteuil and Norris (1996) Powell (1992) Dyksterhuis and Piasek (2010) Williams et al. (1993)	Italy North Sea North Sea Denmark Northern hemisphere	CSAn 1n 100% NIN 100% NN8 33% NN6 25% Serravallian 50%	12,05 X 10,93 X 10,79 X 13,12 Main 12,72 X		Large error margin Large error margin Large error margin Large error margin Large error margin

		Brown and Downie (1985)	Ireland offshore (All)	Serravallian 100%	11.63 X	
LAD	<i>Cribroperidinium giuseppi</i>	14.21 14.90 13.53 13.53	Soliman et al. (2012) Brinkhuis and Biffi (1993) Firth (1996) Brown and Downie (1984) Bujak and Matsuoka (1986)	Egypt Italy N Atlantic Ireland offshore (All) N Pacific	NN5 100% C13n 75% C11r 25% NP13 0% Langhian 50%	13.53 Main 33.29 Local LAD? 30.44 Local LAD? 50.50 Local LAD? 14.90 X Large error margin
FAD	<i>Cerebrocytota poussani</i>	17.85 17.95 17.76 17.95	Zegarra and Helenes (2011) de Verteuil and Norris (1996)	C America USA offshore (All)	Burdigalian 60% NN3 100%	17.76 X Large error margin 17.95 Main Large error margin
FAD	<i>Unipontidinium aqueductus</i>	14.57 15.16 13.99 15.16	Powell (1992) Brown and Downie (1985) de Verteuil and Norris (1996) Dybäkier and Piasek (2010) Louweyse et al. (2008) Zevenboom (1995) Williams et al. (1993) Bijl et al. (2018)	Northern hemisphere Ireland offshore (All) Denmark Ireland offshore (All) Italy Northern hemisphere Antarctica	North Sea NN5 50% USA offshore (All) NN5 33% NN5 10% Ireland offshore (All) CSBn.1n 75% Northern hemisphere CSBn.2n 0%	14.01 X Large error margin 14.22 X Large error margin 14.45 X Large error margin 14.77 X 14.90 X Large error margin 15.16 Main
FAD	<i>Labyrinthidinium truncatum</i>	16.09 18.12 15.16 18.12	de Verteuil and Norris (1996) Head et al. (1989a) Powell (1992) Louweyse et al. (2008) Köthe (2012) Dybäkier and Piasek (2010) Zevenboom (1995) Soliman et al. (2012)	USA offshore (All) Labrador Sea North Sea Ireland offshore (All) Northern hemisphere N Atlantic France USA offshore (All) Denmark Italy N Atlantic	NN4 75% NN10 <100% NN8 25% CSc.1r 70% C45n 50% NN100% NN2 85% NN2 100% CSDr.1n 100% NN5 75%	15.67 X Large error margin >8.29 Local FAD? 10.81 Local FAD? 15.28 X 15.52 X 15.59 X Large error margin 16.86 X 16.28 X 17.72 X 18.12 Main NN3 50% (with large error margin), but suspected caving, so LO could also be at NN4 60% (16.12 Ma).
LAD	<i>Cordosphaeridium cantharellum</i>	17.48 20.70 13.88 13.88	Soliman et al. (2012) Powell (1992) Brinkhuis and Biffi (1993) Williams et al. (1993) Firth (1996) Louweyse and Jan du Chêne (1998) de Verteuil and Norris (1996) Dybäkier and Piasek (2010) Zevenboom (1995) Fensome et al. (2008)	Egypt North Sea Italy Northern hemisphere N Atlantic France USA offshore (All) Denmark Italy N Atlantic	NN4 25% NN4 80% P19.0% Northern hemisphere C45n 50% NN100% NN2 85% NN2 100% CSDr.1n 100% NN5 75%	17.19 X Large error margin 15.52 X Local FAD? 32.10 X 20.07 X Large error margin 35.15 Local LAD? 17.59 X 18.86 X Large error margin 18.28 X 17.72 X 13.88 Main Dated as 14.00 Ma by Fensome et al. (2008).
FAD	<i>Sumatradinium druggii</i>	17.74 18.28 17.19 18.28	de Verteuil and Norris (1996) Soliman et al. (2012)	USA offshore (All) Egypt	NN3 0% NN4 25%	18.28 Main Large error margin 17.19 X
FAD	<i>Sumatradinium hispidum</i>	18.28 18.28 18.28 18.28	Soliman et al. (2012)	Egypt	NN2 100%	18.28 Main NN2 <100%, but unclear how much, because lower part of NN2 truncated by hiatus.
FAD	<i>Coustonidinium aubryae</i>	19.74 21.69 17.80 21.69	Zevenboom (1995) de Verteuil and Norris (1996) Dybäkier and Piasek (2010)	Italy USA offshore (All) Denmark	CSBn.1n 0% NN2 25% NN4 5%	14.87 Local FAD? 21.69 Main Large error margin 17.80 X
FAD	<i>Pyxidinopodus tuberculata</i>	21.68 23.23 20.13 23.23	de Schepper and Head (2009) Vorstegh and Zevenboom (1995) Montanari et al. (1997) Bijl et al. (2018)	N Atlantic Mediterranean Italy Antarctica	C2An.1n 39% NN12 0% CSAn.1n 50% CScn.3n 100%	2.86 Local FAD? 3.30 Local FAD? 20.13 X 23.23 Main
FAD	<i>Melitasphaeridium chaonophorum</i>	21.60 22.96 20.10 22.96	Bujak and Matsuoka (1986) Head et al. (1989a) Powell (1992) Williams et al. (1993) de Schepper and Head (2009) Louweyse and Jan du Chêne (1998) Soliman et al. (2012) Duffield and Stein (1986)	N Pacific Labrador Sea North Sea Northern hemisphere N Atlantic France Egypt USA offshore (All)	Tortonian 0% NN10 <100% NN4 0% Aquitanian 50% NN15 <100% NN100% NN2 100% NN10 0%	11.63 Local FAD? >8.29 Local FAD?; Present in lowest sample. 22.96 Main Large error margin 21.74 X Large error margin >3.70 Local FAD?; Present in lowest sample. 20.10 X 18.28 Local FAD? 14.24 Local FAD?
FAD	<i>Sumatradinium soucuyantiae</i>	19.89 21.69 18.51 21.69	de Verteuil and Norris (1992) Montanari et al. (1997) Soliman et al. (2012)	USA offshore (All) Italy Egypt	NN2 25% C6n 25% NN2 95%	21.69 Main Large error margin 19.48 X 18.51 X
FAD	<i>Exochasphaeridium insigne</i>	19.11 20.10 18.28 20.10	de Verteuil and Norris (1996) Dybäkier and Piasek (2010) Soliman et al. (2012)	USA offshore (All) Denmark Egypt	NN2 50% NN2 85% NN2 100%	20.10 Main Large error margin 18.99 X 18.28 X
LAD	<i>Caligodinium amicum</i>	21.85 22.98 21.23 21.23	Firth (1996) Biffi and Manum (1988) Brinkhuis and Biffi (1993) Williams et al. (1993) de Verteuil and Norris (1996) Dybäkier and Piasek (2010)	N Atlantic Italy Northern hemisphere USA offshore (All) Denmark	C16r 50% NN1 50% C13n 60% Aquitanian 50% NN2 30% NN2 35%	36.83 Local LAD? 22.98 X 33.38 Local LAD? 21.74 X Large error margin 21.46 X Large error margin 21.23 Main
FAD	<i>Operculodinium piseckii</i>	15.29 16.93 14.04 16.93	Zegarra and Helenes (2011) Zevenboom (1995)	Egypt C America Italy	NN5 0% Langhian 90% CSCr 60%	14.91 X 14.04 X 16.93 Main
FAD	<i>Batiacapsaera sphaerica</i>	18.76 22.12 16.98 22.12	Williams et al. (2012) Williams et al. (1993) Bijl et al. (2018)	Egypt Northern hemisphere Antarctica	NN4 25% Aquitanian 35% CSc.1r 50%	17.19 X 22.12 Main Large error margin 16.93 X
FAD	<i>Operculodinium janduchense</i>	23.96 23.96 23.96 23.96	Soliman et al. (2012) Head et al. (1989a) Bijl et al. (2018)	Egypt Labrador Sea Antarctica	NN4 100% NN10 100% C7n.1n 100%	14.91 Occurs in single sample. 8.29 Local FAD? 23.96 Main
FAD	<i>Invertocysta tabulata</i>	24.71 25.80 23.63 25.80	Powell (1992) Louweyse et al. (2008) Williams et al. (1993) Zegarra and Helenes (2011) Bijl et al. (2018)	North Sea Ireland offshore (All) Northern hemisphere C America Antarctica	P22 33% CSAb 25% Seravallian 75% Seravallian 80% CSc.5r 50%	25.80 Main Large error margin 13.71 Local FAD? 12.17 Local FAD? 12.06 Local FAD? 23.63 X
LAD	<i>Chiropteridium galeo</i>	24.04 28.23 20.55 20.55	Fensome et al. (2008) Dybäkier and Piasek (2010) Slivinská et al. (2012) de Verteuil and Norris (1996) Head and Norris (1989) Biffi and Manum (1988) Brinkhuis and Biffi (1993)	N Atlantic Denmark Norway France Labrador Sea Italy	<50% between NP25 0% - NN2 0% NN2 20% C9r 10% NN2 25% NP24 50% NN2 50% C13r 75%	24.83 Error margin too large; Dated as 21.90 Ma by Fensome et al. (2008), based on Williams et al. (2004). 21.91 X 27.82 X 21.69 X Large error margin 28.23 X 20.55 Main 34.03 Local LAD?
LAD	<i>Chiropteridium lobospinosum</i>	25.93 28.23 22.98 22.98	Powell (1992) Head and Norris (1989) Köthe (2012) Grädelstein et al. (1992) Biffi and Manum (1988)	North Sea Labrador Sea Germany North Sea	P22 15% NP24 50% NP24 60% NN1 50% NP25 75%	26.42 X Large error margin 28.23 X 27.95 X 22.98 Main 24.06 X
FAD	<i>Aptedinium spiridoides</i>	28.17 30.58 25.56 30.58	Powell (1992) Köthe (2012) Williams et al. (1993) Biffi and Manum (1988)	North Sea Germany Northern hemisphere	NN2 45% NN2 60% C11r 50% C11r 50%	28.27 X Large error margin 30.58 Main 25.55 X Large error margin 16.43 Local FAD?
FAD	<i>Leptodinium italicum</i>	29.46 29.46 29.46 29.46	Biffi and Manum (1988)	Italy	P20 75%	29.46 Main
LAD	<i>Licracysta semicirculata</i>	27.08 29.62 25.82 25.82	Brinkhuis et al. (2003) Powell (1992) Grädelstein et al. (1992) Brinkhuis and Biffi (1993) Pross et al. (2010) Slivinská et al. (2012) Egger et al. (2016) Van Simaeys et al. (2004)	Australia North Sea North Sea Italy Italy Denmark Canada offshore (All) Belgium	C9r 50% P22 15% NP24 0% C13n 60% C7n 75% C8n.2n 55% C9n 85% NP24 100%	27.65 X 26.45 X Large error margin 29.63 X 33.38 Local LAD? 26.67 X 25.82 Main 26.57 X 26.84 X
LAD	<i>Achilleodinium biformoides</i>	28.12 30.58 25.99 25.99	Powell (1992) Brown and Downie (1984) Williams et al. (1993) Firth (1996) Van Simaeys et al. (2004) Pross et al. (2010) Brinkhuis and Biffi (1993) Ačkalinić et al. (2015)	North Sea Ireland offshore (All) Northern hemisphere N Atlantic Italy Italy W Turkey	NP23 60% NP13 75% Rupelian 80% C17n.1r 75% NP24 66% C8r 100% P16/P17 100% P1b 50%	30.58 X Large error margin 49.46 Local LAD? 29.25 Large error margin 37.78 Local LAD? 27.79 X 25.99 Main 34.03 Local LAD? 64.58 Local LAD?
LAD	<i>Enneadocysta arcuata</i>	32.11 33.39 30.82 30.82	Powell (1992) Head and Norris (1989)	North Sea Labrador Sea	P18 43% NP23 50%	33.39 X Large error margin 30.82 Main
FAD	<i>Chiropteridium lobospinosum</i>	31.79 33.16 30.46 33.16	Egger et al. (2016) Eldrett and Harding (2009) Firth (1996) Powell (1992) Head and Norris (1989) Köthe (2012) Grädelstein et al. (1992) Van Simaeys et al. (2004)	N Atlantic N Atlantic North Sea Labrador Sea Germany North Sea	C12r 50% C13n 100% C12r 25% NP23 65% NP23 50% P10r 100% C12n 33%	32.10 X 33.16 Main 32.63 X 30.46 X Large error margin 30.10 X 32.27 X 32.02 X 30.89 X
FAD	<i>Heteraulacysta campanula</i>	35.52 37.99 31.54 37.99	Brinkhuis (1994) Brinkhuis and Biffi (1993) Powell (1992)	Italy Italy North Sea	NP18 80% C17n 25% NP23 20%	37.04 X 37.99 Main 31.54 X Large error margin



		Barron Diatom Catalog in Lazarus et al. (2014)	Barron (2003), based on: Barron (1992); Shackleton et al. (1995); unpublished notes of Barron	North Pacific	Bio- and magnetostratigraphy of Barron (1992); Integrated cyclo-, bio- and magnetostratigraphy of Shackleton et al. (1995)	14,9 Gradstein et al. (2004)	14,9 X
FAD Diatom <i>Denticulopsis lauta</i>	15,8 15,9 15,57 15,9	Cody et al. (2008) Cody et al. (2008) Barron et al. (2013)	Antarctic Antarctic Yanagisawa and Akiba (1998), based on: Barron and Gladenkov (1995)	New Jersey Shelf	Total range CONOP model Average range CONOP model Confirmation only	15,57 (total range) Gradstein et al. (2004) 15,67–15,7 (average range) Gradstein et al. (2004) 15,9 Gradstein et al. (2004)	15,57 X 15,69 X 15,9 Main
		Barron et al. (1985a) Barron Diatom Catalog in Lazarus et al. (2014)	Barron (2003), based on: Barron (1992); Shackleton et al. (1995); unpublished notes of Barron	Eastern Tropical Pacific North Pacific	Biostratigraphic interpolation Bio- and magnetostratigraphy of Barron (1992); Integrated cyclo-, bio- and magnetostratigraphy of Shackleton et al. (1995)	16,1 i.e. Berggren et al. (1985) 15,9 Gradstein et al. (2004)	15,9 X 15,9 Main
		Barron (1985a)		Eastern Equatorial Pacific	Biostratigraphic interpolation	15,9 i.e. Berggren et al. (1985)	15,7 X
FAD Diatom <i>Cestodiscus peplum</i>	16,2 16,4 16,15 16,4	Pälike et al. (2010) Barron et al. (1985b) Barron Diatom Catalog in Lazarus et al. (2014)	Barron (1985a), based on: Barron (1985b) Barron (2003), based on: Barron (1992); Shackleton et al. (1995); unpublished notes of Barron	Eastern Equatorial Pacific Eastern Equatorial Pacific Equatorial Pacific	Confirmation only Magnetostratigraphy Bio- and magnetostratigraphy of Barron (1992); Integrated cyclo-, bio- and magnetostratigraphy of Shackleton et al. (1995)	16,15 Gradstein et al. (2004) 16,4 i.e. Berggren et al. (1985) 16,4 Gradstein et al. (2004)	16,15 X 16,2 X 16,4 Main
LAD Diatom <i>Thalassiosira fraga</i>	16,2 16,5 15,96 15,96	Pälike et al. (2010) Barron (2003)	Barron (1983) Barron (1992); Shackleton et al. (1995); unpublished notes of Barron	Eastern Equatorial Pacific Equatorial Pacific	Confirmation only Bio- and magnetostratigraphy of Barron (1992); Integrated cyclo-, bio- and magnetostratigraphy of Shackleton et al. (1995)	15,96 Gradstein et al. (2004) 16,5 Berggren et al. (1995)	15,96 Main 16,5 X
		Barron Diatom Catalog in Lazarus et al. (2014)	Barron (1985a)	Eastern Equatorial Pacific Eastern Tropical Pacific	Biostratigraphic interpolation Biostratigraphic interpolation	16,3 Gradstein et al. (2004) 16,4 i.e. Berggren et al. (1985)	16,3 X 16,2 X
FAD Diatom <i>Actinocyclus ingens</i>	16,1 18,2 15,25 18,2	Cody et al. (2008) Cody et al. (2008) Pälike et al. (2010) Barron et al. (2013) Bohaty et al. (2003)	Antarctic Antarctic Barron (1983) Barron (1985a) Baldauf and Barron (1991); Harwood and Maruyama (1992); Censarek and Gersonde (2002)	Eastern Equatorial Pacific New Jersey Shelf Kerguelen Plateau	Total range CONOP model Average range CONOP model Confirmation only Confirmation only Magnetostratigraphy; Confirmation from Ar/Ar dating	15,78 (total range) Gradstein et al. (2004) 15,84–15,89 (average range) Gradstein et al. (2004) 15,25 Gradstein et al. (2004) 15,5 Gradstein et al. (2004) 16,2 (First Common Occurrence) Berggren et al. (1995)	15,78 X 15,87 X 15,25 X 15,5 X 16,2 X
LAD Diatom <i>Triceratium pileus</i>	17,4 17,6 17,3 17,3	Pälike et al. (2010) Barron (1985a) Barron Diatom Catalog in Lazarus et al. (2014)	Barron (2005)	Eastern Equatorial Pacific Eastern Equatorial Pacific Central Tropical Pacific	Biostratigraphic interpolation Magnetostratigraphy Magnetostratigraphy	17,35 Gradstein et al. (2004) 17,6 i.e. Berggren et al. (1985) 17,6 Gradstein et al. (2004)	17,35 X 17,3 Main 17,6 X
LAD Diatom <i>Thalassiosira spinosa</i>	17,6 17,64 17,5 17,5	Pälike et al. (2010) Barron (1985a)		Eastern Equatorial Pacific Eastern Equatorial Pacific	Biostratigraphic interpolation Magnetostratigraphy	17,64 Gradstein et al. (2004) 17,9 i.e. Berggren et al. (1985)	17,64 X 17,5 Main
FAD Radiolaria <i>Cyrtocapsella tetrapera</i> an	21,84 21,92 21,77 21,92	Nigrini et al. (2005)		Central Equatorial Pacific ODP Site 1218	Magnetostratigraphy	22,52–22,65 Berggren et al. (1995)	21,77 X
		Nigrini et al. (2005)		Central Equatorial Pacific ODP Site 1219	Magnetostratigraphy	22,6–22,86 Berggren et al. (1995)	21,92 Main
		Nigrini et al. (2005)		Central Equatorial Pacific ODP Site 1220	Magnetostratigraphy	22,25–23,01 Berggren et al. (1995)	21,85 X
FAD Diatom <i>Thalassiosira fraga</i>	19,7 20,4 19,21 20,4	Pälike et al. (2010) Barron (2003)	Barron (1983) Barron (1992); Shackleton et al. (1995); unpublished notes of Barron	Eastern Equatorial Pacific Equatorial Pacific	Confirmation only Bio- and magnetostratigraphy of Barron (1992); Integrated cyclo-, bio- and magnetostratigraphy of Shackleton et al. (1995)	19,21 Gradstein et al. (2004) 20,3 Berggren et al. (1995)	19,21 X 19,9 X
		Barron (1985a) Gladenkov and Barron (1995) Harwood and Maruyama (1992)		Eastern Equatorial Pacific North Pacific Kerguelen Plateau	Biostratigraphic extrapolation Magnetostratigraphy Magnetostratigraphy	19,9 i.e. Berggren et al. (1985) 20,1 i.e. Berggren et al. (1985) 21,2 Berggren et al. (1985)	19,2 X 19,4 X 20,3 X
		Barron Diatom Catalog in Lazarus et al. (2014)	Barron (2005)	Central Tropical Pacific Eastern Tropical Pacific	Magnetostratigraphy Biostratigraphic extrapolation	20,4 Gradstein et al. (2004) 19,9 i.e. Berggren et al. (1985)	20,4 Main 19,2 X

TABLE S11

## Summary

Sample	Core	Section	Interval (cm)	Half	Depth (mbsf)	Depth (m) Material
T1	1XX	6	46.25	W	148.26	
T2	1XX	1	46.25	W	148.21	138.79 Sandine
T3	2XX	3	128.10	W	199.58	212.9 Sandine
T4	2XX	2	148.10	W	257.08	273.49 Sandine

Negative $^{37}\text{Ar}$ intensities are used in age calculations										Negative $^{37}\text{Ar}$ intensities are set to zero									
Plateau					Full External Error					Full External Error					Full External Error				
	Full	External	Total	fusion	Normal	Isochron	Full	External	Inverse	Full	External	Total	External	Full	External	Total	External	Comments	
T1	17.23	0.47	17.70	0.47	16.47	1.71	17.94	1.46	17.59	0.47	17.76	0.59							
T2	28.75	1.45	24.20	1.45	28.75	1.79	1.96	18.45	0.76	28.21	0.50	27.57	1.47						
T3	22X	3	128.10	W	59.36	3.86	54.32	1.93	54.83	33.97	61.61	3.84	-29.11	251.62	57.71	1.41	No reliable results produced		
T4	28X	2	148.10	W	18.02	0.24	16.74	0.38	18.76	0.33	17.93	0.28	18.07	0.21	18.24	0.39	No diagnostic results produced		

Sample T3  
Negative  $^{37}\text{Ar}$  intensities are used in age calculations

Relative Abundance	36Ar (%)	%1σ	37Ar (%)	%1σ	38Ar (%)	%1σ	39Ar (%)	%1σ	40Ar (%)	%1σ	40(n/39k) ± 1σ	Age ± 1σ (Ma)	40Ar(f) (%)	39Ar(k) (%)	K/Ca ± 1σ	
329_VU107_A	0.0546880	1.33	89.4308	1.29	0.055795	10.50	1.89788	0.215	16.4500	0.227	2.09 ± 0.36	7.44	0.02 ± 0.01			
330_VU107_A	0.0547307	3.042	81.620	0.709097	9.129	5.48483	0.191	5.4251	0.141	1.00670	0.4669	9.19 ± 3.73	36.88	5.57	0.04 ± 0.02	
331_VU107_A	0.0548048	4.204	81.620	0.709097	9.129	5.48483	0.191	5.4251	0.141	1.00670	0.4669	9.19 ± 3.73	36.88	5.57	0.04 ± 0.02	
334_VU107_A	0.0548105	3.020130	0.434	44.6007	45.567	0.07105	0.989	10.27	0.222	93.922	0.005	1.08865	0.47327	2.75	18.46	0.10 ± 0.05
298_VU107_A	0.0507229	57.540	10.04	0.038049	25.678	0.08848	0.897	2.3816	0.305	1.05043	0.41626	16.32 ± 1.18	80.89	1.73	0.14 ± 0.03	
215_VU107_A	0.0508211	15.207	42.006	0.024861	28.776	0.07264	0.897	2.3816	0.305	1.05043	0.41626	17.00 ± 1.70	69.22	2.18	0.439 ± 0.188	
216_VU107_A	0.0508211	15.207	42.006	0.024861	28.776	0.07264	0.897	2.3816	0.305	1.05043	0.41626	17.22 ± 1.10	71.34	2.18	0.439 ± 0.188	
209_VU107_A	0.0509051	0.910	2.23055	26.318	0.000452	142.800	0.000682	0.031	4.0211	0.219	2.10507	0.17697	17.89 ± 1.45	40.26	1.40	0.19 ± 0.04
308_VU107_A	0.0508261	0.456	51.18865	49.720	0.260558	2.700	0.024956	0.332	42.8869	0.032	2.10330	0.17250	16.00 ± 1.01	10.15	3.54	0.27 ± 0.06
323_VU107_A	0.0508261	3.923	60.480	0.10527	1.028	0.024956	0.332	42.8869	0.032	2.10330	0.17250	22.81 ± 2.20	10.50	0.57	0.04 ± 0.02	
212_VU107_A	0.0509050	3.914	6.20196	19.237	0.000452	270.000	0.00012	0.001	4.6949	0.269	2.09057	0.16017	19.97	0.51	0.88 ± 0.71	

Σ

4.146784

0.335

23.97162

271.521

148.0646

1.800

51.25997

0.986

136.2122

0.805

## Information on Analysis and Constraints Used in Calculations

## Results

	40(p/y)36(a) ± 1σ	40(n/39k) ± 1σ	Age ± 1σ (Ma)	Nδ	SBA(k) (%)	K/Ca ± 1σ
Age Plateau	2.00056 ± 0.2510	17.23 ± 0.47	16.45 ± 0.47	0.46	8.87	0.14 ± 0.08

## Total Plateau Age

	1.86443 ± 0.1138	15.80 ± 0.97	12	1.03 ± 2.00

## Normal Isotopes

	330.37 ± 10.01	1.01847	1.71	8.87

## Normal Isotopes

	330.37 ± 10.01	1.01847	1.71	8.87

## Inverse Isotopes

	330.80 ± 10.37	2.00595	8.58%	8.87

## Inverse Isotopes

	330.80 ± 10.37	2.00595	8.58%	8.87

## Information on Analysis and Constraints Used in Calculations

## Results

	40(p/y)36(a) ± 1σ	40(n/39k) ± 1σ	Age ± 1σ (Ma)	Nδ	SBA(k) (%)	K/Ca ± 1σ
Age Plateau	2.18191 ± 0.0804	18.29 ± 0.73	0.12	73.08	0.025 ± 0.059	

## Total Plateau Age

	1.70279 ± 0.2496	14.79 ± 1.30%	10	0.107 ± 0.079

## Normal Isotopes

	288.76 ± 4.08	2.20571 ± 0.0826	18.45 ± 0.74	0.33	73.08

## Normal Isotopes

	288.76 ± 4.08	2.20571 ± 0.0826	18.45 ± 0.74	0.33	73.08

## Inverse Isotopes

	320.46 ± 4.51	2.14604 ± 0.1165	17.98 ± 0.97	0.11	73.08

## Inverse Isotopes

	320.46 ± 4.51	2.14604 ± 0.1165	17.98 ± 0.97	0.11	73.08

## Information on Analysis and Constraints Used in Calculations

## Results

	36Ar(a) [A]	37Ar(a) [A]	38Ar(c) [A]	39Ar(k) [A]	40Ar(f) [A]	Age ± 1σ (Ma)	Nδ	SBA(k) (%)	K/Ca ± 1σ

<tbl\_r cells="10" ix="1" maxcspan="1" maxrspan="

G28_VU107	0 °C	✓	0.008203	5.675	42.376750	57.066	0.004135	135.855	0.087921	12.348	0.9325	1.662	53.99684 + 28.40942	521.00 + 317.51	636.00	0.33	0.001 ± 0.000
190_VU107	0 °C	✓	0.008203	12.676	2.14688	21.524	0.0111189	62.988	0.09047	52.278	4.5980	1.722	31.0194 + 25.1824	306.80 + 253.52	52.20	0.03	0.002 ± 0.001
181_VU107	0 °C	✓	0.008203	0.649684	2.14688	12.675	0.0111189	39.020	0.023338	27.585	2.4020	0.258	27.01410 + 11.02404	242.3 + 105.72	11.69	0.06	0.002 ± 0.001
182_VU107	0 °C	✓	0.008203	0.729	2.14688	12.675	0.0111189	73.524	0.023338	27.585	2.4020	0.257	24.71010 + 11.02404	228.2 + 105.72	11.69	0.06	0.002 ± 0.001
609_VU107	0 °C	✓	0.008203	4.212	6.354023	48.272	0.008037	532.609	0.07595	11.559	1.1414	0.043	22.9941 + 21.57090	195.6 + 301.34	119.65	0.19	0.004 ± 0.010
187_VU107	0 °C	✓	0.008203	3.478	0.71759	71.186	0.026798	30.017	0.09507	52.439	5.125	0.162	20.3026 + 20.67098	179.0 + 191.22	19.98	0.05	0.006 ± 0.005
188_VU107	0 °C	✓	0.008203	3.938	1.12503	56.822	0.011033	65.023	0.04388	18.983	2.0683	0.051	9.6424 + 3.4465	82.0 + 82.52	18.95	0.13	0.007 ± 0.005
184_VU107	0 °C	✓	0.008203	0.729	2.14688	12.675	0.0111189	73.524	0.023338	27.585	2.4020	0.257	24.71010 + 11.02404	228.2 + 105.72	11.69	0.06	0.002 ± 0.001
194_VU107	0 °C	✓	0.008203	10.112	1.00798	54.029	0.016498	58.650	0.020903	29.133	1.2726	0.010	0.0001 + 5.4049	0.8 + 46.26	0.09	0.07	0.010 ± 0.006
628_VU107	0 °C	✓	0.008203	26.088	41.36407	86.126	0.003980	169.346	0.08972	29.718	36.211	0.007	307.010 + 814.36319	0.0 + 102.32	782.97	0.00	0.000 ± 0.000
186_VU107	0 °C	✓	0.008203	2.033	2.04047	21.321	0.008017	85.877	0.091515	52.082	0.673	0.162	64.0120 + 36.02405	0.0 + 101.59	1.36	0.00	0.000 ± 0.002
185_VU107	0 °C	✓	0.008203	4.393	2.04047	21.321	0.008017	85.877	0.091515	52.082	0.673	0.162	64.0120 + 36.02405	0.0 + 101.59	1.36	0.00	0.000 ± 0.002
634_VU107	0 °C	✓	0.008203	4.393	2.04047	21.321	0.008017	85.877	0.091515	52.082	0.673	0.162	64.0120 + 36.02405	0.0 + 101.59	1.36	0.00	0.000 ± 0.002
183_VU107	0 °C	✓	0.008203	2.033	2.04047	21.321	0.008017	85.877	0.091515	52.082	0.673	0.162	64.0120 + 36.02405	0.0 + 101.59	1.36	0.00	0.000 ± 0.002
J-0.00485730 + 0.0000193	24.453	1.07745	27.335	0.007234	144.471	0.04116	14.197	0.6534	1.388	5.61908 + 3.80232	46.61 ± 3.55	34.22	0.12	0.000 ± 0.003			
FCA = 28.201 ± 0.023 Ma																	
622_VU107	0 °C	✓	0.0157627	1.719	4.70769	58.152	0.12102	4.571	0.10460	0.072	85.3770	0.018	7.4423 + 0.1839	61.14 + 1.59	94.05	32.72	1.001 ± 0.867
633_VU107	0 °C	✓	0.1877277	0.488	36.36200	65.264	0.252608	2.758	0.185218	0.051	18.3216	0.011	7.60416 + 0.10104	62.88 + 1.31	89.21	54.42	0.138 ± 0.080

Σ 3.207704 0.191 26.17037 343.139 0.0414028 3.517 32.821028 0.000 119.0804 0.005

G28_VU107-T	0 °C	✓	0.008203	5.675	42.376750	57.066	0.004135	135.855	0.087921	12.348	0.9325	1.662	53.99684 + 28.40942	521.00 + 317.51	636.00	0.33	0.001 ± 0.000
028_VU107-T	0 °C	✓	0.008203	5.675	42.376750	57.066	0.004135	135.855	0.087921	12.348	0.9325	1.662	53.99684 + 28.40942	521.00 + 317.51	636.00	0.33	0.001 ± 0.000
029_VU107-T	0 °C	✓	0.008203	5.675	42.376750	57.066	0.004135	135.855	0.087921	12.348	0.9325	1.662	53.99684 + 28.40942	521.00 + 317.51	636.00	0.33	0.001 ± 0.000
182_VU107-T	0 °C	✓	0.008203	5.675	42.376750	57.066	0.004135	135.855	0.087921	12.348	0.9325	1.662	53.99684 + 28.40942	521.00 + 317.51	636.00	0.33	0.001 ± 0.000
183_VU107-T	0 °C	✓	0.008203	5.675	42.376750	57.066	0.004135	135.855	0.087921	12.348	0.9325	1.662	53.99684 + 28.40942	521.00 + 317.51	636.00	0.33	0.001 ± 0.000
184_VU107-T	0 °C	✓	0.008203	5.675	42.376750	57.066	0.004135	135.855	0.087921	12.348	0.9325	1.662	53.99684 + 28.40942	521.00 + 317.51	636.00	0.33	0.001 ± 0.000
185_VU107-T	0 °C	✓	0.008203	5.675	42.376750	57.066	0.004135	135.855	0.087921	12.348	0.9325	1.662	53.99684 + 28.40942	521.00 + 317.51	636.00	0.33	0.001 ± 0.000
186_VU107-T	0 °C	✓	0.008203	5.675	42.376750	57.066	0.004135	135.855	0.087921	12.348	0.9325	1.662	53.99684 + 28.40942	521.00 + 317.51	636.00	0.33	0.001 ± 0.000
187_VU107-T	0 °C	✓	0.008203	5.675	42.376750	57.066	0.004135	135.855	0.087921	12.348	0.9325	1.662	53.99684 + 28.40942	521.00 + 317.51	636.00	0.33	0.001 ± 0.000
188_VU107-T	0 °C	✓	0.008203	5.675	42.376750	57.066	0.004135	135.855	0.087921	12.348	0.9325	1.662	53.99684 + 28.40942	521.00 + 317.51	636.00	0.33	0.001 ± 0.000
189_VU107-T	0 °C	✓	0.008203	5.675	42.376750	57.066	0.004135	135.855	0.087921	12.348	0.9325	1.662	53.99684 + 28.40942	521.00 + 317.51	636.00	0.33	0.001 ± 0.000
190_VU107-T	0 °C	✓	0.008203	5.675	42.376750	57.066	0.004135	135.855	0.087921	12.348	0.9325	1.662	53.99684 + 28.40942	521.00 + 317.51	636.00	0.33	0.001 ± 0.000
191_VU107-T	0 °C	✓	0.008203	5.675	42.376750	57.066	0.004135	135.855	0.087921	12.348	0.9325	1.662	53.99684 + 28.40942	521.00 + 317.51	636.00	0.33	0.001 ± 0.000
192_VU107-T	0 °C	✓	0.008203	5.675	42.376750	57.066	0.004135	135.855	0.087921	12.348	0.9325	1.662	53.99684 + 28.40942	521.00 + 317.51	636.00	0.33	0.001 ± 0.000
193_VU107-T	0 °C	✓	0.008203	5.675	42.376750	57.066	0.004135	135.855	0.087921	12.348	0.9325	1.662	53.99684 + 28.40942	521.00 + 317.51	636.00	0.33	0.001 ± 0.000
194_VU107-T	0 °C	✓	0.008203	5.675	42.376750	57.066	0.004135	135.855	0.087921	12.348	0.9325	1.662	53.99684 + 28.40942	521.00 + 317.51	636.00	0.33	0.001 ± 0.000
195_VU107-T	0 °C	✓	0.008203	5.675	42.376750	57.066	0.004135	135.855	0.087921	12.348	0.9325	1.662	53.99684 + 28.40942	521.00 + 317.51	636.00	0.33	0.001 ± 0.000
196_VU107-T	0 °C	✓	0.008203	5.675	42.376750	57.066	0.004135	135.855	0.087921	12.348	0.9325	1.662	53.99684 + 28.40942	521.00 + 317.51	636.00	0.33	0.001 ± 0.000
197_VU107-T	0 °C	✓	0.008203	5.675	42.376750	57.066	0.004135	135.855	0.087921	12.348	0.9325	1.662	53.99684 + 28.40942	521.00 + 317.51	636.00	0.33	0.001 ± 0.000
198_VU107-T	0 °C	✓	0.008203	5.675	42.376750	57.066	0.004135	135.855	0.087921	12.348	0.9325	1.662	53.99684 + 28.40942	521.00 + 317.51	636.00	0.33	0.001 ± 0.000
199_VU107-T	0 °C	✓	0.008203	5.675	42.376750	57.066	0.004135	135.855	0.087921	12.348	0.9325	1.662	53.99684 + 28.40942	521.00 + 317.51	636.00	0.33	0.001 ± 0.000
200_VU107-T	0 °C	✓	0.008203	5.675	42.376750	57.066	0.004135	135.855	0.087921	12.348	0.9325	1.662	53.99684 + 28.40942	521.00 + 317.51	636.00	0.33	0.001 ± 0.000
201_VU107-T	0 °C	✓	0.008203	5.675	42.376750	57.066	0.004135	135.855	0.087921	12.348	0.9325	1.662	53.99684 + 28.40942	521.00 + 317.51	636.00	0.33	0.001 ± 0.000
202_VU107-T	0 °C	✓	0.008203	5.675	42.376750	57.066	0.004135	135.855	0.087921	12.348	0.9325	1.662	53.99684 + 28.40942	521.00 + 317.51	636.00	0.33	0.001 ± 0.000
203_VU107-T	0 °C	✓	0.008203	5.675	42.376750	57.066	0.004135	135.855	0.087921	12.348	0.9325	1.662	53.99684 + 28.40942	521.00 + 317.51	636.00	0.33	0.001 ± 0.000
204_VU107-T	0 °C	✓	0.008203	5.675	42.376750	57.066	0.004135	135.855	0.087921	12.348	0.9325	1.662	53.99684 + 28.40942	521.00 + 317.51	636.00	0.33	0.001 ± 0.000
205_VU107-T	0 °C	✓	0.008203	5.675	42.376750	57.066	0.004135	135.855	0.087921	12.348	0.9325	1.662	53.99684 + 28.40942	521.00 + 317.51	636.00	0.33	0.001 ± 0.000
206_VU107-T	0 °C	✓	0.008203	5.675	42.376750	57.066	0.004135	135.855	0.087921	12.348	0.9325	1.662					

TABLES12

104-643-A8H3-24-26	65.55	6.46	-72.7	75.8	-76.7	67.3	R	24.6	247.3	4.32	-0.39	0.92	581.3	221.3	221.3	221.3	70.10	221.3	-76.7	R	0.33	6,76
104-643-A8H3-37-59	65.88	0.47	-31.0	77.7	-47.3	42.2	R	60.9	222.2	3.88	-0.74	0.67	556.2	196.2	196.2	196.2	70.43	196.2	-67.3	R	0.37	6,81
104-643-A8H3-39-45	66.25	17.45	61.9	63.1	48.0	28.5	R	28.5	228.0	3.98	-0.67	0.74	562.0	202.0	202.0	202.0	70.48	202.0	-63.1	R	0.37	6,86
104-643-A8H3-131-133	66.25	14.01	14.01	62.0	62.0	33.9	R	24.3	219.5	3.88	-0.58	0.58	563.7	197.3	197.3	197.3	70.48	197.3	-63.1	R	0.37	6,91
104-643-A8H3-24-26	67.05	0.90	-48.9	76.5	-64.8	55.8	R	25.8	235.8	3.04	-0.70	0.72	558.9	199.8	199.8	199.8	71.60	199.8	-64.8	R	0.38	6,97
104-643-A8H3-47-59	67.38	6.17	26.8	83.0	-68.3	55.9	R	12.1	235.9	4.12	-0.56	0.83	569.9	209.9	209.9	209.9	71.93	209.9	-68.3	R	0.36	7,01
104-643-A8H3-93-95	67.74	0.30	58.4	95.9	70.3	50.4	R	23.0	230.4	4.02	-0.64	0.77	564.4	204.4	204.4	204.4	72.49	204.4	-70.3	R	0.38	7,06
104-643-A8H4-131-133	68.12	0.09	-47.2	93.9	-79.4	38.0	R	14.2	218.0	3.86	-0.79	0.62	562.0	192.0	192.0	192.0	72.67	192.0	-79.4	R	0.43	7,11
104-643-A8H4-131-133	68.55	0.17	65.2	70.2	64.6	62.6	R	47.8	62.6	1.09	0.46	0.89	576.6	216.6	216.6	216.6	73.10	216.6	-64.6	R	0.34	7,15
104-643-A8H4-55-69	68.89	0.07	10.4	10.4	10.4	10.4	R	17.8	181.1	0.93	-0.53	0.53	569.3	209.3	209.3	209.3	72.60	209.3	-73.8	R	0.38	7,18
104-643-A8H5-93-97	69.24	0.09	-11.7	58.2	175.2	175.2	N	32.8	175.2	3.06	-1.00	0.08	569.2	232.2	232.2	232.2	73.79	232.2	-58.2	N	0.38	7,20
104-643-A8H5-131-133	69.62	0.08	32.4	120.2	57.6	189.1	N	25.4	189.1	3.30	-0.99	0.16	703.1	343.1	343.1	343.1	74.17	343.1	-57.6	N	0.43	7,22
104-643-A8H6-24-26	70.05	22.56	76.0	197.6	76.0	205.1	N	38.6	205.1	3.55	-0.91	0.42	719.1	359.1	359.1	359.1	74.60	359.1	-76.8	N	0.33	7,25
104-643-A8H6-57-59	70.38	2.26	7.9	118.4	62.2	155.2	N	36.4	155.2	2.71	-0.91	0.42	669.2	309.2	309.2	309.2	74.93	309.2	-62.1	N	0.35	7,27
104-643-A8H6-131-133	70.73	0.65	113.9	119.9	45.9	100.8	N	30.2	100.8	2.64	-0.97	0.04	622.8	267.2	267.2	267.2	75.28	267.2	-45.9	(excursion)	0.40	7,36
104-643-A8H6-132-134	70.73	0.09	113.9	119.9	45.9	100.8	N	30.2	100.8	2.64	-0.97	0.04	703.1	359.1	359.1	359.1	75.28	359.1	-45.9	(gap below)	0.40	7,36
104-643-A8H7-135-137	72.06	15.09	77.0	113.3	74.6	104.7	N	78	104.7	1.83	-0.57	0.57	582.9	32.8	32.8	32.8	73.11	32.8	-74.6	N	0.30	7,50
104-643-A8H9-155-97	72.36	13.23	66.1	108.7	71.0	99.2	N	40.7	99.2	1.73	-0.16	0.99	387.3	27.3	27.3	27.3	73.87	27.3	-71.0	N	0.40	7,62
104-643-A8H9-135-137	72.76	2.50	82.3	94.4	74.3	98.2	N	36.6	98.2	1.71	-0.14	0.99	386.3	26.3	26.3	26.3	73.86	26.3	-74.3	N	0.40	7,66
104-643-A8H9-135-137	73.16	12.88	73.3	82.8	73.0	83.7	N	36.7	83.7	1.41	0.11	0.99	373.6	11.8	11.8	11.8	73.18	27.18	-73.0	N	0.35	7,69
104-643-A8H9-24-26	73.50	20.02	36.1	36.1	36.1	36.1	N	39.4	88.1	1.49	-0.01	0.00	359.4	32.8	32.8	32.8	73.44	32.8	-74.0	N	0.40	7,76
104-643-A8H9-25-57	73.86	1.07	13.0	13.0	13.0	13.0	N	40.8	98.8	1.21	-0.19	0.09	358.2	32.8	32.8	32.8	73.90	32.8	-74.0	N	0.40	7,76
104-643-A8H9-131-133	74.26	13.77	74.4	110.9	73.9	110.1	N	36.6	110.1	1.92	-0.34	0.34	402.3	42.3	42.3	42.3	74.03	42.3	-67.4	N	0.40	7,83
104-643-A8H9-3-25-27	75.06	16.46	70.5	60.0	66.6	69.0	N	34.5	69.0	1.20	0.36	0.93	351.1	357.1	357.1	357.1	80.11	357.1	-66.6	N	0.30	7,86
104-643-A8H9-33-57	75.36	20.75	65.7	72.5	67.0	67.8	N	27.7	67.8	1.38	0.53	0.93	355.9	355.9	355.9	355.9	80.41	355.9	-67.0	N	0.40	7,89
104-643-A8H9-33-57	75.75	1.07	13.0	13.0	13.0	13.0	N	41.5	13.0	1.41	-0.14	0.04	350.9	350.9	350.9	350.9	80.41	350.9	-67.0	N	0.30	7,92
104-643-A8H9-135-137	76.16	20.59	69.1	69.1	62.6	70.6	N	30.3	62.6	1.09	0.46	0.89	360.7	23.1	23.1	23.1	81.21	23.1	-70.6	N	0.40	7,96
104-643-A8H9-4-25-27	76.56	12.70	71.0	86.4	69.5	86.0	N	33	86.0	1.50	-0.07	1.00	374.1	14.1	14.1	14.1	81.61	374.1	-69.5	N	0.30	7,99
104-643-A8H9-45-57	76.86	12.26	74.2	10.8	71.7	67.3	N	28.3	67.3	1.17	0.37	0.92	354.5	354.5	354.5	354.5	81.91	354.5	-71.7	N	0.40	8,02
104-643-A8H9-45-57	77.26	15.26	75.6	85.8	74.0	63.8	N	31.6	63.8	1.18	0.44	0.90	351.9	351.9	351.9	351.9	81.91	351.9	-74.0	N	0.40	8,06
104-643-A8H9-131-133	77.66	1.07	8.0	8.0	8.0	8.0	N	30.1	8.0	0.55	0.44	0.56	357.6	357.6	357.6	357.6	82.17	357.6	-72.5	N	0.40	8,09
104-643-A8H9-131-133	78.06	1.07	8.0	8.0	8.0	8.0	N	30.1	8.0	0.55	0.44	0.56	357.1	357.1	357.1	357.1	82.30	357.1	-73.0	N	0.40	8,12
104-643-A8H9-131-133	78.36	10.39	75.4	25.2	74.3	245.6	R	36	245.6	7.50	0.35	0.94	357.3	17.7	17.7	17.7	83.45	17.7	-73.3	R	0.40	8,14
104-643-A8H9-6-25-27	78.76	1.76	73.6	16.5	68.5	49.3	R	8.4	49.3	7.45	0.38	0.92	353.6	15.6	15.6	15.6	83.81	15.6	-49.3	R	0.40	8,17
104-643-A8H9-6-25-27	79.16	0.76	10.3	10.3	80.0	80.0	R	4.4	80.0	0.76	0.44	0.44	435.1	8.4	8.4	8.4	84.93	8.4	-80.2	R	0.40	8,25
104-643-A8H9-131-133	80.00	5.61	56.2	56.2	56.2	56.2	R	31.6	56.2	0.76	0.44	0.44	314.8	8.4	8.4	8.4	85.24	8.4	-80.8	R	0.40	8,28
104-643-A8H9-131-133	80.66	1.07	8.2	8.2	97.1	97.1	R	5.7	97.1	0.57	0.35	0.94	308.8	8.8	8.8	8.8	86.69	8.8	-66.9	R	0.40	8,31
104-643-A8H9-131-133	81.06	2.92	74.2	16.2	72.6	142.2	R	7.3	142.2	0.56	0.60	0.62	402.7	7.0	7.0	7.0	81.11	7.0	-72.6	R	1.71	gap below
104-643-A10H-155-57	81.86	2.56	18.8	182.2	89.2	201.4	R	47.2	201.4	0.93	0.36	0.66	540.5	180.5	180.5	180.5	180.8	180.5	-69.2	R	0.40	8,63
104-643-A10H-155-57	82.26	4.22	73.7	166.8	78.3	192.1	R	8.3	192.1	0.72	0.48	0.51	531.2	17.1	17.1	17.1	88.22	17.1	-78.3	R	0.40	8,69
104-643-A10H-155-57	82.66	9.33	20.2	20.2	68.9	198.0	R	36.5	198.0	0.95	0.31	0.51	537.1	17.7	17.7	17.7	88.12	17.7	-68.9	R	0.40	8,74
104-643-A10H-155-57	83.06	1.37	13.0	13.0	13.0	13.0	R	34.1	13.0	0.72	0.49	0.51	341.7	2.4	2.4	2.4	89.02	2.4	-70.5	R	0.40	8,78
104-643-A10H-155-57	83.46	1.07	13.0	13.0	13.0	13.0	R	34.1	13.0	0.72	0.49	0.51	341.7	1.4	1.4	1.4	89.02	1.4	-70.5	R	0.40	8,82
104-643-A10H-155-57	83.86	1.07	13.0	13.0	13.0	13.0	R	34.1	13.0	0.72	0.49	0.51	341.7	1.4	1.4	1.4	89.02	1.4	-70.5	R	0.40	8,86
104-643-A10H-155-57	84.26	1.07	13.0	13.0	13.0	13.0	R	34.1	13.0	0.72	0.49	0.51	341.7	1.4	1.4	1.4	89.02	1.4	-70.5	R	0.40	8,90
104-643-A10H-155-57	84.66	1.07	13.0	13.0	13.0	13.0	R	34.1	13.0	0.72	0.49	0.51	341.7	1.4	1.4	1.4	89.02	1.4	-70.5	R	0.40	8,94
104-643-A10H-155-57	85.06	1.07	13.0	13.0	13.0	13.0	R	34.1	13.0	0.72	0.49	0.51	341.7	1.4	1.4	1.4	89.02	1.4	-70.5	R	0.40	8,98
104-643-A10H-155-57	85.46	1.07	13.0	13.0	13.0	13.0	R	34.1	13.0	0.72	0.49	0.51	341.7	1.4	1.4	1.4	89.02	1.4	-70.5	R	0.40	9,02
104-643-A10H-155-57	85.86	1.07	13.0	13.0	13.0	1																

104-643A15H-3,135-137	133.16	0.09	13.9	231.5	<b>-55.8</b>	223.2	R	4.7	403.2	7.04	0.73	0.68	7.04	0.73	0.68	511.3	151.3	151.3	151.3	<b>-55.8</b>	R	0.40	15,02			
104-643A15H-4,135-137	133.56	0.07	-37.6	206.8	<b>-71.2</b>	218.7	R	38.3	398.7	6.96	0.78	0.63	7.11	0.68	0.74	506.8	146.8	146.8	146.8	<b>-71.2</b>	R	0.30	15,02			
104-643A15H-4,135-137	133.56	0.05	56.6	244.6	<b>-66.2</b>	227.5	R	9	407.5	7.11	0.68	0.74	7.11	0.68	0.74	515.6	155.6	155.6	155.6	<b>-66.2</b>	R	0.40	15,03			
104-643A15H-4,135-137	133.56	0.05	56.6	244.6	<b>-66.2</b>	227.5	R	9	364.8	6.96	0.78	0.63	7.11	0.68	0.74	515.6	155.6	155.6	155.6	<b>-66.2</b>	R	0.40	15,03			
104-643A15H-4,135-137	134.66	0.10	80.7	133.3	72.5	121.3	N	12.8	131.3	2.12	-0.52	0.85	7.27	0.57	0.57	409.4	49.4	54.4	409.4	48.4	54.4	72.5	N	0.40	16,30	
104-643A15H-4,135-137	135.06	0.30	20.3	136.6	64.7	126.9	N	32.6	126.9	2.21	-0.60	0.80	7.27	0.57	0.57	415.0	55.0	55.0	415.0	44.26	415.0	64.7	N	0.30	16,32	
104-643A15H-5,55-57	135.36	0.40	52.7	107.7	67.6	106.8	N	10.6	108.8	1.86	-0.29	0.96	7.27	0.57	0.57	394.9	34.9	34.9	394.9	144.56	394.9	67.6	N	0.40	16,33	
104-643A15H-5,55-57	135.76	0.84	86.4	272.0	70.3	129.5	N	38.7	129.5	2.20	-0.64	0.77	7.27	0.57	0.57	417.6	57.6	57.6	417.6	144.96	417.6	70.3	N	0.80	16,35	
104-643A15H-5,55-57	136.56	0.50	63.2	114.6	<b>-65.0</b>	114.4	N	25.3	114.4	2.00	-0.41	0.91	7.27	0.57	0.57	402.5	42.5	42.5	402.5	145.46	402.5	65.0	N	0.30	16,39	
104-643A15H-5,55-57	136.56	0.50	63.2	114.6	<b>-65.0</b>	114.4	N	25.3	114.4	2.00	-0.41	0.91	7.27	0.57	0.57	407.4	47.4	47.4	407.4	145.46	407.4	65.0	N	0.40	16,40	
104-643A15H-5,55-57	137.26	0.12	61.9	232.2	70.2	125.7	N	12.1	125.7	2.19	-0.58	0.81	7.27	0.57	0.57	413.8	53.8	53.8	413.8	146.46	413.8	70.2	N	0.40	16,42	
104-643A15H-5,55-57	137.66	0.28	79.2	113.0	73.9	107.5	N	31.7	107.5	1.88	-0.30	0.95	7.27	0.57	0.57	395.6	35.6	35.6	395.6	146.86	395.6	73.9	N	0.40	16,43	
104-643A15H-7,25-27	138.06	0.46	44.5	315.4	69.8	322.8	N	36	322.8	5.63	0.80	-0.60	0.75	7.27	0.57	0.57	310.9	250.9	250.9	310.9	147.26	250.9	69.8	N	1.00	16,45
104-643A16H-1,25-27	138.56	0.16	40.9	169.3	<b>-59.0</b>	168.3	R	12.7	348.3	6.08	0.98	0.20	7.27	0.57	0.57	505.9	145.9	145.9	505.9	<b>-59.0</b>	R	0.30	16,50			
104-643A16H-1,25-27	138.56	0.21	40.9	169.3	<b>-59.0</b>	168.3	R	12.7	303.8	0.57	0.58	0.55	7.27	0.57	0.57	465.5	99.5	99.5	465.5	<b>-59.0</b>	R	0.40	16,51			
104-643A16H-1,25-27	139.26	0.44	37.4	176.6	<b>-56.5</b>	176.6	R	13.1	311.2	5.68	0.75	0.75	7.27	0.57	0.57	468.4	136.4	136.4	468.4	136.4	136.4	56.5	R	0.40	16,53	
104-643A16H-1,25-27	139.66	0.19	47.2	356.9	48.5	40.9	N	5.2	40.9	0.71	0.76	0.65	7.27	0.57	0.57	378.5	18.5	18.5	378.5	146.36	378.5	48.5	N	0.40	16,55	
104-643A16H-1,25-27	140.06	0.17	69.7	317.6	68.2	286.6	N	4.7	286.6	0.50	0.88	0.48	7.27	0.57	0.57	366.2	6.2	6.2	366.2	149.76	366.2	68.2	N	0.26	16,58	
104-643A16H-1,25-27	140.32	0.35	73.2	322.5	75.3	204.4	N	34.2	204.4	0.50	0.94	0.35	7.27	0.57	0.57	350.0	358.0	358.0	350.0	150.2	358.0	75.3	N	0.40	16,59	
104-643A16H-1,25-27	140.76	0.31	73.6	55.1	73.9	24.7	N	24	24.7	0.40	0.91	0.42	7.27	0.57	0.57	362.3	2.3	2.3	362.3	150.46	362.3	73.9	N	0.40	16,62	
104-643A16H-1,25-27	141.16	0.12	73.6	74.5	68.6	19.4	N	19.4	19.4	0.09	0.78	0.77	7.27	0.57	0.57	342.8	342.8	342.8	342.8	149.46	342.8	6.0	N	0.30	16,64	
104-643A16H-1,25-27	141.56	0.13	73.6	93.4	58.0	37.3	N	19.3	37.3	0.08	0.61	0.61	7.27	0.57	0.57	359.5	14.6	14.6	359.5	146.36	359.5	6.0	N	0.36	16,67	
104-643A16H-1,25-27	141.82	0.09	73.6	61.9	74.8	71.4	N	12.1	72.4	0.48	0.89	0.46	7.27	0.57	0.57	365.2	5.2	5.2	365.2	151.52	365.2	71.4	N	0.44	16,68	
104-643A16H-1,25-27	142.26	0.13	73.6	83.0	74.7	41.9	N	22	41.9	0.73	0.74	0.67	7.27	0.57	0.57	379.5	19.5	19.5	379.5	146.36	379.5	74.7	N	0.40	16,71	
104-643A16H-1,25-27	142.66	0.15	73.1	73.1	<b>-51.9</b>	66.2	R	15.4	24.5	4.24	-0.40	0.91	7.27	0.57	0.57	403.8	43.8	43.8	403.8	152.36	403.8	<b>-51.9</b>	R	0.40	16,72	
104-643A16H-1,25-27	143.06	0.19	43.5	97.9	<b>-79.9</b>	198.6	R	15.5	19.5	0.55	0.92	0.32	7.27	0.57	0.57	356.2	176.2	176.2	356.2	<b>-79.9</b>	R	0.26	16,73			
104-643A16H-1,25-27	143.46	0.11	43.5	252.9	<b>-80.1</b>	239.8	R	20.1	219.8	7.3	0.50	0.66	7.27	0.57	0.57	327.0	217.4	217.4	327.0	<b>-80.1</b>	R	0.40	16,74			
104-643A16H-1,25-27	143.86	0.13	43.5	252.9	<b>-80.1</b>	239.8	R	20.1	219.8	7.3	0.50	0.66	7.27	0.57	0.57	327.0	217.4	217.4	327.0	<b>-80.1</b>	R	0.40	16,75			
104-643A16H-1,25-27	144.26	0.07	43.5	97.9	<b>-79.9</b>	198.6	R	15.5	19.5	0.55	0.92	0.32	7.27	0.57	0.57	356.2	162.7	162.7	356.2	<b>-79.9</b>	R	0.26	16,76			
104-643A16H-1,25-27	144.66	0.15	35.0	97.9	<b>-41.4</b>	18.0	R	17.8	37.8	0.54	0.99	0.22	7.27	0.57	0.57	348.7	0.14	0.14	348.7	14.84	0.14	18.4	R	0.30	16,78	
104-643A16H-1,25-27	145.06	0.66	32.2	116.2	<b>-65.7</b>	97.7	R	14.7	27.7	0.75	0.99	0.14	7.27	0.57	0.57	342.2	44.2	44.2	342.2	144.96	44.2	97.7	R	9.65	gap below 16,81	
104-643A16X-1,25-27	148.06	0.15	35.0	97.9	<b>-41.4</b>	18.0	R	17.8	37.8	0.54	0.99	0.22	7.27	0.57	0.57	340.2	5.2	5.2	340.2	182.0	5.2	18.0	R	0.30	16,81	
104-643A16X-1,25-27	148.46	0.66	32.2	116.2	<b>-65.7</b>	97.7	R	14.7	27.7	0.75	0.99	0.14	7.27	0.57	0.57	342.2	44.2	44.2	342.2	144.96	44.2	97.7	R	9.65	gap below 16,81	
104-643A16X-1,25-27	148.86	0.15	35.0	97.9	<b>-41.4</b>	18.0	R	17.8	37.8	0.54	0.99	0.22	7.27	0.57	0.57	340.2	5.2	5.2	340.2	182.0	5.2	18.0	R	0.30	16,81	
104-643A16X-1,25-27	149.26	0.15	35.0	97.9	<b>-41.4</b>	18.0	R	17.8	37.8	0.54	0.99	0.22	7.27	0.57	0.57	340.2	5.2	5.2	340.2	182.0	5.2	18.0	R	0.30	16,81	
104-643A16X-1,25-27	149.66	0.15	35.0	97.9	<b>-41.4</b>	18.0	R	17.8	37.8	0.54	0.99	0.22	7.27	0.57	0.57	340.2	5.2	5.2	340.2	182.0	5.2	18.0	R	0.30	16,81	
104-643A16X-1,25-27	150.06	0.15	35.0	97.9	<b>-41.4</b>	18.0	R	17.8	37.8	0.54	0.99	0.22	7.27	0.57	0.57	340.2	5.2	5.2	340.2	182.0	5.2	18.0	R	0.30	16,81	
104-643A16X-1,25-27	150.46	0.15	35.0	97.9	<b>-41.4</b>	18.0	R	17.8	37.8	0.54	0.99	0.22	7.27	0.57	0.57	340.2	5.2	5.2	340.2	182.0	5.2	18.0	R	0.30	16,81	
104-643A16X-1,25-27	150.86	0.15	35.0	97.9	<b>-41.4</b>	18.0	R	17.8	37.8	0.54	0.99	0.22	7.27	0.57	0.57	340.2	5.2	5.2	340.2	182.0	5.2	18.0	R	0.30	16,81	
104-643A16X-1,25-27	151.26	0.15	35.0	97.9	<b>-41.4</b>	18.0	R	17.8	37.8	0.54	0.99	0.22	7.27	0.57	0.57	340.2	5.2	5.2	340.2	182.0	5.2	18.0	R	0.30	16,81	
104-643A16X-1,25-27	151.66	0.15	35.0	97.9	<b>-41.4</b>	18.0	R	17.8	37.8	0.54	0.99	0.22	7.27	0.57	0.57	340.2	5.2	5.2	340.2	182.0	5.2	18.0	R	0.30	16,81	
104-643A16X-1,25-27	152.06	0.15	35.0	97.9	<b>-41.4</b>	18.0	R	17.8	37.8	0.54	0.99	0.22	7.27	0.57	0.57	340.2	5.2	5.2	340.2	182.0	5.2	18.0	R	0.30	16,81	
104-643A16X-1,25-27	152.46	0.15	35.0	97.9	<b>-41.4</b>	18.0	R	17.8	37.8	0																

104-643A-26X1.85-87	235.36	0.04	49.3	34.6	<b>-59.2</b>	151.5	R	331.5	5.79	0.88	0.48	495.3	135.3	135.3	135.3	<b>-59.2</b>	R	0.50	17.97	
104-643A-26X1.135-137	235.86	0.02	44.6	71.8	<b>-41.6</b>	152.0	R	332.0	5.79	0.88	0.47	495.8	135.8	135.8	135.8	<b>-41.6</b>	R	0.50	17.98	
104-643A-26X1.35-87	236.36	0.04	73.6	25.9	<b>-56.5</b>	201.5	R	341.5	6.66	0.93	0.37	495.3	135.3	135.3	135.3	<b>-56.5</b>	R	0.50	17.99	
104-643A-26X1.35-87	236.36	0.04	73.6	77.0	<b>-82.5</b>	100.7	R	341.5	6.66	0.93	0.37	495.3	135.3	135.3	135.3	<b>-82.5</b>	R	0.50	18.00	
104-643A-26X1.135-137	237.36	0.04	36.0	313.2	<b>-55.3</b>	203.1	R	348.3	5.61	0.92	0.33	495.8	135.8	135.8	135.8	<b>-55.3</b>	R	0.50	18.05	
104-643A-26X1.35-87	237.86	0.05	37.0	290.7	<b>-64.3</b>	243.2	R	34.4	423.2	7.39	0.45	0.89	496.0	136.0	136.0	136.0	<b>-64.3</b>	R	0.50	18.01
104-643A-26X1.85-87	238.36	0.03	68.6	208.8	<b>-66.0</b>	236.6	R	4.4	416.6	7.27	0.55	0.83	498.0	220.4	220.4	220.4	<b>-66.0</b>	R	0.50	18.02
104-643A-26X3.135-137	238.86	0.06	63.9	188.7	<b>-85.</b>	209.9	R	3.1	389.9	6.81	0.87	0.50	498.0	135.7	135.7	135.7	<b>-85.</b>	R	0.50	18.03
104-643A-26X4.35-87	239.36	0.08	77.4	19.3	<b>-85.6</b>	205.5	R	3.8	239.1	6.81	0.87	0.48	498.5	135.8	135.8	135.8	<b>-85.6</b>	R	0.50	18.04
104-643A-26X3.35-87	239.36	0.08	77.4	39.4	<b>-85.6</b>	205.5	R	3.8	239.1	6.81	0.87	0.48	498.5	135.8	135.8	135.8	<b>-85.6</b>	R	0.50	18.05
104-643A-26X2.35-87	240.86	0.04	82.3	249.8	71.8	236.2	N	9	236.2	5.69	0.83	0.56	500.0	210.0	310.0	310.0	71.8	N	0.50	18.08
104-643A-26X5.135-137	241.36	0.04	77.3	343.6	79.3	353.0	N	4.3	353.0	6.16	0.99	0.12	500.8	136.0	136.0	136.0	<b>-78.5</b>	R	0.50	18.00
104-643A-26X4.35-87	241.86	0.04	75.7	357.7	69.1	12.0	N	12.0	0.21	0.98	0.21	501.3	227.0	227.0	227.0	<b>-64.3</b>	R	0.50	18.01	
104-643A-26X4.35-87	242.36	0.04	85.4	76.5	60.1	345.9	N	14.4	345.9	6.0	0.97	0.24	504.0	329.7	329.7	329.7	60.4	N	0.50	18.12
104-643A-26X4.85-87	242.86	0.04	24.0	74.7	43.6	76.7	354.8	3.4	304.0	6.19	1.00	0.10	504.0	338.3	338.3	338.3	76.7	N	0.50	18.14
104-643A-26X5.135-137	243.36	0.05	77.4	249.8	71.8	246.0	N	4.3	246.0	5.69	0.83	0.56	504.0	227.0	227.0	227.0	<b>-64.3</b>	R	0.50	18.16
104-643A-27X1.35-87	244.66	0.02	84.8	354.8	61.5	68.5	N	1.2	68.5	1.20	0.37	0.93	505.1	152.1	192.3	192.3	61.5	N	0.50	18.26
104-643A-27X1.85-87	245.16	0.03	37.0	130.4	75.5	54.7	N	29.7	54.7	0.95	0.58	0.82	505.7	192.3	192.3	192.3	<b>-85.6</b>	R	0.50	18.28
104-643A-27X1.135-137	245.66	0.06	33.0	190.5	41.4	75.4	N	18.3	75.4	1.32	0.25	0.97	505.8	198.1	198.1	198.1	41.4	N	0.50	18.30
104-643A-27X2.35-87	246.16	0.02	73.2	324.3	57.6	331.6	N	10.3	331.6	5.79	0.88	0.48	506.3	141.0	183.0	183.0	57.6	N	0.50	18.34
104-643A-27X1.135-137	247.16	0.03	4.9	298.6	<b>-80.0</b>	238.7	N	50.7	238.7	5.66	0.86	0.50	507.0	210.0	210.0	210.0	92.4	N	0.50	18.37
104-643A-27X3.135-137	247.66	0.02	9.0	269.9	<b>-56.4</b>	128.2	R	3.4	308.2	5.38	0.62	0.79	507.0	210.1	210.1	210.1	<b>-56.4</b>	R	0.50	18.39
104-643A-27X3.85-87	248.16	0.04	84.5	140.9	50.5	87.4	R	3.4	267.4	4.67	-0.05	-1.00	507.0	210.1	210.1	210.1	<b>-56.5</b>	R	0.50	18.41
104-643A-27X4.29-87	248.66	0.09	16.5	180.0	2.3	184.6	R	3.1	184.6	3.22	-1.00	-0.08	507.0	207.3	207.3	207.3	<b>-56.4</b>	R	0.50	18.43
104-643A-27X4.29-87	249.10	0.04	75.7	34.0	55.8	217.1	N	9.7	217.1	3.79	-0.80	-0.60	507.0	192.3	192.3	192.3	<b>-56.4</b>	R	0.50	18.45
104-643A-27X4.29-87	249.56	0.04	75.7	34.0	55.8	217.1	N	9.7	217.1	3.79	-0.80	-0.60	507.0	192.3	192.3	192.3	<b>-56.4</b>	R	0.50	18.47
104-643A-27X4.29-87	250.16	0.14	73.3	54.4	73.6	154.2	N	8.2	154.2	2.69	-0.90	-0.44	507.0	177.4	177.4	177.4	75.5	N	0.50	18.49
104-643A-27X5.35-87	250.66	0.07	34.0	120.1	52.4	167.1	N	4.1	167.1	2.92	-0.97	-0.22	507.0	198.1	198.1	198.1	41.4	N	0.50	18.51
104-643A-27X5.72-74	251.03	0.08	61.9	77.9	<b>-68.1</b>	64.3	R	14.4	244.3	4.26	-0.43	-0.90	507.0	187.0	187.0	187.0	<b>-68.9</b>	R	0.50	18.53
104-643A-27X5.125-127	251.56	0.12	56.3	73.2	<b>-64.1</b>	64.3	R	18.7	244.3	4.27	-0.43	-0.90	507.0	187.0	187.0	187.0	<b>-64.6</b>	R	0.50	18.55
104-643A-27X6.74-79	252.06	0.05	45.0	123.4	<b>-68.1</b>	64.3	R	4.7	244.4	4.27	-0.43	-0.90	507.0	187.0	187.0	187.0	<b>-64.4</b>	R	0.50	18.58
104-643A-27X6.74-79	252.56	0.12	56.4	73.2	<b>-64.1</b>	64.3	R	14.4	244.4	4.27	-0.43	-0.90	507.0	187.0	187.0	187.0	<b>-64.5</b>	R	0.50	18.59
104-643A-27X6.125-127	253.06	0.07	75.8	134.8	<b>-47.6</b>	63.1	R	14.6	243.1	4.24	-0.45	-0.89	507.0	187.0	187.0	187.0	<b>-65.8</b>	R	0.50	18.61
104-643A-28X1.35-87	254.46	0.08	29.4	351.6	12.5	336.8	R	4.6	516.8	9.02	-0.32	-0.19	507.0	227.0	227.0	227.0	<b>-12.5</b>	R	0.50	18.70
104-643A-28X1.85-87	254.96	0.15	14.4	349.5	51.4	46.9	R	4.7	525.6	3.95	-0.68	-0.73	507.0	90.9	90.9	90.9	<b>-15.4</b>	R	0.50	18.72
104-643A-28X2.35-87	255.46	0.08	32.0	31.1	52.1	285.8	N	27.9	285.8	0.56	-0.88	-0.48	507.0	149.8	149.8	149.8	<b>-43.2</b>	R	0.50	18.75
104-643A-28X2.35-87	255.96	0.05	14.8	51.2	52.5	256.8	N	16.8	256.8	0.69	-0.92	-0.48	507.0	177.4	177.4	177.4	<b>-43.2</b>	R	0.50	18.77
104-643A-28X3.135-137	256.56	0.10	77.8	100.0	<b>-43.2</b>	170.0	N	7.7	170.0	5.36	0.60	0.80	507.0	171.0	171.0	171.0	<b>-43.2</b>	N	0.50	18.78
104-643A-28X3.35-87	257.46	0.08	62.4	84.1	67.1	352.3	N	13.5	352.3	6.15	0.99	0.13	507.0	198.1	198.1	198.1	<b>-39.6</b>	N	0.50	18.79
104-643A-28X3.135-137	257.96	0.12	50.4	283.4	66.1	276.1	N	7.5	276.1	4.82	0.11	0.99	507.0	198.1	198.1	198.1	<b>-39.6</b>	N	0.50	18.80
104-643A-28X3.135-137	260.46	0.10	50.4	32.0	64.1	310.9	N	20.8	310.9	5.41	0.66	0.76	507.0	198.1	198.1	198.1	<b>-39.6</b>	N	0.50	18.81
104-643A-28X3.35-87	260.96	0.08	76.0	76.0	76.0	259.9	N	9.1	259.9	3.23	0.60	0.80	507.0	198.1	198.1	198.1	<b>-39.6</b>	N	0.50	18.82
104-643A-28X3.35-87	261.46	0.05	40.5	292.0	61.0	336.1	N	14.4	336.1	5.87	0.59	0.41	507.0	198.1	198.1	198.1	<b>-39.6</b>	N	0.50	18.83
104-643A-28X4.85-87	261.96	0.04	57.0	76.0	64.9	256.0	N	5.3	256.0	5.35	0.60	0.80	507.0	198.1	198.1	198.1	<b>-39.6</b>	N	0.50	18.84
104-643A-28X4.85-87	262.46	0.05	77.4	278.8	70.7	215.5	N	13.7	215.5	5.51	0.71	0.20	507.0	198.1	198.1	198.1	<b>-39.6</b>	N	0.50	18.85
104-643A-28X5.135-137	262.86	0.05	49.3	97.0	51.2	82.5	N	3.2	82.5	1.44	0.39	0.87	507.0	227.0	227.0	227.0	<b>-12.5</b>	R	0.50	18.96
104-643A-28X1.35-87	264.86	0.05	60.8	62.7	66.3	66.2	N	6.6	66.2	1.16	0.40	0.91	507.0	198.1	198.1	198.1	<b>-85.6</b>	R	0.50	18.97
104-643A-28X1.35-87	265.26	0.08	76.8	282.8	75.5	70.9	N	4.5	70.9	1.33	0.34	0.87	507.0	198.1	198.1	198.1	<b>-85.6</b>	R	0.50	18.98
104-643A-28X2.35-87	265.76	0.06	58.8	53.4	70.3	52.6	N	19.5	52.6	0.92	0.67	0.79	507.0	198.1	198.1	198.1	<b>-85.6</b>	R	0.50	18.99
104-643A-28X2.35-87	266.26	0.05	50.4	22.2	52.6	256.3	N	8.1	256.3	1.03	0.35	0.65	507.0	198.1	198.1	198.1	<b>-85.6</b>	R	0.50	19.00
104-643A-28X2.35-87	266.76	0.04	57.0	81.9	65.9	61.0	N	4	61.0	2.21	0.35	0.								